Marine Biogeochemistry Studies of Iron and Hydrogen Peroxide using Flow Injection -Chemiluminescence

by

Angela Milne

A thesis submitted to the University of Plymouth in partial fulfilment for the

degree of

DOCTOR OF PHILOSOPHY

School of Earth, Ocean and Environmental Sciences

In collaboration with the

Marine Biological Association

June 2007

For Dad

Life is a journey,

achievements are unimportant

it's the people that you meet

who leave the lasting impressions

that you take with on your way.

Authors Declaration

At no time during the registration for the degree of Doctor of philosophy has the author been

registered for any other University award without prior agreement of the Graduate Committee.

A programme of advanced study was undertaken and relevant scientific seminars and conferences

were regularly attended at which work was presented and papers were prepared for publication.

Word count for the main body of the thesis

39,218

Signed. *Angela Mule*

Date.....12/6/07.............

i

Marine Biogeochemistry Studies of Iron and Hydrogen Peroxide using Flow Injection-Chemiluminescence

Angela Milne

Iron is an essential micronutrient for the growth of planktonic species. It is an integral element of numerous enzymes and proteins with important functions in photosynthesis and respiratory electron transport. In contrast to iron, hydrogen peroxide (H_2O_2) is ubiquitous in seawater. Phytoplankton are known to generate reactive oxygen species (ROS) such as superoxide and H_2O_2. This production, in conjunction with membrane bound reductases, may affect an organism's ability to access nutrients such as iron. The work presented in this thesis describes the development and optimisation of sensitive flow injection-chemiluminescence techniques to assess redox processes at the cellular level and their application to investigate marine processes.

Two flow injection methods, one based on direct sample injection and another involving the pre-concentration of iron, were used to determine iron(II) and dissolved iron and assess potential interference from a number of metals and H_2O_2. The results demonstrated the increased oxidation of Fe(II) in the presence of H_2O_2 (half life reduced from 10.4 to 3.5 min at 50 nM H_2O_2) and confirmed the ability of the pre-concentration method to remove this matrix interference. The accuracy and precision of the pre-concentration method were confirmed through analysis of samples collected on two international intercomparison studies. The results demonstrated that the method was precise (~ 8 %RSD) and provided a suitably low limit of detection (17 pM) for the determination of dissolved iron.

Dust deposition is an important source of iron to remote open ocean regions. The solubility of iron and aluminium in North Atlantic waters was assessed through an on-deck dissolution experiment. Calculated solubilities of iron released from six differing dust samples were low and varied from 0.001 to 0.04 %, whereas the release of aluminium ranged from 0.06 - 9.0 %. Solubility was inversely correlated with particle concentration, where higher solubility was observed for lower particle concentrations.

A versatile and adaptable FI system was developed, with a low detection limit (0.4 – 1.3 nM), excellent precision (1.1 – 1.8 %RSD) and the capability of sensitive real-time determination of H_2O_2 over a wide dynamic range. The results from laboratory based assays using a novel in-line filter approach demonstrated H_2O_2 production by the diatom species *Thalassiosira weissflogii* with observed concentrations in the range 30 – 100 nM. In addition, through field studies carried out in two different oceanic regions (English Channel and Ross Sea), a previously unreported correlation between phytoplankton biomass and surface H_2O_2 concentrations was observed.

The FI-CL instrumentation for the determination of Fe(II) was successfully adapted and optimised for the continuous in-line measurements of Fe(II) generated by diatoms. This technique provided a low detection limit (11 pM) and excellent precision (6.3 ± 3.2 % RSD). In further laboratory based assays with *T. weissflogii*, preliminary results indicated pM changes in Fe(II) generation following the reduction of organically bound Fe(III).

Acknowledgements

Presentations and Conferences Attended

Dissertations Symposium on Chemical Oceanography (DISCO), Hawaii. October 2006.

Oral Presentation: *The Determination of Hydrogen Peroxide Production by Diatoms using Flow Injection – Chemiluminescence and the Implications for Iron Speciation.*

Challenger, Scottish Association of Marine Science, Oban, Scotland. September 2006.

Oral Presentation: *The Determination of Hydrogen Peroxide Production by Diatoms using Flow Injection – Chemiluminescence and the Implications for Iron Speciation.*

Analytical Research Forum, RSC, University College Cork, Eire. July 2006.

Poster Presentation: *Flow Injection – Chemiluminescence for the Determination of Hydrogen Peroxide Production by Diatoms and the Implications for Iron Speciation.*

American Geophysical Union, Ocean Sciences Meeting, Honolulu, Hawaii. February 2006.

Oral Presentation: *High Resolution Real Time Determination of Hydrogen Peroxide Determination by Diatoms: Implications for Iron Speciation.*

British Phycological Society, 54th Annual Meeting, University of Plymouth. January 2006.

Poster Presentation: *Generation of extra-cellular reactive oxygen by marine diatoms; the development of real-time in vivo assays to reveal physiological function.*

Analytical Research Forum, Royal Society of Chemistry, University of Plymouth. July 2005.

Poster Presentation: *Dissolution of Iron from Dusts in North Atlantic Surface Seawater.*

American Society of Limnology & Oceanography, Santiago de Compostela, Spain. June 2005.

Oral and Poster Presentation: *Dissolution of Iron from Dusts in North Atlantic Surface Seawater.*

Challenger, Challenger Society, University of Liverpool. September 2004.

Poster Presentation: *Determination of Iron in North Atlantic Seawater using Flow Injection with Chemiluminescence Detection.*

Analytical Research Forum, RSC, University of Central Lancashire. July 2004.

Poster Presentation: *Determination of Iron in North Atlantic Seawater using Flow Injection with Chemiluminescence Detection.*

Western Region Analytical Division, RSC, University of Plymouth, England. July 2004.

Poster Presentation: *Determination of Iron in North Atlantic Seawater using Flow Injection with Chemiluminescence Detection.*

Publications

Milne, A., Davey, M. S., Worsfold, P. J., Achterberg, E. P., Taylor, A. R. Real-time determination of reactive oxygen species generation by marine phytoplankton using flow injection-chemiluminescence. (submitted to Limnology & Oceanography: *Methods*).

Moore, C. Mark, Matthew M. Mills, Rebecca Langlois, Angela Milne, Eric P. Achterberg, Julie La Roche, and Richard J. Geider. (2007). Relative influence of nitrogen and phosphorous availability on phytoplankton physiology and productivity in the Oligotrophic Sub-Tropical North Atlantic Ocean. Limnology & Oceanography (accepted).

Moore, C. M., Mills, M. M., Milne, A., Langois, R., Achterberg, E., Lochte, K., Geider, R. J., and J. La Roche. (2006). Iron limits primary productivity during spring bloom development in the central North Atlantic. *Global Change Biology* **12**:626-634.

Table of Contents

Chapter 1   Iron and Hydrogen Peroxide in Seawater

Chapter 3   A Dissolution Study of Iron and Aluminium from Six Dusts in North Atlantic Ocean Seawater

Chapter 4   Determination of H_2O_2 in Laboratory Cultures and Natural Surface Seawater using Flow Injection with Chemiluminescence Detection

Chapter 5   Effect of Hydrogen Peroxide Production by Diatoms on Iron Speciation in Seawater

Chapter 6   Conclusions & Future Work

References

Tables

Figures

xvi

Abbreviations

8-HQ	8-hydroxyquinoline
CL	Chemiluminescence
dAl	Dissolved aluminium species passing through a 0.2 – 0.4 μm pore size filter (Fe(II) + Fe(III)), analysed after acidification
DFB	Desferrioxamine B
dFe	Dissolved iron species passing through a 0.2 – 0.4 μm pore size filter (Fe(II) + Fe(III)), analysed after acidification
DI method	Determination of an analyte by direct injection of a sample into a reagent stream
Fe(II)	Dissolved iron(II), <0.2 μm, analysed immediately after in-line filtration
Fe'	'Free ' inorganic iron species
FI	Flow injection
FI-CL	Flow injection-chemiluminescence
GF-AAS	Graphite furnace atomic absorption spectrometry
H_2O_2	Hydrogen peroxide
HNLC	High nutrient, low chlorophyll
ICP-MS	Inductively coupled plasma mass spectrometry
LISW	Low iron filtered seawater
LOD	Limit of detection
luminol	5-amino-2,3-dihydo-1,4-phthalazinedione
nM	nmol L^{-1}
pM	pmol L^{-1}

Q-HCl	High purity quartz distilled hydrochloric acid
UHP water	Ultra high purity water
UV-FSW	UV irradiated filtered seawater

Chapter 1

Iron and Hydrogen Peroxide in Seawater

1.1 Introduction

The marine environment is a major contributor to global primary production, producing an estimated 40% of the photosynthesis on Earth (Falkowski, 1994). The turnover of biomass is nearly three orders of magnitude higher than that of terrestrial biomass (Table 1.1), and therefore nutrients that regulate primary production in the marine environment play a key role in the global carbon cycle and on the world's climate.

Table 1.1 Global primary productivity in marine and terrestrial regions

Ecosystem	Net Primary Productivity (10^{15} g / year)	Total Plant Biomass (10^{15} g)	Turnover Time (years)
Marine	35 – 50	1 - 2	0.02 – 0.06
Terrestrial	50 - 70	600 - 1000	9 - 20

(Adapted from Falkowski and Raven (1997))

Iron is an essential nutrient for planktonic species. Vital for plant metabolism, iron occurs in cytochromes and iron-sulphur redox proteins which are involved in key metabolic functions in intracellular respiration and photosynthesis (Sunda, 2001). Iron is also incorporated in proteins for the transport of oxygen and is required for nitrogen fixation and for the reduction of nitrate, nitrite and sulphate (Whitfield, 2001).

Primary production is generally limited by the macro-nutrients (nitrate, phosphate and silicate) and light. However in ~ 40 % of the world's oceans there is an abundance of these major nutrients, yet concentrations of chlorophyll a are low (Falkowski, 1994). These regions have become known as High Nutrient, Low Chlorophyll (HNLC) areas, the most important are the Southern Ocean, the equatorial Pacific and the sub-arctic Pacific. It is now known that these HNLC regions are limited by iron availability (Boyd et al., 2004; Martin et al., 1994). Furthermore, regardless of oceanic region, there is compelling evidence that the supply of iron

2

controls the productivity, species composition, and trophic structure of planktonic communities in large areas of the world's oceans (Sunda, 2001).

Hydrogen peroxide (H_2O_2), a reactive oxygen species (ROS), is ubiquitous in the surface waters of the oceans. The ROS are transient, highly reactive species which also include oxygen ions, free radicals and superoxide (O_2^-). H_2O_2 is a key chemical species in redox reactions and has the potential to affect the cycling of trace metals and organic compounds (e.g. iron, González-Davila et al. (2005); Millero and Sotolongo (1989)). It is known that H_2O_2 is produced by phytoplankton during aerobic respiration and photosynthesis as a metabolic by-product (Falkowski and Raven 1997; Fridovitch 1998). The potential role of cellular redox processes including planktonic H_2O_2 production on the availability of iron is an interesting area of study. In order to elucidate the relationship between biological generation of H_2O_2 and iron, a better understanding is required into the processes governing iron availability and the mechanisms utilised by organisms to access this essential nutrient.

1.2 Iron in Seawater

Iron (Fe) is the fourth most abundant element in the Earth's crust with an average concentration of around 5.6% (Taylor, 1964). However, despite its crustal ubiquity the concentration of iron in the surface waters of the ocean, while variable, is very low (0.02 – 2 nM) (de Baar and de Jong, 2001; Landing and Bruland, 1987; Martin et al., 1990; Measures and Vink, 1999). The variability in surface ocean concentrations is due to large spatial and temporal differences in rates of input and removal (Sunda 2001). The processes which contribute to the low iron concentrations observed in the oceans, and the input and removal pathways of this essential element, are discussed below.

3

1.2.1 Iron Speciation in Seawater

The physicochemical speciation of iron in seawater is dependent on the interactions between the various particulate and dissolved phases and the composition of the seawater. The chemical speciation of an element can have a controlling influence on its biological availability and for metals it is usually the free metal ion that is most readily assimilated (Whitfield 2001). In seawater at pH 8, inorganic iron has a solution chemistry which is dominated by hydrolysis species. Iron exists in the ocean in two oxidation states, iron(II) and iron(III), and both of these form soluble inorganic and organic complexes, colloids (sub-micron particles) and particulate phases (Achterberg et al. 2001). Iron(III) predominates in oxygenated waters. It is highly reactive with respect to water (forming oxyhydroxides), adsorption and complex formation and is highly insoluble (Sunda 2001). In contrast, iron(II) is thermodynamically unstable in oxygenated waters and is rapidly oxidised to iron(III). Figure 1.2 illustrates the different species of iron which exist in seawater.

Inorganic iron(III) exists in solution as the mononuclear iron hydrolysis species ($Fe(OH)_2^+$, $Fe(OH)_3^0$, and $Fe(OH)_4^-$), which are much more kinetically labile with respect to ligand exchanges than organic chelates (Sunda 2001). They can be viewed as a single reactive pool, due to the fact that they rapidly equilibrate with one another. The ratio of these mononuclear hydrolysis species (Fe(III)') to free ferric ions is $\sim 10^{10}$ at pH 8.1 (Hudson et al., 1992). This makes Fe(III)' prone to rapid removal by oxyhydroxide colloid formation and effective scavenging onto falling particles (Whitfield 2001). As previously mentioned, these iron hydrolysis species are sparingly soluble and precipitate as hydroxides. In the absence of organic or inorganic chelators, the total amount of soluble iron in aqueous solution is limited by the solubility of iron hydroxide species. At pH 7.4 and in the absence of chelating ligands, the total amount of soluble iron ($Fe^{3+}_{(aq)}$ + $Fe(OH)^{2+}_{(aq)}$ + $Fe(OH)_2^+_{(aq)}$) is as low as 10^{-10} M (Boukhalfa and Crumbliss, 2002). Over time, these hydroxides undergo dehydration and crystallisation, which ultimately leads to the formation of more stable iron oxides. Aged

hydroxides and iron oxides are less available to biota for uptake as compared with freshly precipitated hydroxides (Sunda 2001). It is therefore important for biota to minimise hydrolysis and dehydration processes and to use alternative mechanisms to keep iron available.
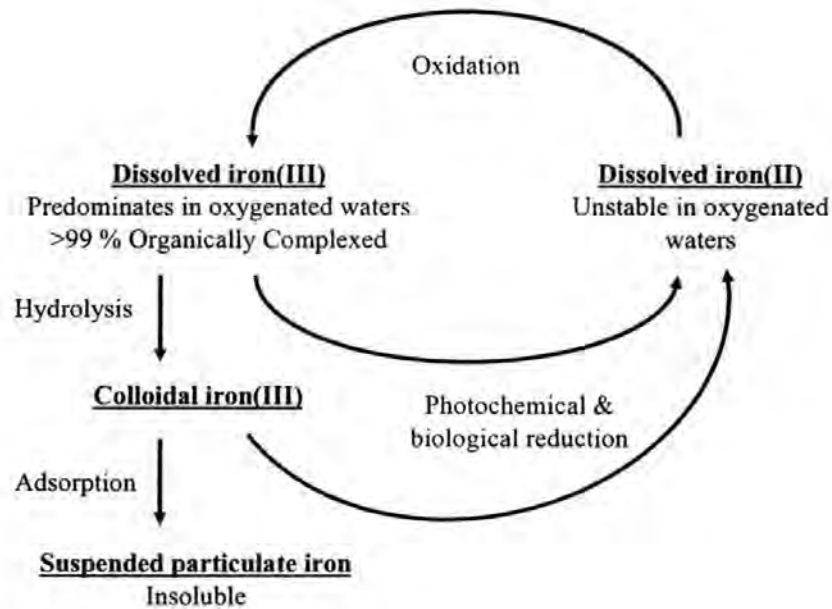
Figure 1.1 The speciation of iron in seawater.

Iron concentrations in the euphotic zone are maintained by iron-binding organic ligands (Whitfield 2001). Over 99% of iron(III) is strongly complexed by organic ligands (van den Berg 1995) with very high stability constants. Complexation with such organic ligands is an important factor in controlling the speciation of iron in seawater and therefore its availability (Wells, 2003). The presence of these ligands increases the solubility of iron and greatly reduces removal by particle scavenging. Two ligand classes have been identified;

	Log K	Concentration (M)
a) a strong ligand found in surface waters	13	$0.4 - 1.0 \times 10^{-9}$
b) a weaker ligand found in depths down to 2000m	11.5	1.5×10^{-9}

(Rue and Bruland, 1995).

where the stability constant (K) is calculated from all inorganic iron (Fe') rather than free Fe^{3+}.

5

While little is known about these ligands, the observed binding strengths resemble those determined for siderophores (specific iron-binding chelators released by marine heterotrophic bacteria to sequester iron) grown in laboratory based cultures (e.g $K_{Fe'L}$ = $10^{11.5}$ – $10^{12.5} M^{-1}$, (Lewis et al., 1995; Macrellis et al., 2001)). Iron chelation maintains concentrations of iron in surface waters, without the presence of iron-chelating ligands the iron concentrations would be much lower and the biology of the oceans would likely look far different (Sunda 2001).

Iron(II) is much more soluble and more kinetically labile and forms much weaker organic chelates (Sunda 2001). Therefore, the reduction of iron(III) through photoreduction of iron -chelates, -hydroxides and -oxides, typically leads to the dissociation of iron chelates or to the dissolution of iron oxyhydroxides. This is due to iron(II) being formed which is much less strongly bound to organic ligands and iron(II) oxyhydroxides being highly soluble (Sunda 2001). Once released the free iron(II) ion is rapidly re-oxidised and the resultant iron(III) is then re-chelated by organic ligands or precipitated as iron hydroxides. This photoreductive cycling enhances the concentration of kinetically labile inorganic species of iron(II) and iron(III) and therefore enhances biological uptake (Sunda 2001).

1.2.2 Sources of Iron to the Oceans

The routes through which iron is transported to the oceans are illustrated in Figure 1.1. These inputs can be grouped into three main pathways: atmospheric deposition, fluvial (riverine) and processes which take place on the sea floor, such as sediment re-suspension, re-suspension and up-welling from continental shelf regions and inputs from hydrothermal vents.

Fluvial inputs

Atmospheric deposition (wet & dry)

Continental shelf

Iron Pool
(Dissolved, colloidal and suspended particulate)

Biological uptake & microbial re-mineralisation

Hydrothermal vents

Ageing & Settling of particulate iron

Dissolution into sub-oxic bottom waters and sediment re-suspension and transport

Sediments
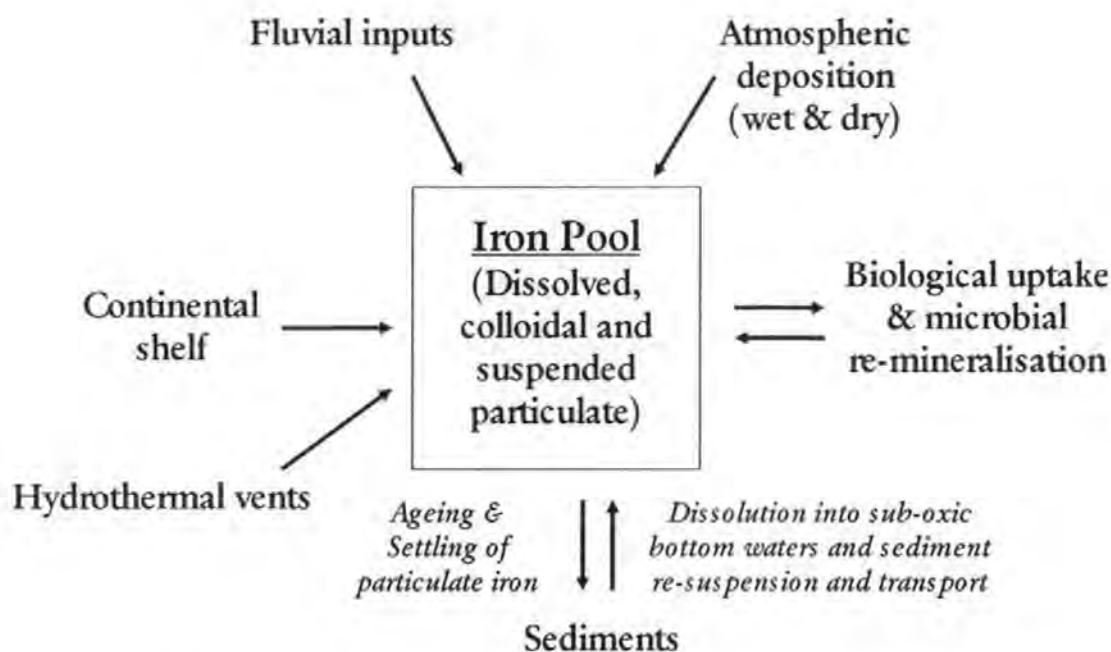
Figure 1.2. Schematic diagram of the input pathways which contribute to the biogeochemical cycling of iron in the ocean.

River systems transport particulate and dissolved iron to coastal zones, following erosion of rocks and soils, which results in increased iron concentrations in these areas. However, up to 95 % of riverine dissolved iron can be lost through estuarine mixing processes (Boyle et al., 1977). The higher salinity and pH of the ocean environment compared to freshwater systems results in scavenging of both dissolved and particulate iron following flocculation (Moore et al., 1979; Sanudo-Wilhelmy et al., 1996; Turner and Millward, 1994). While this pathway is most likely to be the dominant input of iron to coastal regions, the majority of this iron supply is transported only as far as the Continental Shelf (Johnson et al., 2001). How much of the iron is transported further to the open ocean is uncertain, however, in areas of upwelling this input pathway may be of great importance.

Atmospheric deposition is a major pathway for the transport of iron to the oceans. Wind-transported dust arises primarily from desert and semi-arid regions, the majority of which are located in the Northern Hemisphere. Important arid areas include the large deserts

of North Africa, the Arabian Peninsula and Asia. The importance of these areas is in part due to their size, but also through their proximity to oceans (e.g. North Africa and the North Atlantic Ocean). Dependence on meteorological events means that rates of dust production and wet/dry deposition to the ocean are sporadic.

Previous studies have estimated and revised dust inputs to the oceans using available field data (Duce et al. 1991; Duce and Tindale 1991; Moore et al. 2002), these estimates lie in the range $400 - 1000 \times 10^{12}$ g y^{-1} of which ~ 30 % is as a result of wet deposition processes (Jickells and Spokes, 2001). The resultant flux of iron delivered to the surface oceans from the atmosphere is dependant on a number of factors, the most important of these is the amount of iron contained in the aerosol and the solubility of that iron upon deposition into seawater. For crustal aerosols, the iron content is usually assumed to be 3.5 % (Duce and Tindale, 1991). However, there is a large disparity in the reported fraction of iron which is soluble in seawater and values in the literature range from 0.001 – 87 % (Bonnet and Guieu, 2004; Hand et al., 2004; Jickells and Spokes, 2001; Zhuang et al., 1990). Different experimental protocols and analytical techniques used to derive these estimates may account for some of these differences and make results difficult to compare. Aerosol iron solubility is influenced by composition (Zhu et al., 1992) and the degree of cloud processing that an aerosol has undergone (Jickells and Spokes, 2001). Particle loading has also been shown to affect the solubility of iron in seawater, resulting in the re-adsorption of iron at high particle concentrations (Bonnet and Guieu, 2004).

Atmospheric deposition is a crucial source of iron in remote oceans regions. Iron limitation reflects deep water iron-nitrogen concentration ratios that are inadequate to meet the iron requirements of phytoplankton (Watson, 2001). Rapid scavenging of iron, from the subsequent re-mineralisation of the metal from sinking detritus (faecal pellets and dead organisms), at faster rates than nitrogen creates an imbalance in iron-nitrogen concentrations.

In order to sustain primary production, another source of iron is required in addition to that received from upwelling inputs (Jickells et al., 2005). This additional source of iron can be provided through dust deposits. The positive effect of atmospheric deposition on surface water iron concentrations has been observed through raised dissolved iron concentrations (Sarthou et al. 1999). Also dust addition incubations experiments have demonstrated positive growth of the resident phytoplankton community from the input of dust (Moore et al., 2006). These studies demonstrate the importance of this pathway as a source of nutrients including iron.

Inputs from sea-floor processes (hydrothermal vents and sediments) are in general contained to the source region. Hydrothermal vents are potentially the largest supplier of dissolved iron to deep waters, with the global iron flux estimated to be in the region of $1 - 10$ x 10^{12}g y^1 (Chester 2000). Seawater end members produced from these systems have high dissolved iron concentrations ($\sim 1 - 3$ mM, (Von Damm and Bischoff, 1987)). However, sediments enriched in iron in the same vicinity as hydrothermal areas, suggests that the majority of the dissolved iron from hydrothermal activity precipitates out in various mineral forms (mostly oxyhydroxides) close to the source (German et al., 1991). Marine sediments, through the reductive mobilisation of iron, are potentially another major source of dissolved iron. The average iron content of deep-sea clays and coastal muds is 6 % and 6.5 % respectively (Chester 2000), of this about half exists in iron oxide coatings and organic moieties, which are susceptible to reductive dissolution, producing dissolved iron(II). Concentrations of dissolved iron(II) observed in reducing pore waters are commonly in the micro-molar range (Canfield, 1989) though it is unlikely to be transported into the overlying waters due to the rapid oxidation of iron(II) in oxic seawater. Sedimentary inputs of dissolved iron are therefore only expected to be significant in anoxic areas, in places where there is significant turbidity, or gradual release of iron into an organically bound stabilised form.

1.2.3 Iron Cycling in the Oceans

Vertical distribution

The vertical distribution of iron is strongly influenced by biological uptake, recycling and relatively intense scavenging processes. The vertical distribution of dissolved iron (<0.4 – or <0.2 μm filterable iron) in remote open ocean waters, such as HNLC regions, are consistent with nutrient–type elements, i.e. depleted concentrations in the surface waters due to biological uptake and enrichment at depth owing to remineralisation of organic matter (Johnson et al., 1997; Martin and Gordon, 1988). Figure 1.3 illustrates dissolved iron concentrations in the water column from remote areas in the North Pacific and North Atlantic which display the same nutrient-type profile trend. In less productive oligotrophic areas, dissolved iron concentrations in surface and intermediate waters are often less depleted and can exhibit surface water maxima, particularly in areas where sources of iron are more prominent (e.g. high dust input) (Johnson et al., 1997; Measures et al., 1995; Ussher et al., 2004).
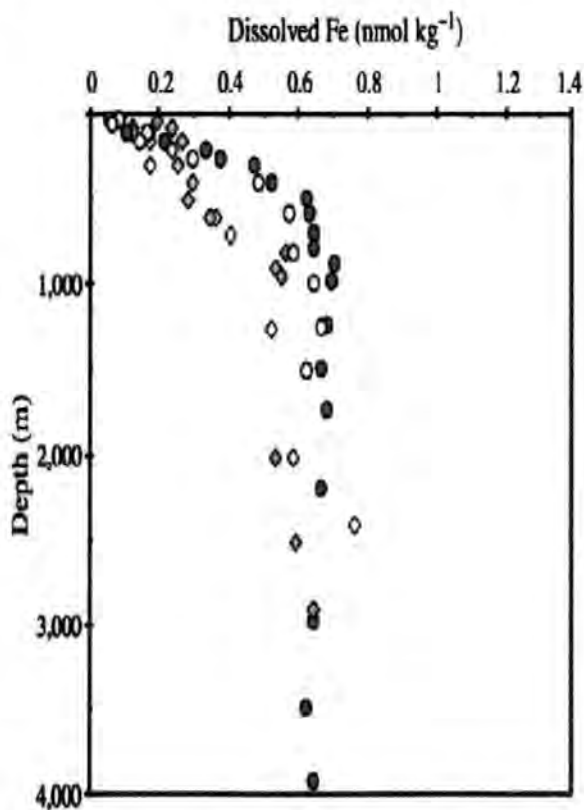
Figure 1.3 Vertical dissolved iron profiles from high latitudes of the North Atlantic ($\bullet$, $\lozenge$) (59° 30' N, 20° 45'W and 47° N, 20° W; data from Martin et al. (1993) and the North Pacific ($\bullet$, $\circ$) (50° N, 145° W and 45° N, 142° 52' W; data from Martin et al., (1989).

In deep water, iron does not exhibit the trend of nutrient type metals, which exhibit a relatively low level of scavenging in the deep sea, and hence their concentrations increase in the circulation of water in the world's oceans as the water ages. Iron, with a residence time of ~ 200 yr, does not exhibit this trend (Bergquist and Boyle, 2006). This is demonstrated in Figure 1.3, the concentrations of dissolved iron below 1000 m do not significantly differ between the two ocean bodies. This is in contrast to nutrients or nutrient-type metals (e.g. zinc) where concentrations in the Pacific are markedly higher that those of the Atlantic. Instead, the deep-water concentrations of dissolved iron appear to be controlled by a balance of remineralization, from the rain of particulates from above and lateral transport, and particulate scavenging (Bergquist and Boyle, 2006; Johnson et al., 1997).

The concentrations of iron in the upper water column, i.e. the euphotic zone, are influenced by and cycled within the biological pool. This has a significant effect on its transport through the water column with respect to concentrations in surface waters (depleted) and at depth (enriched). Due to biological activity, and mixing processes, the transport of iron in the upper water column is far more dynamic than in deep waters (Hutchins et al., 1993) and is reflected in the shorter residence times, e.g. estimates for the upper 100 m of the Sargasso Sea have been calculated to be 250 and 18 days for dissolved and particulate iron respectively (Jickells, 1999).

Biological cycling

The concentrations of iron in the ocean are often correlated with the major nutrients (N and P) which would suggest that iron is also controlled by biological uptake and regeneration cycles (Johnson et al., 1997; Martin and Gordon, 1988; Sunda and Huntsman, 1995). Studies have highlighted the role of biota on the availability and cycling of iron in the upper ocean (Boyd and Harrison, 1999; Price and Morel, 1998) and Figure 1.4 illustrates this

11

cycle. Within the euphotic zone, iron and other nutrients are taken up by phytoplankton and bacteria as part of their growth cycles. Further assimilation occurs through grazing by higher organisms. Following the death of an organism, or through the release of biogenic particles (faecal pellets), the nutrients are transported downwards. Decay processes release the nutrients and iron back into the water column via microbial remineralisation leading to enrichment in dissolved iron concentrations at lower depths (Sunda, 2001). Upwelling and turbulent mixing then return the iron to the euphotic zone.
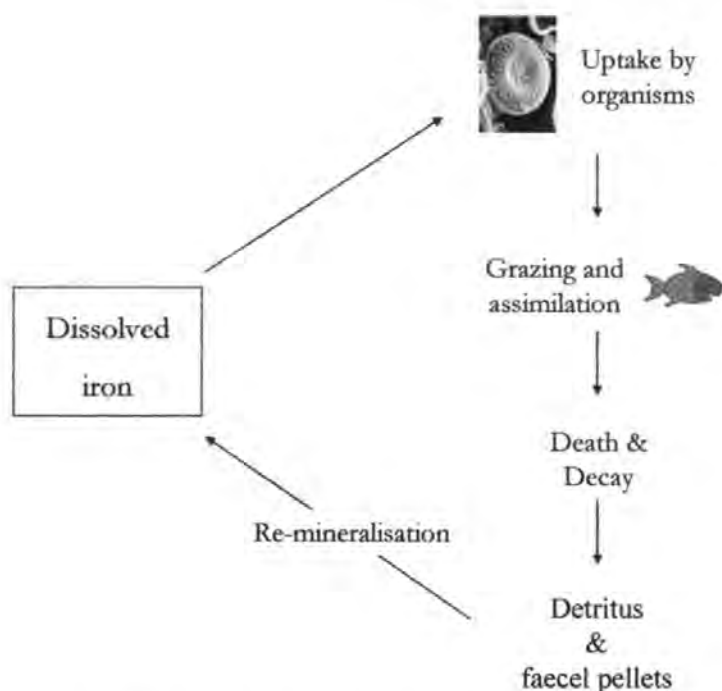
Figure 1.4. The biological cycling of iron in the euphotic zone.

Marine organisms acquire iron by either membrane transporters or through siderophore systems. Marine bacteria (heterotrophic and phototrophic) have been observed to secret siderophores under iron limited conditions and also can access iron from multiple siderophores produced by different organisms (Granger and Price, 1999; Hutchins et al., 1999; Trick and Wilhelm, 1995). Siderophores are low molecular weight (300 – 1000 Da) iron chelators with either hydroxamate or catecholate functional groups which selectively bind

iron(III). The siderophores chelate and solubilise iron present in minerals (e.g. iron oxides), adsorbed onto particle surfaces or bound within existing complexes (Neilands, 1995). The iron-bound siderophores are transported back into the cells via high affinity membrane transporters (Reid et al., 1993). While siderophore production has been observed in heterotrophic and cyanobacteria, there has been no evidence of this method of iron acquisition by marine phytoplankton, although they have been observed to access iron bound to siderophores (Hutchins et al., 1999; Maldonado and Price, 1999). Conditional stability constants in the order of $K_{Fe'LFe} = 10^{11.5} - 10^{12.5}$ M^{-1} have been determined for marine siderophores produced in laboratory cultures which are similar to the two ligand classes indicated in the ocean environment (Rue and Bruland, 1995). It is therefore evident that siderophores constitute part of the iron-binding ligand pool and therefore contribute to maintaining iron concentrations in surface waters.

Iron uptake through ion membrane transporters has been demonstrated to be related to the concentration of inorganic iron species ([Fe']) though the exact mechanisms of acquisition are uncertain (Anderson and Morel, 1982; Hudson and Morel, 1990; Sunda and Huntsman, 1995). However, the concentration of Fe' (estimated to be 0.01 pM (Rue and Bruland, 1995)) would be insufficient for adequate iron uptake (Maldonado and Price, 2000). It is unclear whether membrane transporters are selective either for free iron(II) or iron(III), in addition there is now growing evidence which suggests that organisms can increase the concentrations of [Fe'] by accessing iron from organic complexes. It has been demonstrated that eukaryotic phytoplankton possess inducible reductases at the cell surface through which they can reduce iron(III) bound to organic complexes (Maldonado and Price, 2000; Maldonado and Price, 2001). Following complex dissociation the cells can internalise the inorganic iron via metal transport proteins at the cell surface. In addition to cell mediated processes, as previously mentioned in section 1.2.1, the dissociation of iron from organic ligands can also be propagated through photochemical production, resulting in enhanced Fe'. This light mediated dissociation process may be important in optically transparent waters of

the open ocean, where light can penetrate to the base of the surface mixed layer (Barbeau et al. 2001).

In an environment where an essential growth element is > 99 % organically complexed, all processes which enable cells to acquire iron are important. The biological reduction of organic iron could potentially supply a large fraction of the iron required for cell growth in the oceanic environment (Maldonado and Price, 2000).

1.3 Hydrogen Peroxide in Seawater

The occurrence of H_2O_2 in seawater was first reported by Baalen and Marler in 1966. Since then there have been numerous studies reporting H_2O_2 concentrations in ocean environments (Cooper et al., 1987; Moffett and Zafiriou, 1993; Yuan and Shiller, 2005) and reporting its involvement in redox processes with metal ions (González-Davila et al., 2005; Millero and Sotolongo, 1989; Moffett and Zika, 1987). The concentrations of H_2O_2 in seawater are controlled by a complex set of factors involving light intensity, concentration of organic matter and physical mixing processes. This can result in different concentrations being observed in the surface waters of different aquatic environments.

1.3.1 Sources of Hydrogen Peroxide to the Oceans

There are three main sources of H_2O_2 in surface seawater and these are illustrated in Figure 1.5. The formation of H_2O_2 in seawater involves the single electron reduction of O_2 to form the intermediate O_2^-, subsequent disproportionation produces H_2O_2. The primary in-situ source of H_2O_2 involves photochemical processes as a result of the interaction of UV

light, with O_2, dissolved organic matter and/or trace metals (Cooper et al. 1988; Yocis et al. 2000; Keiber et al. 2003; Millero 2006) (Figure 1.5 (1)). Certain dissolved organic chromophores (org), present in seawater, are light receptors and are raised to a higher (excited) state which leads to the production of O_2^-:

$$org + h\nu \rightarrow org*$$
$$org* + O_2 \rightarrow org^+ + O_2^-$$
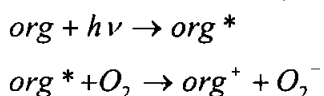
The rapid disproportionation of O_2^- leads to H_2O_2 formation and regeneration of molecular O_2 via

$$2O_2^- + 2H^+ \rightarrow H_2O_2 + O_2$$
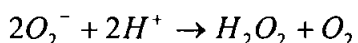
The photochemical processes which lead to the formation of H_2O_2 in seawater, also occur in the atmosphere. As a consequence, atmospheric deposition of H_2O_2 (Figure 1.5 (2)), particularly during wet precipitation events, also results in a significant increase in H_2O_2 concentrations in surface waters (Cooper et al. 1987; Yuan and Shiller, 2000; Croot el al. 2004; Gerringa et al. 2004). Differences in light intensity and dissolved organic matter go some way to explain the differences in surface H_2O_2 concentrations observed in different marine systems. A wide range of H_2O_2 concentrations have been reported in the open ocean from 20 to >200 nM (Zika et al. 1985; Miller & Kester 1994; Sarthou et al. 1997; Yuan & Shiller 2001, 2005; Croot et al. 2004, 2005). The higher concentrations of H_2O_2 (up to 300 nM) have been observed in Equatorial and Tropical regions of the Atlantic where there is also high concentrations of dissolved organic matter in/or as a result of the Amazon Plume entering into the Atlantic (Yuan and Shiller, 2001) and longer periods of light intensity. In regions of low incident radiation and low concentrations of dissolved organic matter, much lower surface values have been reported, e.g. surface concentrations in the Southern Ocean in the range 10 – 20 nM (Sarthou et al., 1997).
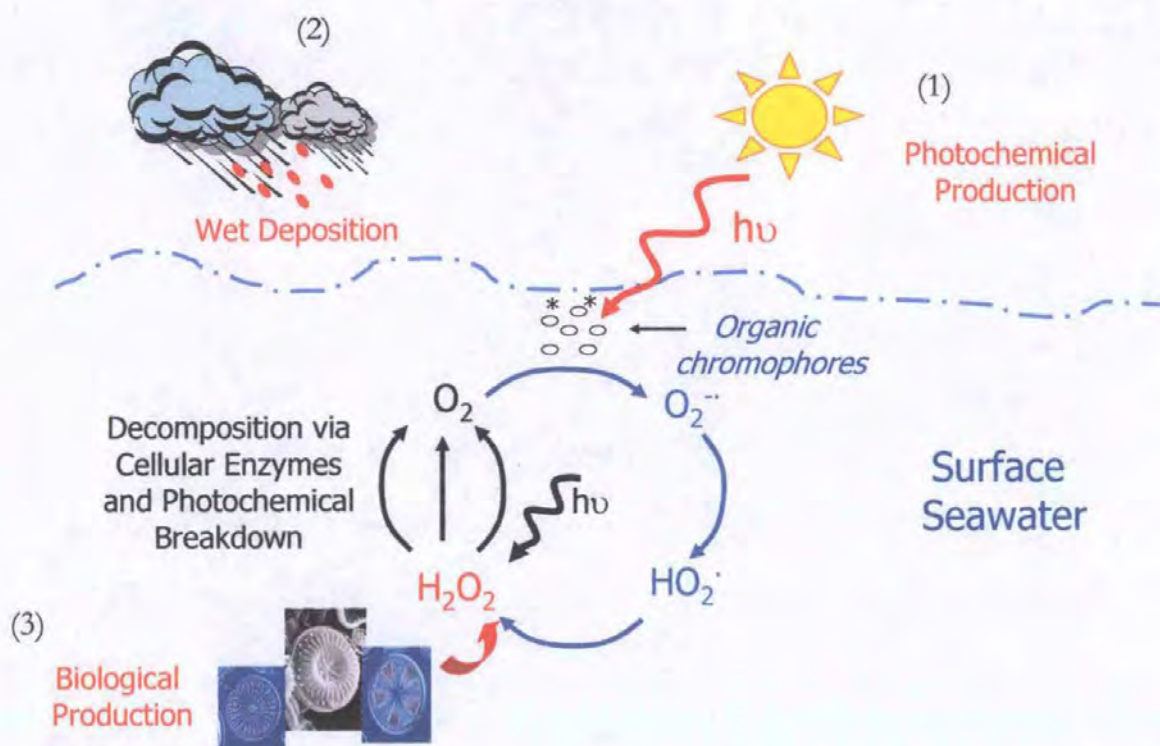
Figure 1.5 The sources and decomposition pathways of hydrogen peroxide in surface seawater. (1) Photochemical production and decomposition, (2) deposition of peroxides through rainfall and finally (3) biological production and decomposition through cellular enzymens (e.g. catalases).

The biological production of H_2O_2 constitutes the final source of this reactive species to surface seawater (Figure 1.5 (3)), and is also a major contributor to its decomposition through cellular enzymes.

1.3.2 Hydrogen Peroxide Cycling in the Oceans

Vertical distribution

As discussed in the section above, spatial and temporal factors, as well as seawater composition, determine H_2O_2 concentrations observed in surface waters. The sources of H_2O_2, photochemical production, wet deposition and biological production (Figure 1.5), all impact on the upper water column. As a result, observed profiles for H_2O_2 typically depict a

surface maximum followed by depletion with depth (Croot et al., 2004b; Yuan and Shiller, 2001) as illustrated in Figure 1.6. The cycling of H_2O_2, both production and also decomposition, therefore mainly occurs in the photic zone. These processes are further illustrated in Figure 1.7.
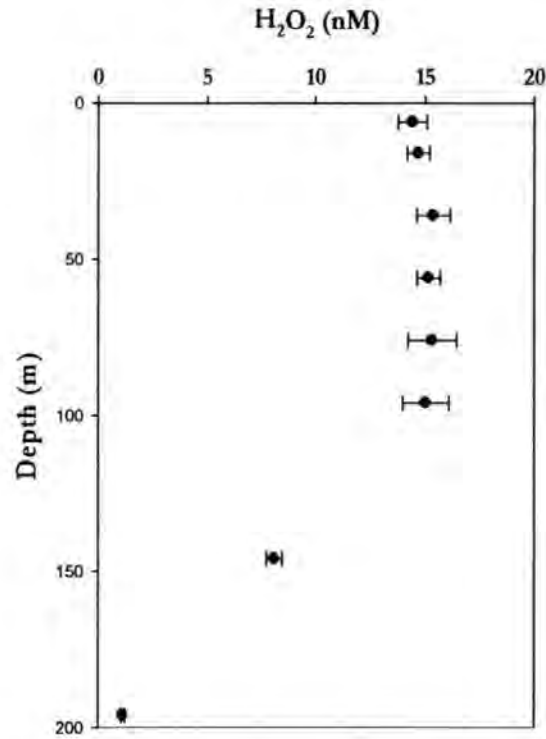
Figure 1.6 Vertical profile of H_2O_2 concentrations from the Ross Sea (CORSACS II 2006, NX14) (Milne et al. unpublished, 2006)
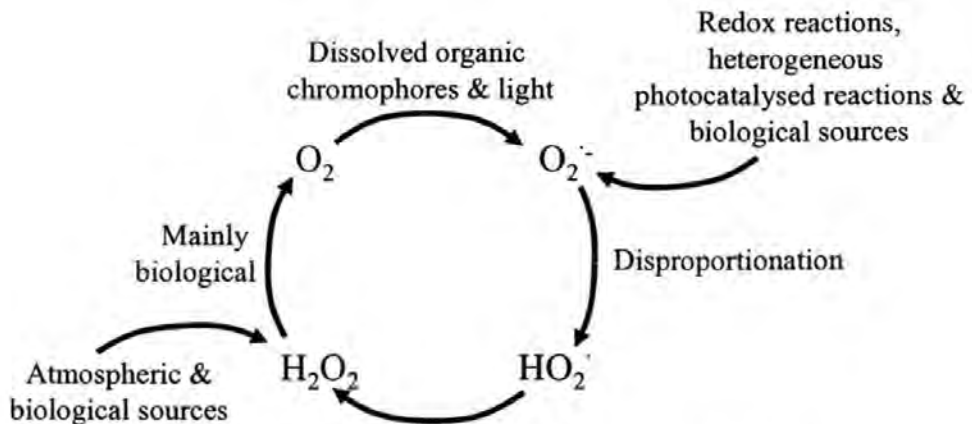
Figure 1.7 The cycling of H_2O_2 in surface seawater.

H_2O_2 is the most stable ROS intermediate, with a half-life ranging from hours to days (Cooper et al. 1994, Petasne and Zika 1997; Yuan and Shiller 2001, 2005). Its decomposition arises mainly through substances produced by biological organisms (e.g. catalase) (Cooper and Zepp, 1990), however photochemical decomposition also occurs (Moffett and Zafiriou, 1993) and transition metals, e.g. iron, can also catalyse decomposition (through redox reactions). The oxidation of iron(II) with H_2O_2 has been investigated by a number of authors (e.g. Millero and Sotolongo, 1989; Millero et al., 1991; Moffett and Zika, 1987). The mechanism for the reaction between iron(II) and H_2O_2 has been widely assumed to proceed predominantly according to the Haber-Weiss (1934) mechanism,

$$Fe(II) + O_2 \rightarrow Fe(III) + O_2^-$$
$$Fe(II) + O_2^- + 2H^+ \rightarrow Fe(III) + H_2O_2$$
$$Fe(II) + H_2O_2 \rightarrow Fe(III) + HO^- + OH^-$$
$$Fe(II) + HO^- \rightarrow Fe(III) + OH^-$$
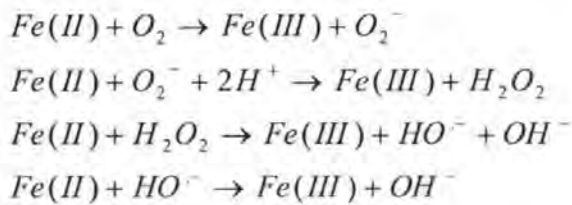
This mechanism illustrates the importance of O_2 and H_2O_2 on iron(II) oxidation, furthermore the cyclic relationship between these species is highlighted, this is demonstrated and simplified in Figure 1.8.
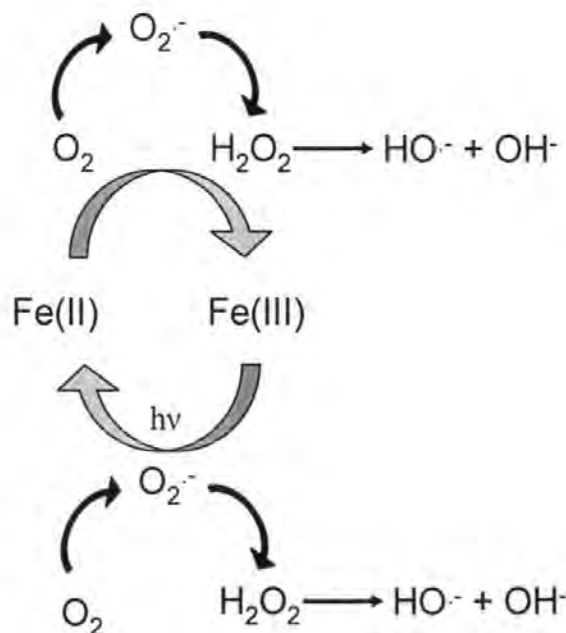
Figure 1.8 A simplified illustration of the oxidation and reduction of iron.

In contrast to the physical and chemical factors which result in H_2O_2 production in surface waters, relatively little is known about the biological contributions to the hydrogen peroxide pool. Biological production of H_2O_2 occurs as a by-product of respiration and photosynthesis (Falkowski and Raven, 1997). The functioning of these essential metabolic processes requires the transfer of electrons across internal and external plasma membranes. In the presence of molecular oxygen, an excellent oxidising agent and terminal electron acceptor (Wolfe-Simon et al., 2005), this electron transfer leads to the production of reactive oxygen species, initially O_2^- and then H_2O_2, through disproportionation. Production of H_2O_2 therefore, occurs both intra and extra-cellularly, although only H_2O_2 is capable of diffusing passively across the outer plasma membrane. Subsequently biological H_2O_2 production is the sum of both internal and external processes. A schematic of a diatom cell is presented in Figure 1.9 to illustrate the production process of H_2O_2.

Production of all reactive oxygen species, including O_2^- and H_2O_2, by phytoplankton is highly dependent on the prevailing conditions. Both abiotic e.g. light, nutrient status and temperature, as well as biotic factors such as pathogen interactions (Evans et al., 2006) can influence the degree of oxidative stress and hence H_2O_2 production and release to the surrounding medium by phytoplankton. The target, if any, of this production is not well understood, though there are a number of different processes in which these reactive species may be involved to the benefit of the organism. Two such processes are cell signalling (cell-to-cell communication) and defence (against pathogens), however, as a key species in redox reactions, the production of H_2O_2 (and O_2^- as its precursor) may also affect an organisms ability to access nutrients such as iron.
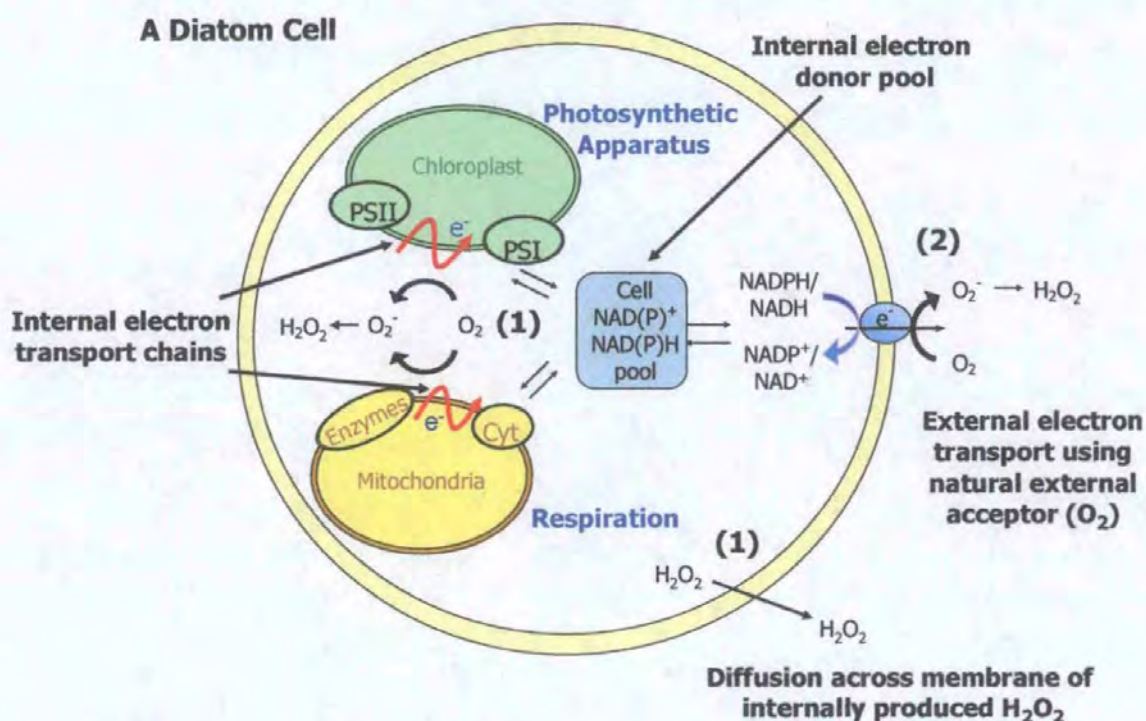
Figure 1.9 A schematic figure of H_2O_2 production by a diatom. (1) Internally produced H_2O_2, arises as a result of reduction of O_2 and subsequent disproportionation to H_2O_2. This is known to occur via electron leakage from the electron transport processes of the mitochondria and chloroplast. H_2O_2 is membrane permeable and if not quenched by intracellular antioxidant mechanisms may diffuse across the outer plasma membrane. (2) Externally produced H_2O_2, following the disproportionation of O_2^{-}, through the cell surface reduction of O_2, the natural terminal electron acceptor.

H_2O_2 and other reactive oxygen species, produced as a result of cellular processes, are also toxic to micro-organisms at high concentrations. Enzymes specific to the catalytic decomposition of these reactive species are therefore also produced by organisms for detoxification, and include the H_2O_2 specific enzyme catalase. Peroxidases, such as horseradish peroxidase and cytochrome c peroxidase, are also enzymes. They reduce H_2O_2 (and hence decompose) by transferring H_2O_2 oxygen to substances which are oxidisable. For many of these enzymes H_2O_2 is the optimal substrate and is therefore utilised during enzymatic processes (Sharp 1990).

1.4 Aims and Objectives

The aim of the work presented in this thesis was to investigate the biogeochemical cycling of iron and H_2O_2 both at a cellular level and in the surface waters of the oceanic environment. In order to achieve this two integrated approaches, laboratory experiments and field based observational campaigns, were undertaken. In addition, suitable analytical methods had to be developed in order to observe processes at the cellular level and in the global oceanic environment. The key objectives of the project were to:

1. Optimise analytical techniques to enable the determination of low concentrations of iron (pM) for use in field studies in the oceanic environment and in laboratory based studies.

2. Gain further understanding of the solubility, and hence bioavailablility, of iron in North Atlantic seawater from dust deposition, and to investigate whether aluminium/iron ratios are a good proxy for estimating dust deposition events.

3. Develop an analytical technique for the sensitive (nM) and real time detection of H_2O_2, transferable between the laboratory and field studies, in order to investigate and assess the biological production of H_2O_2 at the cellular level and in the open ocean environment.

4. Investigate the reduction of Fe(III)-organic complexes at the cell surface and assess the role of biological reactive oxygen species and membrane bound reductase enzymes in this process.

Chapter 2

The Determination of Dissolved Iron in Seawater using Flow Injection with Chemiluminescence Detection

2.1 Introduction

The very low, sub-nanomolar concentrations of iron in seawater and ubiquitous sources of contamination have hindered studies relating to the distribution and behaviour of iron in seawater and make shipboard analysis difficult. The presence of iron in research vessels, laboratories and manufactured items is a constant source of possible contamination and ultra-clean sampling and sample handling practices have to be adhered to. The desire to elucidate the role of iron, now well established as a growth limiting nutrient, has created a demand for reliable protocols and precise, accurate and rapid techniques capable of sub-nanomolar measurements, particularly whilst at sea.

Whilst highly precise analytical techniques exist for iron analyses, such as GFAAS and ICP-MS (Gordon et al., 1982; Wu and Boyle, 1998), they are relatively expensive, require time consuming sample preparation and unsuitable for use onboard research vessels. Furthermore, the storage of samples for laboratory based analyses increases the potential for changes in chemical speciation, therefore many speciation measurements can only be made in the field. Flow injection is a recognized analytical tool for various chemical analyses which can be coupled to a range of detection systems. The technique has some major advantages over other techniques including robustness, low cost instrumentation, ease of automation and portability. These benefits, coupled with the low risk of contamination, redox speciation capability, high sample throughput and excellent sensitivity make flow injection instrumentation ideal for the determination of iron particularly at sea (Achterberg et al., 2001). The technique is not, however, limited to the measurement of trace elements and many flow injection methods exist for determining other inorganic species that require high temporal and spatial resolution, e.g. H_2O_2 (Price et al., 1994; Yuan and Shiller, 2001; 2005), O_2^- (Asai et al., 1999).

In this study, flow injection coupled with chemiluminescence detection (FI-CL) was utilised in order to achieve the following aims:

1. To determine dissolved iron(II) and total dissolved iron(II + III) in seawater for both laboratory studies and shipboard analyses.

2. To assess and optimise the method by investigating potential interferences from a selection of metals, sodium sulphite, iron(III) and hydrogen peroxide.

3. To confirm the use of FI-CL to investigate the production of dissolved iron(II) in laboratory based experiments with phytoplankton cultures (presented in chapter five).

To achieve these aims two FI-CL methods were used, one involving sample pre-concentration and the other direct injection (without sample pre-concentration). An automated FI analyser highly selective to the detection of iron(II), with an 8-hydroxyquinoline (8-HQ) pre-concentration column, was used for the determination of sub-nanomolar concentrations of dissolved iron(II) in seawater. Following sample manipulation, this method can also incorporate the determination of dissolved iron(II + III) following reduction of iron(III) to iron(II). In order to confirm the specificity of the iron(II) method for use in studies involving the production of iron(II) by phytoplankton (presented in chapter five), a direct injection method was also employed. Both methods are described.

2.1.1 Background

Chemiluminescence (CL) is the emission of light (luminescence) as a result of a chemical reaction. FI-CL utilises a chemical reaction to quantitatively determine an analyte's concentration following its reaction with a chemiluminescent dye. The decay of the electronically excited state of the dye to a lower energy level is responsible for the emission of light, which is therefore relative to the quantum yield of photons after reacting with an analyte.
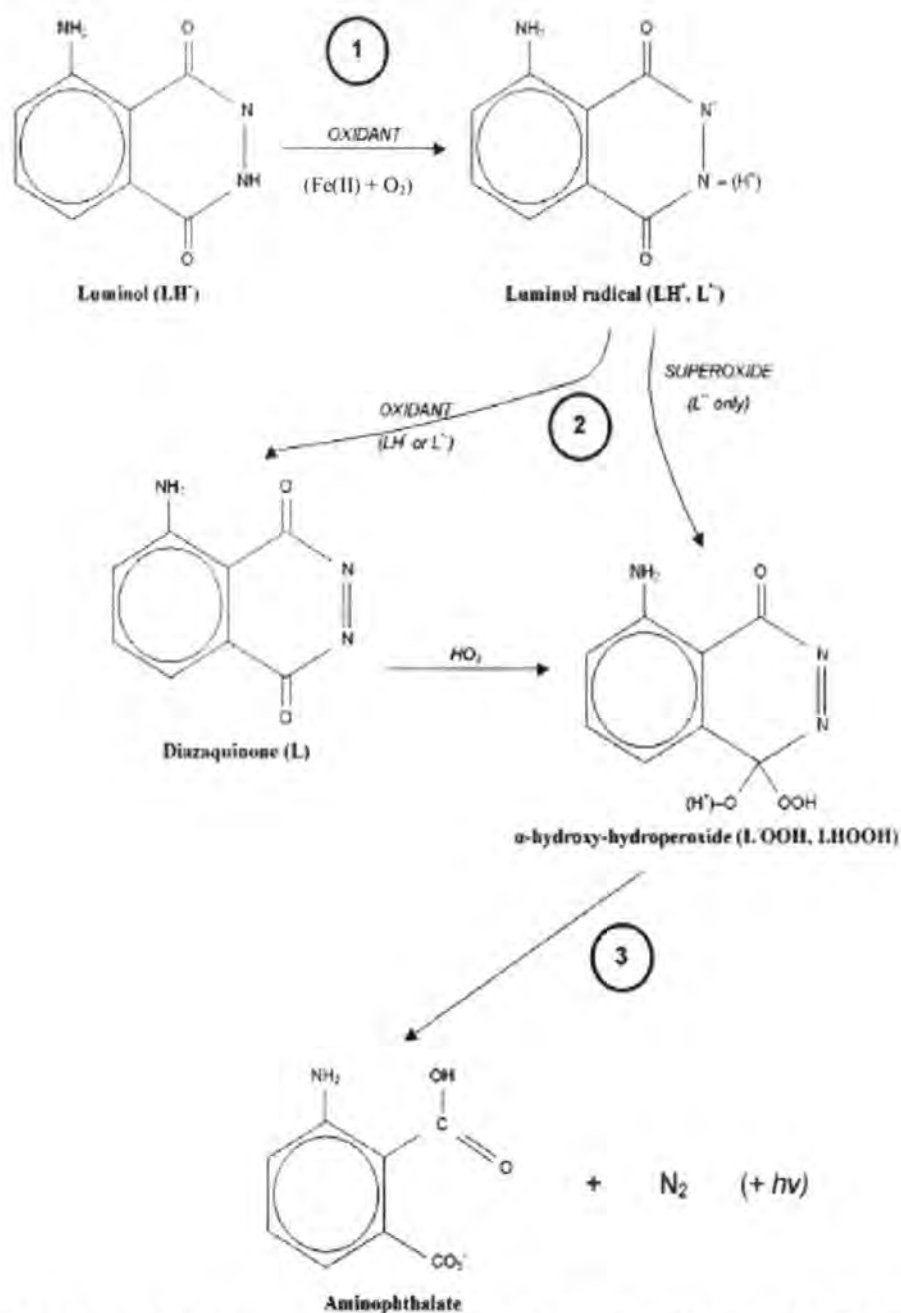
Figure 2.1 Oxidation of luminol indicating the three major steps (adapted from Rose and Waite, (2001)).

One of the most sensitive chemiluminescent dyes for the determination of dissolved iron in seawater is luminol (5-amino-2,3-dihydrphthalazine-1,4-dione) (Achterberg et al., 2001). Unlike methods developed for other trace metals, where the presence of an oxidising agent such H_2O_2 is necessary, the luminol - iron(II) reaction can produce strong CL in the

presence of O_2 only (Rose and Waite, 2001). The mechanisms proposed by Merenyi and co-workers (1990), in which the oxidation of luminol results in CL, is summarised in Figure 2.1. The primary oxidation of luminol to the luminol radical (denoted as (1) in Figure 2.1) in the Fe(II)-O_2 system likely occurs through OH$^{\bullet}$ or its radical derivatives which are produced in significant quantities during the oxidation of Fe(II) (King et al., 1995). The formation of the key intermediate α–hydroxy hydroperoxide (α-HHP) (Figure 2.1, reaction (2)) is propagated through the oxidants O_2 and O_2^- (formed from the initial oxidation of luminol). The final decomposition step (Figure 2.1 (3)) and generation of CL is dependent on the prototrophic state of α-HHP (pK of 8.2, Merenyi et al. 1990) and subsequently depends only on pH. The optimum reaction pH is 10.5 (O' Sullivan et al., 1995).

The luminol CL reaction provides an effective and highly sensitive method for iron(II) determination and has been used to determine dissolved iron(II) in seawater without pre-concentration (King et al., 1995; O' Sullivan et al., 1995). Following reduction of iron(III) to iron(II) using sodium sulphite, the method has been used to determine total dissolvable iron in unfiltered samples after sample pre-concentration onto an 8-HQ pre-concentration column (Bowie et al., 1998; Powell et al., 1995). Determination of low concentrations (pM) of dissolved iron(II), using 8-HQ pre-concentration resin, has also been reported (Bowie et al., 2002; Croot and Laan, 2002). Alternatively, altering the type of oxidant used in the luminol CL reaction can change the iron redox species determined. Obata et al. (1997; 1993) used H_2O_2 as an added oxidant to determine iron(III). In this instance iron(III) was selectively pre-concentrated at pH 3.0 onto an 8-HQ column prior to determination.

It is now common for FI systems to determine dissolved iron in seawater to use a pre-concentrating chelating resin. This resin both concentrates and separates the iron from the seawater matrix (e.g. the major sea salt ions), thereby removing potential interferences from other analytes present in the seawater. Without pre-concentration, sensitivity would be

insufficient to detect the low levels (pM) of iron in open ocean surface waters (Bruland and Rue, 2001). One of the most documented chelating resins for trace metal analysis is the immobilized 8-HQ (Landing et al., 1986), though the recent development of the commercially available nitrilotriacetic acid (NTA) chelating resin has also been demonstrated to be an effective resin for iron analyses (Lohan et al., 2005; Lohan and Bruland, 2006).

The recovery of iron onto a pre-concentration resin is dependent on pH and speciation. Figure 2.2 demonstrates the relationship between pH and the recovery of iron(II) and iron(III) for 8-HQ resin. Dissolved iron is strongly complexed, >99%, (Gledhill and van den Berg 1994; Rue and Bruland, 1995; van den Berg 1995) by organic ligands present in seawater. Complexation and the dissociation kinetics of the various forms of iron can regulate the recovered fraction during the samples contact time with the resin. Sample flow rate and geometry of the column are also factors that determine the amount of iron recovered. The pre-concentration process, therefore, is operationally defined as a measure of labile iron(III), recovered at pH 3 – 4.2, or labile iron(II) and iron(III), if recovered at pH 5.2 – 6.
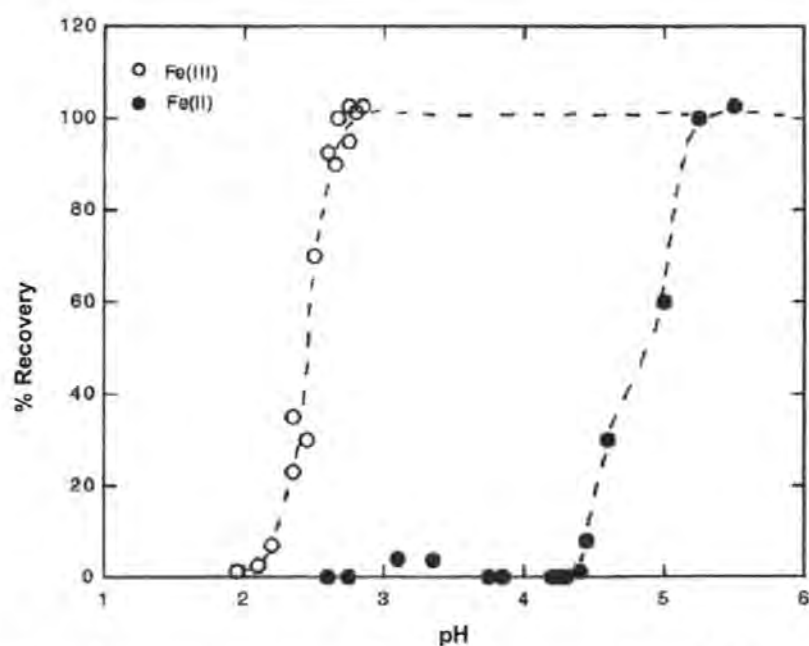
Figure 2.2 pH dependent recovery of iron for 8- hydroxyquinoline (8-HQ). (Adapted from Obata et al. (1993)).

Central to the FI manifold is the CL detector, the photomultiplier tube (PMT) where the photons produced during the chemical reaction are detected and transformed into a signal. A high voltage PMT was typical of early instrumentation, though low power (5V) miniature photon counting heads are now more common (de Jong et al. 1998). The concentration of iron is determined by measurement of the CL intensity, i.e. the rate of photons produced.

2.2 Experimental

A fully automated and portable FI-CL instrument for the determination of iron(II) and dissolved iron(II + III) (Bowie et al., 1998; 2002) is described. The system incorporated a low power (5 V) PMT, micro-columns containing 8-HQ immobilised on a vinyl co-polymer resin (Landing et al., 1986) for sample pre-concentration, and luminol chemistry, without added oxidant, for detection. Instrument control, data acquisition and off-line peak analysis was facilitated by using LabVIEW programs. The design and operation of the system is described. Optimisation and potential interference from a number of metals was investigated and the accuracy of the method assessed through the analyses of two recognized low iron reference materials (an IRONAGES and SAFe sample). The instrument was used to determine dissolved iron(II + III) in seawater samples in shipboard analyses and to investigate the production of dissolved iron(II) in laboratory based experiments with phytoplankton cultures.

A manually operated, portable flow injection instrument with chemiluminescence detection (King et al., 1995; Ussher et al., 2005) was used for the determination of dissolved iron(II). This system did not incorporate a pre-concentration step and the sample was

injection directly (direct injection (DI)) into the luminol stream. The principal aim of developing this system was to facilitate investigations into phytoplankton mechanisms for iron acquisition, a study which is presented in chapter five. It was necessary to examine potential interferences from parameters which would be used in that study, such as iron(III) and the reactive oxygen species hydrogen peroxide (H_2O_2), and what effect if any these would have on the CL signal. The investigations presented here required maintaining iron(II) in solution in order to observe and compare possible changes in the CL signal, this required modification of the manifold to enable the removal of oxygen from both sample and eluent in order to minimise oxidation of iron(II). The rapid oxidation of iron(II) at seawater pH ($\sim$ 8.2) determined the use of the direct injection method, the time taken for pre-concentration and analysis would have resulted in the loss of iron(II) in the seawater samples. The oxygen contained in the luminol reagent maintained the reaction chemistry.

During all experimental analyses, solutions and sample manipulation were either contained or carried out in either a class 100 clean room facility or in a class 100 laminar flow hood.

2.2.1 Operationally Defined Iron Fractions

The measurement of trace metal species in seawater samples is generally operationally defined by the sample pre-treatment process and the analytical method of analysis. The pore size of the filtration process, if used, defines the fraction of iron being measured and includes dissolvable, total dissolvable and total dissolved iron. Table 2.1 defines the fractions analysed in this study and previously reported in literature. Early analyses were carried out without filtration, these measurements were defined as dissolvable iron. The presence of abiotic particulate matter and living cells, and their lack of homogeneity in seawater, meant that iron concentrations increased over time, samples took longer to stabilise and results were more variable. However, it is the dissolved iron fraction that is of the most interest. This is the

fraction that is available to marine organisms and is void of living cells (Bruland and Rue, 2001). The dissolved fraction is usually defined as that which passes through either a 0.2 or 0.4 μm filter. This will still contain small colloids, therefore recent studies have included a further ultra-filtration step (<0.02 μm) to remove these colloids and this has been used to determine an operationally defined 'soluble' iron fraction in seawater (Liu and Millero, 1999; Wu et al., 2001).

Table 2.1 Operationally defined fractions for iron analyses.

Fraction	Filtration	Pre-treatment	Ref
Total dissolved iron (dFe)	<0.2 μm	Acidified (pH 2, HCl) 12 h acidification and 12 h sulphite reduction	This study
Dissolved iron(II) (Fe(II))	<0.2 μm	Analysed immediately after in-line filtration	This study
Total dissolvable iron	unfiltered	Acidified (pH 2, HCl) for 6 months. Sulphite reduction before analysis	(Bowie et al., 1998)
Dissolved iron	0.45 μm	Acidified (pH 1.7, HCl) for 6 months.	(Bruland et al., 2005)
Soluble iron	<0.02 μm	Acidified (pH 2, HCl) for 3 months. Sulphite reduction before analysis	(Sanudo-Wilhelmy et al., 1996)
Colloidal iron	0.02 – 0.2 μm	See note[a]	

[a] value obtained by subtracting dFe (<0.02 μm) from dFe

The filtration process is one factor which affects the iron fraction analysed. Sample acidification is another and different pHs have been suggested for stored samples; e.g. pH 3 (Obata et al., 1993) and pH 2 have been used (Bowie et al., 1998; Sarthou and Jeandel, 2001) and more recently a pH of 1.7 (Lohan et al., 2005). The variations in sample preparation (acidification pH and period of acidification) reported by different workers are due to investigations into the recovery of leachable iron present in colloidal material contained in the filtered fractions. It has been demonstrated that in acidified samples stored over time (>1

week) some of the dissolved iron present is reduced to iron(II) (Lohan et al., 2005; Ussher et al., 2005). Acidification and storage of acidified samples therefore favours methods which determine the iron(II) redox state, though the addition of a reducing agent also ensures reduction of iron(III) to iron(II). For methods which analyse the iron(III) redox state, the addition of H_2O_2 to samples is needed to oxidise the iron(II) to iron(III) prior to analysis. From recent studies it has been demonstrated that acidification of samples to a pH of < 1.8 is required to release all iron from colloids and iron binding ligands (Lohan et al. 2005; Johnson et al. 2007) and to achieve a stable sample within hours of collection. To be able to compare results and interpret differences, operational definitions (pore size of filtration, acidification pH and period) must be clearly stated.

In this study, total dissolved iron(II + III) (dFe) is defined as the fraction which passes through a 0.2 μm filter (Sartorius) and determined after sequential 12 h acidification (pH 2, HCl) and 12 h sulphite reduction. This acidification and reduction period was chosen to achieve the aims of this study and to carry out dFe analyses on board ship and this procedure was maintained throughout all dFe analyses performed in this study. Dissolved iron(II) (Fe(II)) measurements were made by immediate FI-CL analysis with in-line filtration (< 0.2 μm).

2.2.2 Cleaning Protocols

The very low, sub-nanomolar concentrations of iron in seawater and the numerous sources of contamination from dust and manufactured items mean that strict protocols relating to cleaning, solution preparation and sample manipulation are required. The following relates to the cleaning procedures followed for the preparation of plasticware and solutions used in all experiments.

Table 2.2 Protocols for washing of plasticware

Step	Procedure
In general laboratory	
1	Immerse in detergent bath (Decon 5%) for 1 week
2	Rinse 3 times with distilled water
3	Rinse 3 times with UHP water
4	Immerse in 30% HCl (VWR, Aristar grade) for 1 week
5	Rinse 3 times with UHP water
In clean air (class-100) laboratory	
6	Immerse in 20% HNO_3 (VWR, Aristar grade) for 1 week
7	Rinse 3 times with UHP water
For sample bottle storage	
8	Part fill with UHP water and acidify to pH 2 with quartz distilled HCl (Q-HCl)
9	Triple bag in clean (acid rinsed) plastic bags & store in clean plastic container

UHP = ultra high purity (Millipore, 18 MΩ cm^{-1})

Low density polyethylene (LDPE) containers (Nalgene) were used for all solution (standards, reagents, samples) preparations including sample collection and storage. Trace metal cleaning protocols were adhered to for the cleaning of all containers prior to use. Table 2.2 details the protocols followed.

Concentrated hydrochloric acid (VWR, Aristar grade) was distilled using a Teflon™ still in order to remove trace metal impurities. The clean solution was collected in a clean LDPE container, double bagged and stored in a class-100 laminar flow hood. The molarity of the acid after distillation was approximately 9 M.

Ammonia solution was prepared using isopiestic distillation. For this procedure, a trace metal clean 1 L LDPE bottle containing ultra high purity (UHP) water was placed inside a larger clean, sealable container (Figure 2.3). Aristar grade (VWR) ammonia was poured around the 1 L bottle and the large container sealed, this was left for three months. After this

time, clean ammonia (6 M) was contained in the 1L bottle.
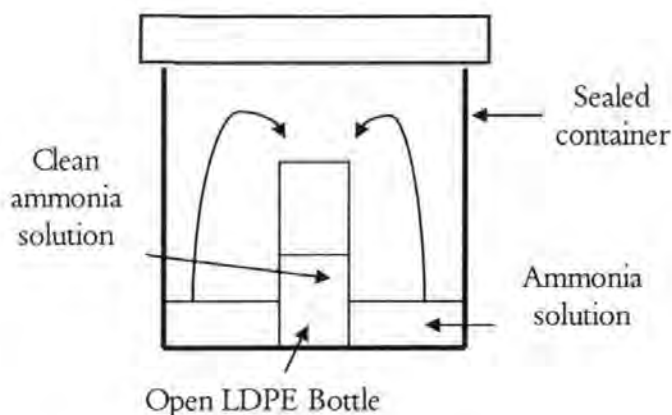
Figure 2.3 Isopiestic distillation of ammonia.

2.2.3 Reagents and Solutions

All chemicals were obtained from Sigma-Aldrich unless otherwise stated and prepared in UHP water (Millipore, 18 MΩ cm^{-1}). Stock solutions of 0.01 M luminol (5-amino-2,3-dihydro-1,4-phthalazinedione) in 0.1 M Na$_2$CO$_3$ were prepared and left for 24 hours to ensure dissolution. This stock was stable for three months. From the stock, a 1 x 10^{-5} M working solution mixed in 0.14 M Na$_2$CO$_3$ buffer was prepared the day prior to each experimental analysis. The pH was adjusted with 2 M NaOH to pH 11.8. This solution was passed through a Chelex-100 (iminodiacetic acid) chelating resin column prior to use to remove any iron or metal impurities.

Stock solutions of 0.02 M ammonium ferrous Fe(II) sulphate (AnalaR; VWR) were prepared by diluting 0.7843 g in acidified (0.1 M, Q-HCl) UHP water. The solutions were refrigerated and used for one week whereupon a new stock was prepared. 40 μM and 200 nM working solutions were prepared in 0.01 M Q-HCl by serial dilution. The working solutions were prepared immediately prior to analysis. The stock and lowest working solutions were

spiked with sodium sulphite to ensure that the iron in the standard remained in the reduced ferrous form.

For the analysis of dissolved Fe(II) and total dFe involving a pre-concentration step, samples were buffered in line using 0.4 M ammonium acetate. This was prepared from a 2.0 M stock (100 mL isopiestic distilled ammonia, 30 mL acetic acid (ROMIL, UpA) in 250 mL UHP water) and adjusted to pH 5.5 with acetic acid. A 0.05 M Q-HCl solution was used as an eluent. An iron(III) reducing agent, sodium sulphite (0.04 M, Na_2SO_3, (S(IV)) was prepared by dissolving 0.1008 g in 15 mL UHP water and 5 mL ammonium acetate buffer (0.4 M at pH 5.5). This solution was passed through two sequential 8-HQ columns prior to use and added to standards and samples (for dFe analyses) at 2.5 μL aliquots per mL of solution to achieve a final concentration of 100 μM. Low iron seawater (LISW) previously obtained from surface waters of the open ocean was used for all calibrations.

For the direct injection (DI) method, UHP water was used as the eluent. Additionally, coastal seawater was filtered, UV irradiated (UV-FSW) and passed through a series of sequential columns filled with resins (Amberlite XAD16, Duolite A7, Amberlite GT73, two Chelex resins and two C18 Sep-Pak columns) following a procedure described by Donat and Bruland (1988). This was to remove dissolved organic carbon and metals. When necessary, purified N_2 was used to remove oxygen from samples and eluent through acid clean PTFE lines fed directly into a laminar flow hood.

A number of solutions were prepared for interference studies. The metals aluminium (Al), cadmium (Cd), chromium (Cr), cobalt (Co), copper (Cu), manganese (Mn), nickel (Ni), silver (Ag) and zinc (Zn) were assessed. Working stock solutions of 5 μM and 100 μM were prepared for each metal by serial dilution of stock Spectrosol standards (1000 mg L^{-1}) in acidified (0.01 M, HCl) 100 mL UHP water. Additionally, a 0.005 M stock solution of ammonium iron(III) sulphate (AnalaR, VWR) was prepared by diluting 0.24109 g in 100 mL

UHP water. The solution was left for 2 h to ensure complete oxidation of iron and then acidified (0.1 M, Q-HCl). Working solutions of 1 and 10 μM in 0.01 M Q-HCL were prepared by serial dilution prior to use. 10 mM and 50 μM H_2O_2 solutions were prepared in UHP water by serial dilution from a stock solution of H_2O_2 (30 %, AnalaR, Fisher). These were prepared immediately prior to use. A solution of S(IV) (0.04 M) was prepared as described above.

2.2.4 Optimisation and Interference Procedures

The parameters of the two different FI methods used in this study for the determination of iron in seawater were previously optimized (Bowie et al., 1998; 2002; King et al., 1995; Ussher et al., 2005). These optimal parameters (detailed in Table 2.3) are the same, where applicable, for both FI methods (i.e. flow rate and reaction pH) and were applied for all analyses performed.

Both of the methods, the pre-concentration method (Bowie et al., 1998; 2002) and the direct injection (DI) method (King et al., 1995; Ussher et al., 2005), were used to determine the iron(II) redox state. Studies were carried out to assess potential interferences from a number of sources, including metals and H_2O_2, utilising both methods and instrumental set-up. The sample preparation for each interference assessment is detailed below.

Table 2.3 Optimal parameters for the determination of iron using FI-CL used in this study (Bowie et al., 1998; 2002; King et al., 1995; Ussher et al., 2005).

Parameter	Fe(II)	dFe
Flow rate	1.6 ml min^{-1}	
Reaction pH	10.5*	
Sample pre-concentration pH	5.5*	5.0*
Sample pre-concentration time	1.5 min	30 s
HCl eluent	0.05 M	

*After mixing with seawater sample and, for reaction pH, also with eluent.

Sample pre-treatment for all analyses

Either UHP water or low iron filtered seawater (0.2 μm) was used during optimisation and the interference studies, therefore filtration was unnecessary. For determination of the Fe(II) fraction, no pre-treatment of samples was required, these were analysed immediately without prior acidification or reduction treatment. Samples for dFe determination were acidified to pH 2 with Q-HCl and spiked with Na_2SO_3. A 12 hour acidification was followed by a 12 hour reduction period prior to analysis.

For the purposes of the investigative study carried out here, only Fe(II) was determined using the DI method. However, both Fe(II) and dFe fractions were determined using the analyser with pre-concentration column. To selectively determine the iron(II) redox state of the two fractions using the 8-HQ pre-concentration column incorporated within the analyser (Figure 2.4), the samples were buffered in-line to pH 5 (Figure 2.2). This process is described in more detail in Analytical Procedure below.

Sodium sulphite interference on iron(II) determination

The reducing agent sodium sulphite is used to reduce the Fe(III) to Fe(II) prior to analysis. A study was performed to ensure that sodium sulphite did not interfere with the Fe(II) chemiluminescence signal. This investigation was carried out in UHP water using the DI method. Increasing concentrations of sulphite were added to 30 mL samples of UHP water (concentrations are detailed in Table 2.4), to each of these a further addition of 20 nM Fe(II) standard was added and the sample immediately analysed. A control sample solely containing an addition of 20 nM Fe(II) standard was also prepared and analysed at the same time. The results from the sodium sulphite additions were compared to the control for evidence of interference on the signal.

Interference of metals on iron(II) determination using the pre-concentration method

Initial studies were carried out to assess the potential interference from a number of metals; Al, Cd, Cr, Co, Cu, Mn, Ni, Ag and Zn. Each metal was added to two samples of 60 mL LISW to achieve a final concentration of 5 nM. A concentration above that observed for these metals in the ocean environment was used, as this would provide indication as to whether there was interference with the CL signal. Additions of 60 μL were taken from working metal solutions of 5 μM to ensure the volume added was consistent for all samples. The samples were left to equilibrate for 24 h before being acidified in preparation for dFe analyses.

Immediately after acidification and prior to reduction, 1 nM of Fe(II) standard was added to one half of the samples. Controls of LISW were prepared with and without the 1 nM addition for comparison of results. For the metal Mn, additional samples were prepared and equilibrated for 72 h. After the reduction period samples were analysed for dFe using the pre-concentration method.

Interference of iron(III) and H$_2$O$_2$ on iron(II) determination

Additional studies were performed to investigate interference from Fe(III) and H$_2$O$_2$, two parameters which would be encountered in future research. This was performed using both the DI and pre-concentration methods.

For investigations using the DI method, 30 mL samples of UHP water were prepared. Following N$_2$ purging, Fe(III) and H$_2$O$_2$ were added to the samples to achieve a range of final concentrations, these are detailed in Table 2.4. To each of these 30 mL aliquots a further addition of 20 nM Fe(II) standard was made and the sample immediately analysed. A control

sample solely containing an addition of 20 nM Fe(II) standard was also prepared and analysed. The addition volume of all solutions is also detailed in Table 2.4. To maintain the volume of addition (50 μL) for the Fe(II) standard, Fe(III) and H_2O_2 (regardless of final concentration), the serial dilutions of the working stocks were adjusted. Additions of S(IV), however, were made in the range 50 to 200 μL. Controls of the Fe(II) standard were added at 100 μL.

Table 2.4. Parameters for the interference study performed using the DI method.

Sample	Concentration (nM)	Addition (μL)
Control Fe(II)	20	100
Fe(III)*	10 and 100	50
H_2O_2*	10 and 100	50
S(IV)*	67, 100, 130 and 267	50, 75, 100 and 200

*Plus 50 μL addition of Fe(II) standard to achieve final concentration of 20 nM

For the investigation using the pre-concentration method, aliquots (30 mL) of UV-FSW were manually buffered to pH 5.0 with ammonium acetate. Fe(III) standard or H_2O_2 were added to achieve a final concentration of either 10 or 100 nM (Fe(III)) or 10 or 50 nM (H_2O_2). The use of the pre-concentration method meant that a lower concentration of Fe(II) could be used, therefore either 1 nM Fe(II) standard or 2 nM Fe(II) (for the H_2O_2 study) was added to the solutions containing Fe(III) and H_2O_2. After the addition of Fe(II) the samples were immediately analysed. For each study a control was performed at the relevant concentration of Fe(II) standard, the timing of the experiment (t = 0) began from the addition of Fe(II).

2.2.5 Instrumentation

The two FI-CL methods, direct injection and sample pre-concentration, required different FI manifolds. The first method (and manifold) detailed is a fully automated, software driven technique with a pre-concentration column. The second method details a

manually operated direct injection technique (without pre-concentration).

Automated analyser with pre-concentration

A schematic diagram of the manifold detailing flow rates is illustrated in Figure 2.4. Three peristaltic pumps (Minipuls 3, Gilson) were used to transport solutions through the system. All manifold tubing was polytetrafluoroethylene (PTFE) (0.75 mm i.d., Fisher) with the exception of the peristaltic pump tubing which was flow rated silicone (Elkay, UK) and the acrylic polymer Perspex™ casings of the T-piece and 8-HQ columns. Pre-concentration, matrix elimination and sample buffer clean-up was performed using in-line micro-columns containing 8-HQ immobilised on a vinyl co-polymer resin (Figure 2.4, inset), synthesized according to Landing et al. (1986).

An electronic 3-way, two position direct lift solenoid switching valve, containing PTFE wetted parts and zero dead volume (model EW-01367-72, Cole-Parmer Instrument Co., Hanwell) was used to change between sample load and UHP water rinse of the column. Sample injections were performed using a 6-port Cheminert low pressure valve (model C22, Valco Instruments Co., Houston). Pumps and switches were operated at 5 V dc (TTL) and 12 V dc, respectively, supplied from the main control unit.

The detection system consisted of a T-piece, where reagent and sample were mixed, and positioned immediately prior to the flow cell. The flow cell was constructed from coiled transparent polyvinyl chloride (PVC) tubing (1.0 mm i.d., Altec, Hants) and mounted on the window of a side-on photon counting head (model H6240-01, Hamamatsu Photonics, Welwyn Garden City). This compact unit incorporated a low noise photomultiplier tube (PMT) and high voltage power supply. It was supplied with 5 V dc source from the main control unit. The photon counting circuitry produced a TTL output pulse train, modulated by the light intensity received at the PMT window. This pulse train was integrated in a resistor -

capacitor network to produce a low level voltage, which in turn was amplified and filtered resulting in a clean signal suitable for collection at the analogue-to-digital converter (National Instruments DAQCard-700).
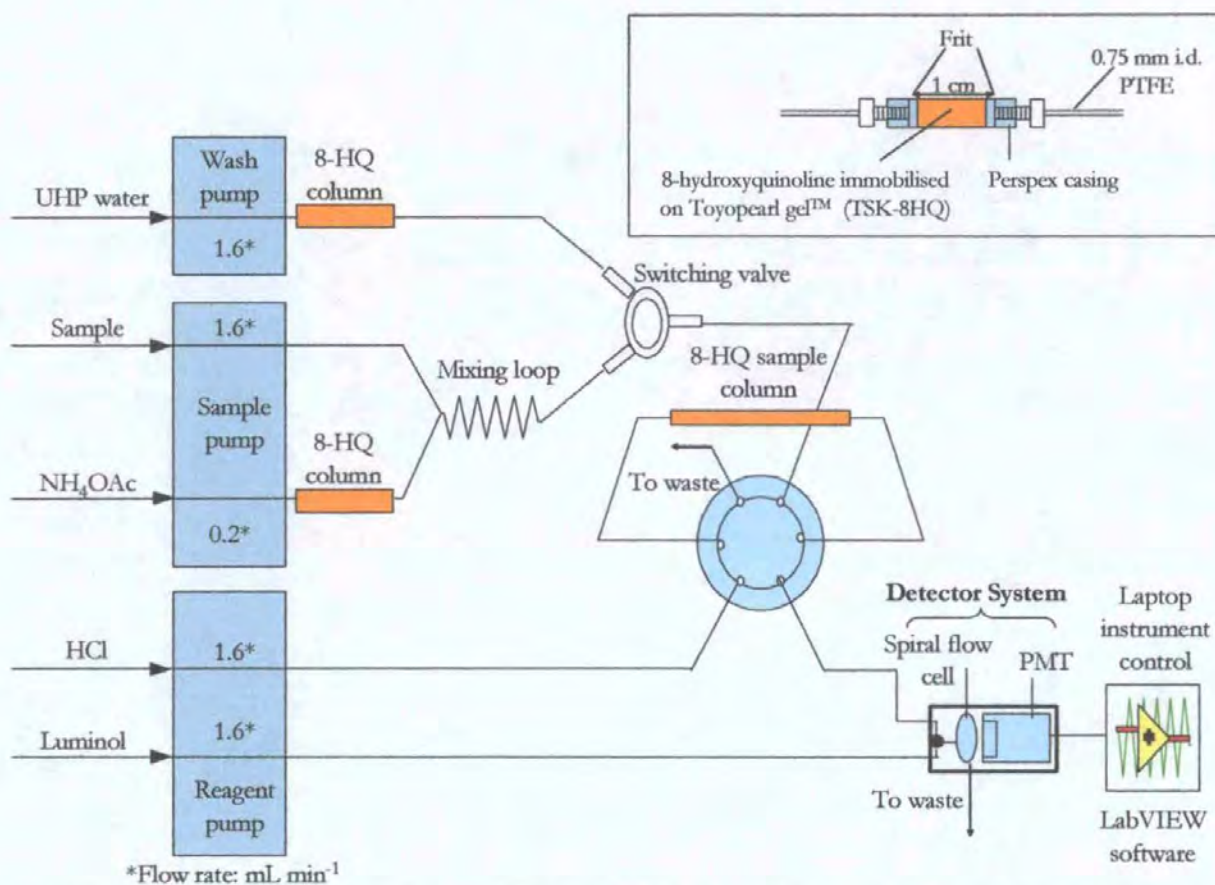
Figure 2.4 Schematic of FI-CL manifold for the automated determination of iron(II) with pre-concentration column (inset).

Instrument control was performed using two cards, a type II PCMCIA DAQCard-DIO-24 I/O card and a multifunction NI DAQCard-700 (National Instruments Corp., Newbury, Berks). Both cards were operated through a laptop computer using LabView version 5.1 (National Instruments Corp.) software with programs (VIs) produced by Ruthern Instruments Ltd. (Bodmin, Cornwall). The pumps, valve and detector, as shown in Figure 2.4, were coupled via a main control unit to the laptop where the LabView software provided automated analyses.

The FI manifold for direct injection analyses (Figure 2.5) consisted of one peristaltic pump (Minipuls 3, Gilson), used to transport all solutions through the system. The tubing, as with the automated system, was all PTFE (0.75 mm i.d., Fisher Scientific) with the exception of the peristaltic pump tubing (flow rated silicone, Elkay) and the Perspex™ casing of the T-piece.
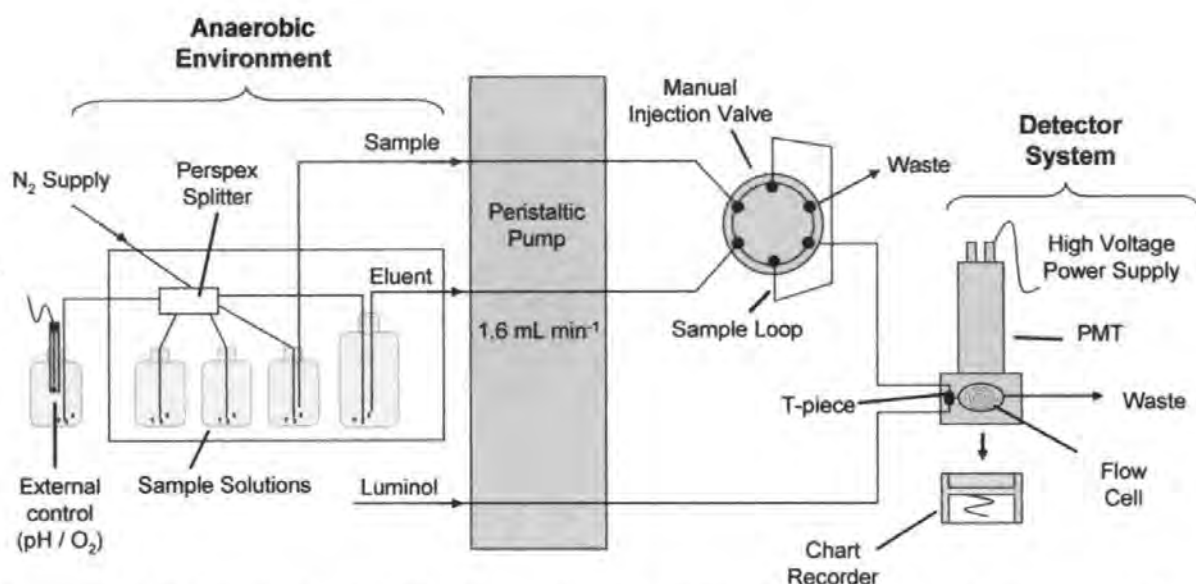
Figure 2.5 FI manifold for the direct injection (DI) of iron(II) under de-oxygenated conditions.

Manual injections were made using a 6-port 2-position rotary injection valve (Anachem, Figure 2.6) fitted with a 60 μL injection loop. This sample loop could be removed and replaced with an 8-HQ column if and when necessary. A continuous supply of N₂ gas was fed into a laminar flow hood through acid clean PTFE tubing and split (y-piece, Cole Parmer) into two lines, one line was fed directly to the eluent solution while the other was connected to a 12-channel Perspex™ splitter. Twelve individual acid clean PTFE lines

delivered N_2 to samples and a control solution. Samples and eluent were bagged and housed within a plastic container to provide an oxygen depleted environment. The control solution, bagged and contained outside of the clean area, monitored pH and oxygen concentrations.
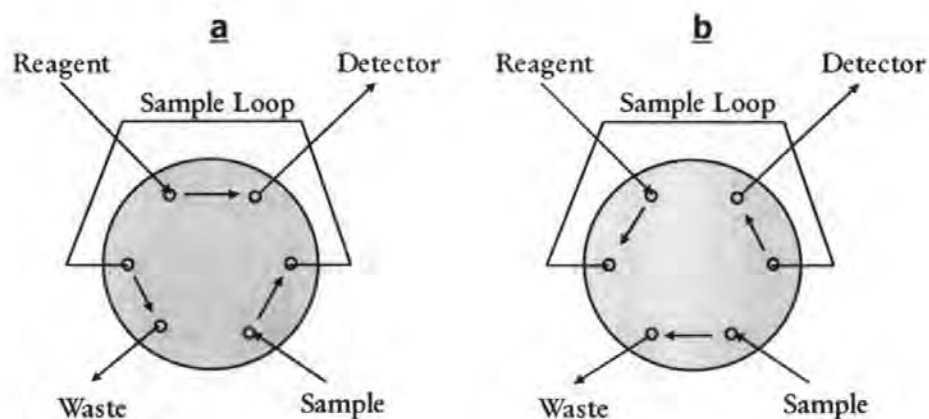
Figure 2.6 Manual injection valve showing (a) load and (b) elute positions.

The detection system consisted of a T-piece, where reagent and sample were mixed, and positioned immediately prior to the coiled quartz flow cell housed in an end-window photomultiplier tube (PMT, Thorn EMI 9789QA). High power voltage was supplied to the PMT using a 1.1 kV power supply (PM 28B, Thorn EMI).

2.2.6 Analytical Procedures

Automated analyses using the pre-concentration method

Prior to use of either instrument all tubing, fittings and connections of the FI manifold were cleaned with 0.5 M Q-HCl followed by rinsing with UHP water for at least 4 h. Before analyses, each system would be operational with reagents flowing through for at least 1 h to ensure baseline stability and to condition sample lines.

On initiation of an analytical cycle, the injection valve was placed in the load position

and the 3-way switching valve open in favour of the sample line (Figure 2.4). The sample was pumped through the FI manifold where it was buffered in-line to pH 5.5 following merging of the two solutions through a 0.57 m (250 μL) mixing coil. For Fe(II) analyses, the Fe(II) in the buffered unacidified sample was pre-concentrated and extracted from the seawater matrix for 1.5 min as it passed through the 8-HQ micro-column. For dFe analyses, the buffered acidified and reduced samples were pre-concentrated for a shorter time of 30 s. Following pre-concentration, the switching valve was changed to pump UHP water and the column rinsed for 30s to remove any residual matrix ions present (Figure 2.4). The 8-HQ reactive iron(II) was then eluted in the reverse direction with HCl (0.05 M) and combined with the continuous luminol stream at the flow cell housed in the detector system. The photons produced generated a signal in the form of a narrow peak. The injection valve was then returned to the load position and washed with UHP water to remove residual HCl prior to the next sample load sequence.

For the determination of Fe(II) an analytical cycle was completed in 3 min, each sample was analysed in triplicate and the mean of the three peaks heights taken as the 8-HQ reactive iron(II) concentration. For dFe analyses, an analytical cycle was completed in 2.5 min, quadruple measurements were performed for each sample and again the mean height of the four peaks used to calculate the iron concentration.

Manual analyses using the direct injection method

Specially prepared 30 mL LDPE bottles with two small holes drilled into the bottle lids were cleaned according to the stated protocols (Table 2.3). The holes were for use during the de-oxygenated experiments, one hole was for the delivery of N_2 gas, while the other was used for injections of solutions and for the sample line. Aliquots (30 mL) of either UHP water or UV-FSW were measured into the cleaned, specially prepared LDPE bottles.

In preparation for analyses, N_2 was first passed through the carrier (UHP water) solution for 6 h and the 30 mL samples, either UHP water or UV-FSW, for 30 min. Samples were spiked with an interference solution (sulphite/Fe(III)/H_2O_2) and / or iron(II) from the working standard solution. Timings commenced at the time of the iron(II) addition and the sample was immediately analysed. The sample solution was pumped to the sample loop of the injection valve which was manually loaded for ~10 s. The sample was eluted with UHP water and combined with the continuous luminol stream at the flow cell housed in the detector system. The photons produced by the CL reaction generated a signal in the form of a narrow peak, this was recorded on a chart recorder and the peak height used as an indication of Fe(II) concentration. The injection valve was then returned to the load position. One sample injection was completed in ~1 min. Samples were analysed over time and / or until no sample solution was left (up to ~15 min).

2.2.7 Calibration

For the pre-concentration method, calibration was performed using two different approaches, depending on whether the Fe(II) or dFe fractions were being determined. For calibration of the Fe(II) fraction, LISW was buffered to pH 5.5 with ammonium acetate stock (2 M). Whereas for calibration of the dFe fraction, the LISW was acidified to pH 2 using Q-HCl and then sodium sulphite added. This ensured that the matrix used for calibration received the same treatment as samples under analyses. Standard additions of iron(II) working stock were made to the treated LISW in the range 0.2 -1.0 nM, equating to 20 – 100 μL addition to 20 mL samples, and immediately analysed.

For the DI method, calibrations were performed to test the response of the system rather than to quantify samples. For all experiments, an Fe(II) control was used and responses were compared to this.

2.3 Results and Discussion

The methods for the determination of Fe(II) and dFe utilised throughout this study had been previously optimised and the reported parameters were used without further investigation or change (Table 2.3). However, a number of experiments were performed to check the validity of operational protocols (the use of the reducing agent sodium sulphite) and to examine potential interference from metals and the reactive oxygen species H_2O_2 on the Fe(II) chemiluminescence signal. The results from these investigations are presented here. Finally, the accuracy and precision of the pre-concentration method, the primary method used, was also assessed and the results discussed.

2.3.1 Optimisation and Interference Studies

Sodium sulphite interference on iron(II) determination

The interference of sodium sulphite on the Fe(II) chemiluminescence signal was investigated. The affect of increasing concentrations of sodium sulphite (67 to 267 μM) added to 20 nM Fe(II) is presented in Figure 2.7.
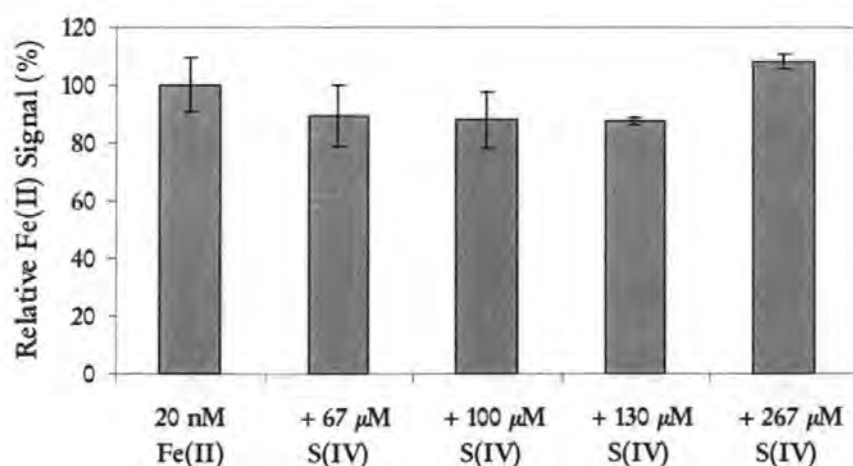
Figure 2.7 Comparison of chemiluminescence signal response to increasing concentrations of sodium sulphite added to 20 nM Fe(II) in UHP water. (Error bars represent ± 2 standard deviations of the results).

The results for the sodium sulphite additions are all within two standard deviations of the 20 nM Fe(II) control, which suggests no direct interference from the addition of sodium sulphite on the determination of Fe(II).

Interferences of metals on iron(II) determination using the pre-concentration method

An interference study involving a range of metals was carried out to assess the potential adverse effects these metals may have on the Fe(II) chemiluminescence signal. The results from this study are shown in Figure 2.8. Excluded from these graphs are the results for the Co addition which are dealt with separately.

The results from the metal additions (5 nM) combined with a 1 nM Fe(II) addition are illustrated in the upper graph (a) of Figure 2.8. All the metals added, with the exception of Mn, had no effect on the 1 nM Fe(II) CL signal. The addition of Mn however, equilibrated both for 24 h and 72 h, resulted in approximately 40 % reduction in the observed Fe(II) signal. From these results, Mn presents a negative interference on the Fe(II) signal at 5 nM. However, 5 nM is relatively high compared with concentrations observed above 1000 m in the North Pacific (0.2 - 0.8 nM, (Landing and Bruland, 1987)) and in the surface waters of the Atlantic Ocean (~ 2 nM, (Bergquist and Boyle, 2006; Statham et al., 1998)). Results from previous analyses to determine dFe carried out in the Atlantic, where the higher concentrations of Mn (~ 2 nM) have been observed, have been comparable with other workers using different analytical techniques for determining dFe (Bowie et al., 2006; 2007). This would suggest that in the surface waters of the Atlantic Mn does not appear to interfere with the Fe(II) CL signal.

The results of the analyses of the metal additions to LISW without added Fe(II) are shown in the lower graph (b) of Figure 2.8. The signal from the LISW control, is ~ 60 % lower than the CL signal produced by the 1 nM Fe(II) standard and would indicate that the

LISW used for this study contained a dFe concentration of ~ 0.3 nM. The CL signals produced from the metal additions, while variable, are all within ± two standard deviations of the LISW control signal. These results suggest that these metals do not interfere with the Fe(II) CL signal.
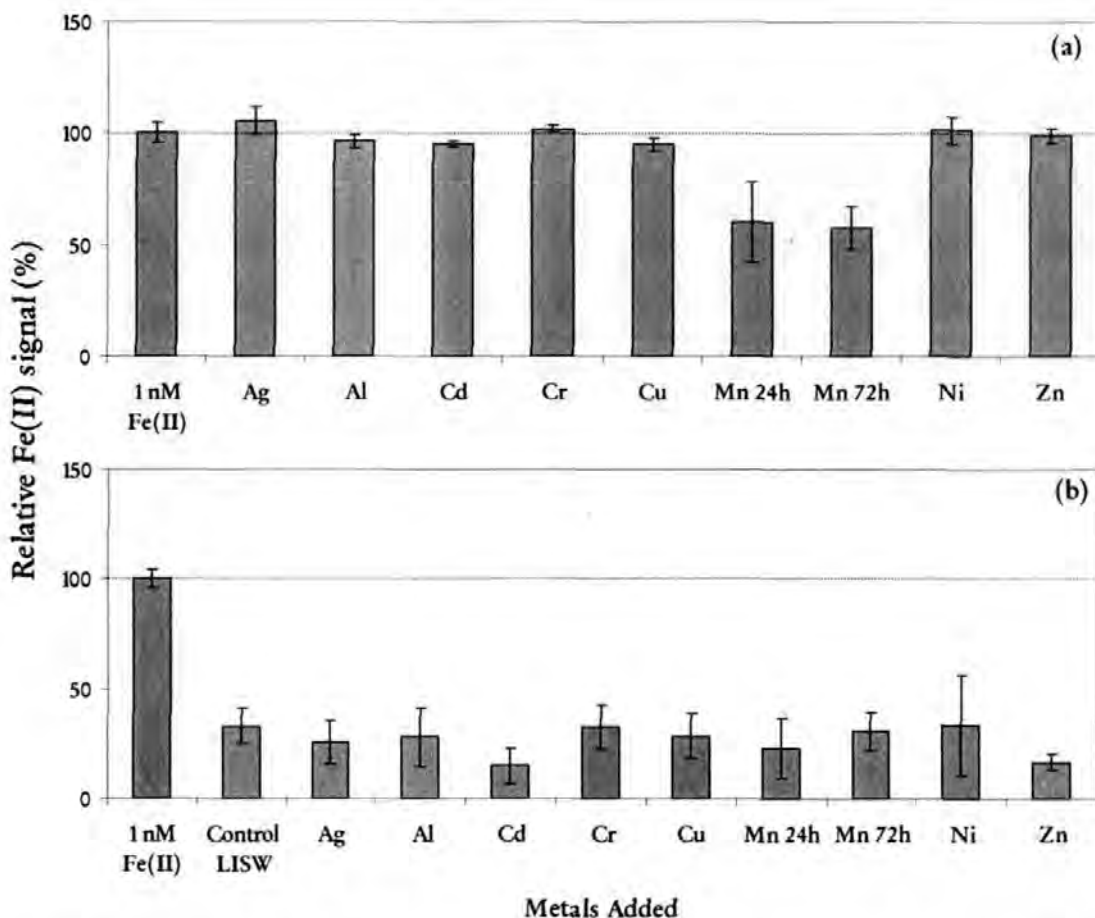
Figure 2.8 Results from additions of 5 nM of various metals in LISW. (a) plus 1 nM Fe(II), and (b) without addition of Fe(II). (Error bars ± 2 standard deviations of the results).

Cobalt was investigated separately as it was already known to positively interfere with the Fe(II) CL signal (Holland, 2001). The results from the Co addition of 5 nM to LISW, without addition of Fe(II), are shown in Figure 2.9. These results demonstrate a large positive interference (550 % increase) from the Co addition. The 5 nM addition of Co is one to two orders of magnitude higher than levels observed in the open ocean where concentrations in the range of 3 – 200 pM (Saito and Moffett, 2002) are more common.

A further experiment, performed using sub-nanomolar additions of Co to LISW at pH 8, demonstrated that at concentrations < 200 pM there was no interference from Co on the Fe(II) signal (Figure 2.10). However, during open ocean research cruises seawater conditions can change, different water masses can be encountered and concentrations of all seawater constituents can vary, e.g. in upwelling conditions concentrations of Co can increase to ~ 1 nM (Saito et al., 2004; 2006). To ensure the removal of any potential interference from cobalt, the cobalt signal was masked through the addition of a cobalt and nickel specific complexing agent, dimethylglyoxime (100 μM in methanol), to the luminol reagent (Bowie et al., 2002).
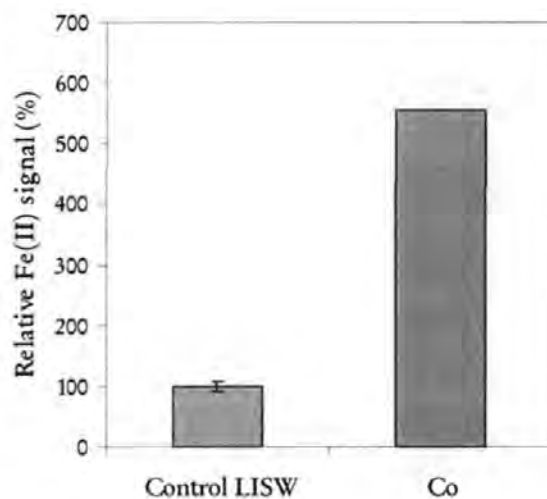
Figure 2.9 The response of a 5 nM addition of cobalt to LISW in comparison to a LISW control. (Error bars represent $\pm$ 2 standard deviations).
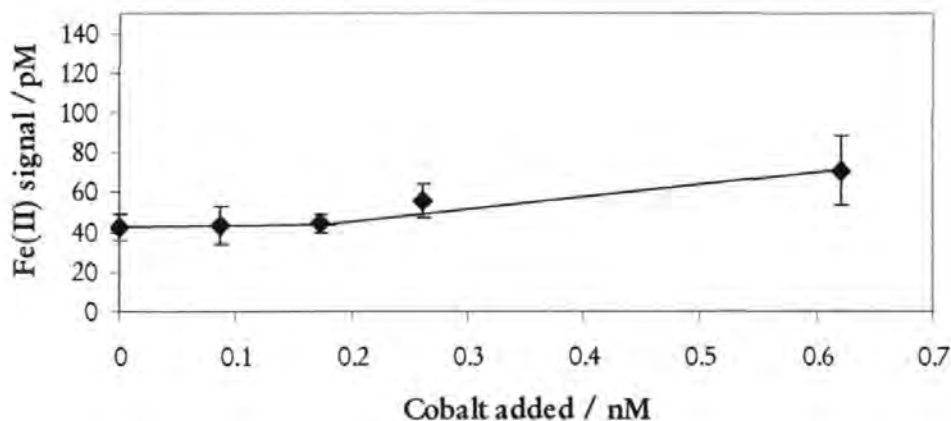
Figure 2.10 The response of increasing additions of cobalt on the Fe(II) signal. (Data provided by Dr Simon Ussher, error bars represent $\pm$ 1 standard deviation).

Initial experiments investigating the effect of Fe(III) and H_2O_2 on the determination of Fe(II) were carried out using the direct injection method. Figure 2.11 illustrates the results from tests carried out in (a) an aerobic and (b) a de-oxygenated environment.
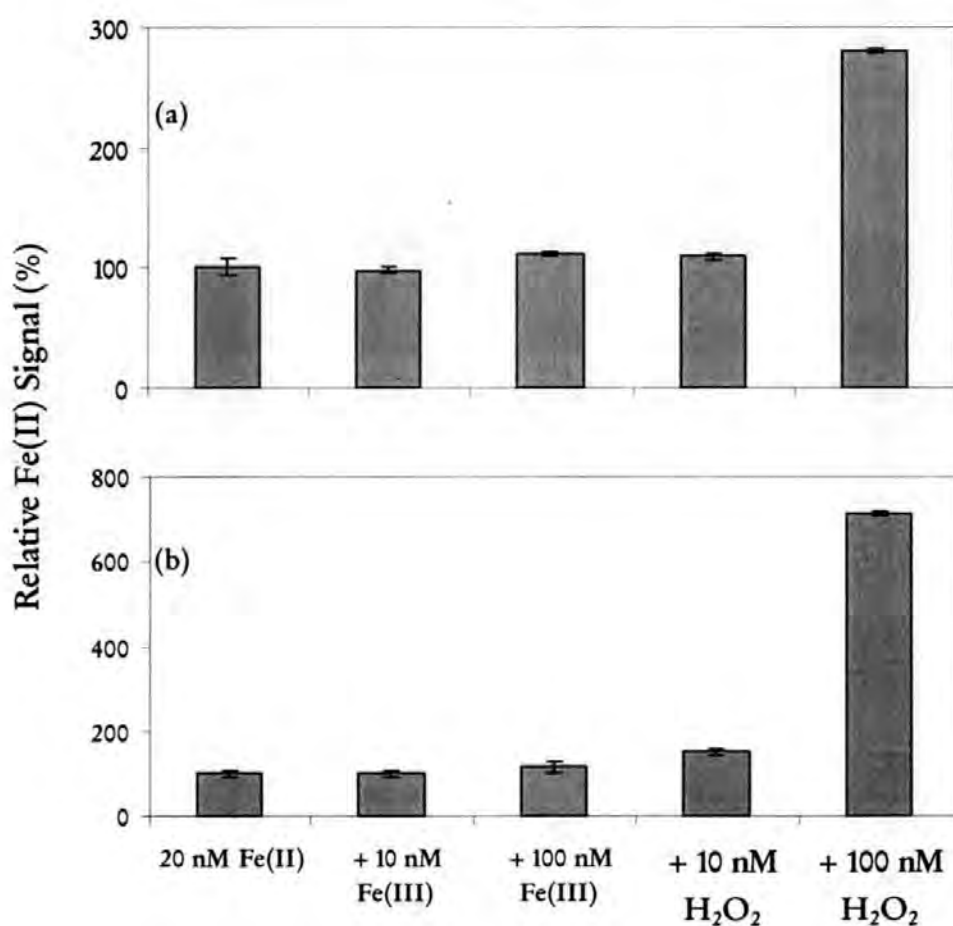
Figure 2.11 CL signal response to increasing additions of Fe(III) and H_2O_2 to 20 nM Fe(II) in UHP water. (a) Aerobic and (b) de-oxygenated conditions using the DI method. The response is compared to a 20 nM Fe(II) control. (Error bars represent ± 2 standard deviations of the results).

No significant effect was observed for the additions of Fe(III) at concentrations of 10 and 100 nM (t-test, $P > 0.05$) in either the aerobic environment or an environment with

oxygen removed. For the H_2O_2 additions, in aerobic conditions no observable increase in CL signal was observed for the addition of 10 nM H_2O_2, however, a 50 % increase was observed under de-oxygenated conditions for the same concentration. This difference in response to the presence of H_2O_2 in the sample was magnified with the 100 nM H_2O_2 addition, in aerobic conditions the CL signal increased by ~ 200 % compared to the control and the effect was further amplified (~ 600 %) under de-oxygenated conditions. These results demonstrate the need for removal of this reactive oxygen species from the sample matrix prior to determination of Fe(II).

Following on from these experiments, a similar interference study was undertaken to investigate the effect of Fe(III) and H_2O_2 on Fe(II) determination using the pre-concentration method. This was performed in an aerobic environment and the additions of Fe(III) and H_2O_2 were carried out using buffered (pH 5.7) UV-FSW, this enabled pre-concentration onto the 8-HQ micro-column and also minimised oxidation. The results from this study are shown in Figures 2.12 (Fe(III)) and 2.13 (H_2O_2). In contrast to the results of the Fe(III) additions performed using the DI method, where no effect on the CL signal was observed (Figure 2.11), when using the pre-concentration method a 70 % increase in the Fe(II) CL signal was observed following the addition of 10 nM Fe(III), illustrated in Figure 2.12. This signal response was further increased following the addition of 100 nM Fe(III) (~ 1500 %).

The recovery of iron onto the 8-HQ pre-concentration resin is not specific to Fe(II), at pH 5.2 – 6.0 both labile Fe(II) and labile Fe(III) are recovered (Figure 2.2). The cumulative effect of pre-concentrating both Fe redox species has resulted in this observed increase in the Fe(II) CL signal. Dissolved iron in the surface waters of the open ocean exists at much lower concentrations (< 1 nM) than used in this study. In a recent inter-comparison a concentration of 0.59 ± 0.21 nM was reported for dissolved iron in Atlantic surface water (Bowie et al., 2006). Dissolved iron is predominantly (> 99 %) bound to organic ligands (Gledhill and Vandenberg, 1994; Powell and Donat, 2001; Rue and Bruland, 1995; Wu and Luther, 1995).
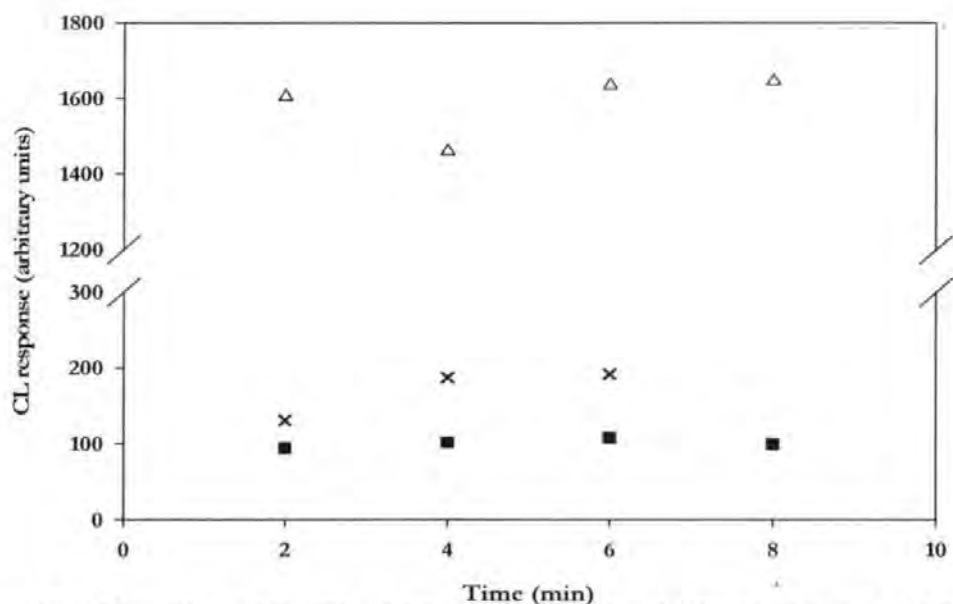
Figure 2.12 The effect of Fe(III) additions. (x) 10 nM and (Δ) 100 nM to 1 nM Fe(II) in UV-FSW compared to a (■) 1 nM Fe(II) control, performed in aerobic conditions using the pre-concentration method.
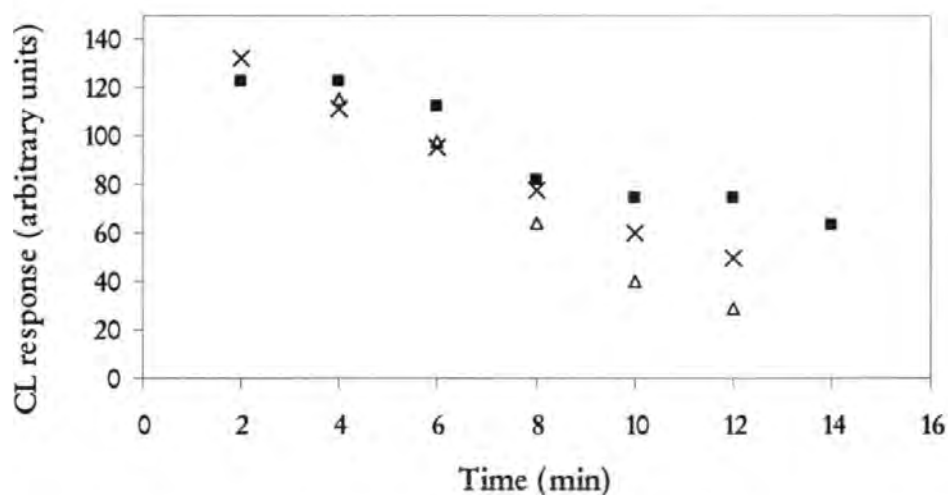
Figure 2.13 The effect of H_2O_2 additions. (x) 10 nM and (Δ) 50 nM to 2 nM Fe(II) in UV-FSW is compared to a (■) 2 nM Fe(II) control, performed in aerobic conditions using the pre-concentration method.

Therefore, if the maximum concentration of dFe is assumed at 0.80 nM (taken from the maximum error limit of the reported value for Atlantic waters) this would result in a labile Fe(III) concentration of 8 pM. The potential for interference from labile Fe(III) is therefore minimal and below the detection limit for dFe analyses.

With regards to H_2O_2, no observable enhancement of the Fe(II) CL signal was observed for the additions of 10 and 50 nM H_2O_2 (Figure 2.13) when compared to the 2 nM Fe(II) control. The presence of the 8-HQ pre-concentration column, and the subsequent removal of H_2O_2 from the sample matrix, has removed the interference on the Fe(II) CL signal from this reactive species. However, the one noticeable effect from both H_2O_2 additions was the reduction in the Fe(II) signal over time when compared to the control, even though the UV-FSW was buffered. This reduction was most likely due to enhanced oxidation of the Fe(II) in the sample by the H_2O_2.

In order to estimate an oxidation rate for Fe(II), in the presence of H_2O_2, it was necessary to estimate the concentration of Fe(II) in the samples. These had been analysed at 7 time points over ~ 14 min. To achieve this, the observed CL response for the 2 nM Fe(II) control observed after ~ 2 min (Figure 2.13) was assumed to equal 100 % and all subsequent measurements, both of the Fe(II) control and the samples with added H_2O_2, were based on a percentage of this signal. This method of calculation provided an estimate of the Fe(II) concentration in all the samples analysed at the seven time points during the short study period (~ 14 min). Based on these calculations, the oxidation rate data Fe(II) at pH 5.7 are shown in Figure 2.14. For first-order kinetics with respect to Fe(II), a linear plot should be obtained when plotting the natural logarithm of the Fe(II) concentrations against time. The pseudo first-order oxidation rates for the three samples together with the corresponding Fe(II) half life are presented in Table 2.5.
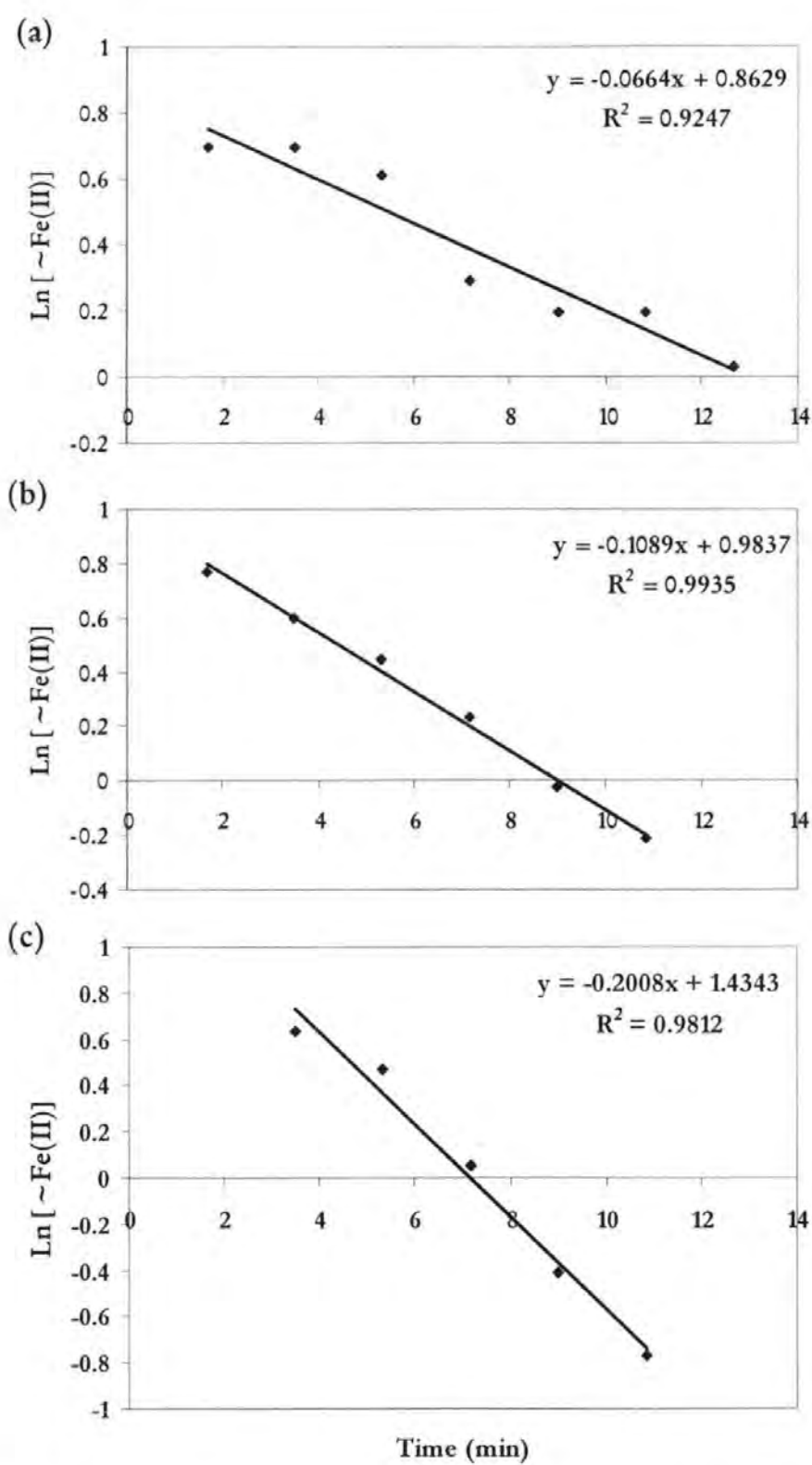
Figure 2.14 Estimated oxidation rate data of 2 nM Fe(II). (a) Without added oxidant, (b) with 10 nM H_2O_2 and (c) 50 nM H_2O in buffered (pH 5.7) UV-FSW.

The half-life of Fe(II) was calculated from the equation:

$$t_{1/2} = \frac{Ln\ (2)}{\lambda}$$

Where Ln(2) in the natural logarithm of 2 and the rate constant is taken from the linear plots (Figure 2.14). H_2O_2 is a known strong oxidant, therefore the Fe(II) half life is decreased in the presence of 10 nM H_2O_2, from 10.4 to 6.4 min. This is further decreased to 3.5 min when the H_2O_2 concentration is increased to 50 nM. This data demonstrates that H_2O_2 increases the oxidation of Fe(II). In addition, the results also show that, even at a pH of 5.7, the half life of Fe(II) is still in the order of minutes. The determination of this transient species must therefore be rapid to minimise loss through oxidation. During this study, samples were analysed immediately and with a short (~1 min) pre-concentration time.

Table 2.5. Data for the rate constant and half life of Fe(II). Performed without and in the presence of H_2O_2

Sample	Rate constant (min^{-1})	Fe(II) half life (min)
Fe(II)	0.0664	10.4
Plus 10 nM H_2O_2	0.1089	6.4
Plus 50 nM H_2O_2	0.2008	3.5

2.3.2 Analytical Figures of Merit and Blank Measurements

Blank measurements were not performed for the DI method as this was solely used for interference investigations on the CL signal and all measurements were compared to a control sample. The automated analyser with pre-concentration was used for sample analysis in both the field and laboratory experiments and regular blank measurements were performed. The figures of merit (summarised in Table 2.6) and blank measurements detailed here refer solely to the pre-concentration method and are based on data acquired during the Meteor 60 research cruise (M60/5) on-board the German research vessel FS Meteor (9th March and 15th
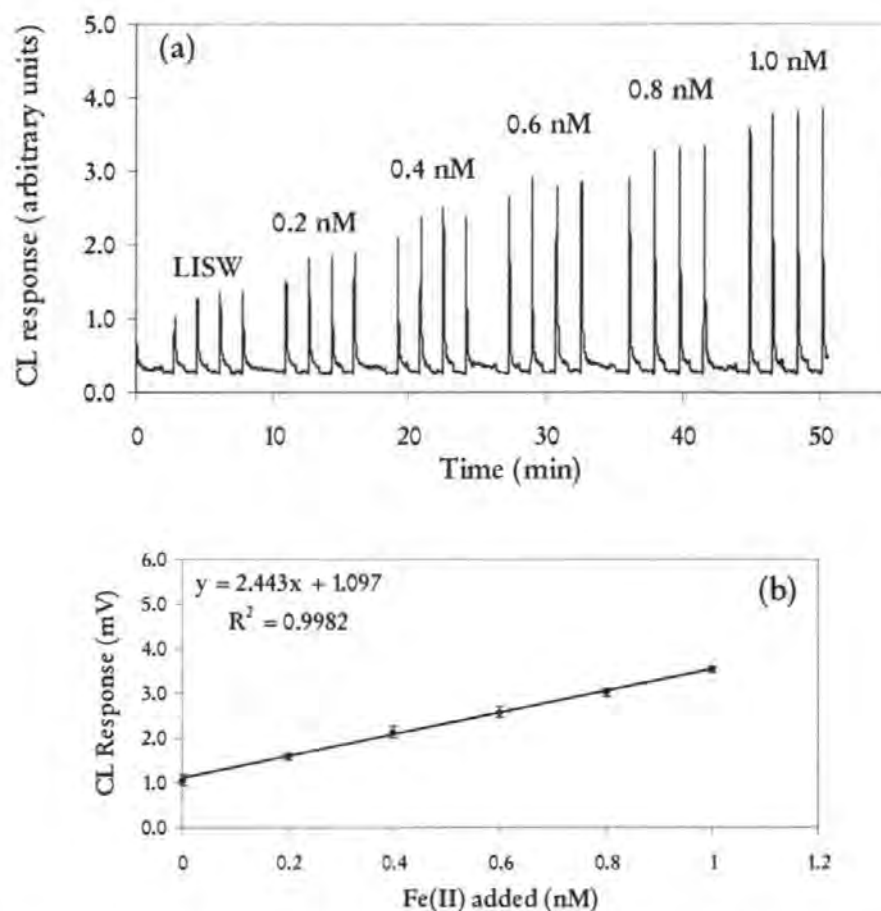
Figure 2.15 Shipboard calibration of Fe(II). (a) Peaks generated by LabView software and (b) corresponding standard addition graph plotted using peak height over the range 0.2 – 1.0 nM (error bars represent ± 2 standard deviations).

The mean blank signal produced was 56 ± 24 pM, (n = 59) resulting in a limit of detection of 17 ± 9 pM (defined as three times the standard deviation on replicate analyses of the blank (n = 4)). Blank determinations were the result of three components; the reagent blank, and additionally for dFe, an acid blank and sulphite blank (from the acid and sulphite used in sample pre-treatment). The reagent blank (typically ~50 pM), was obtained from an analytical cycle (performed >3 times) where only the ammonium acetate buffer solution and UHP water rinse (without sample) were loaded onto the 8-HQ column. These were then eluted into the luminol reagent stream. The signal produced from this procedure includes any signal associated with the reagents (luminol, ammonium acetate buffer, UHP water wash and acid eluent) and the manifold. This procedure, achieved by disconnecting the sample line, was

performed prior to each batch of sample analyses.

The sulphite and acid blanks were determined by separate standard addition analyses. Aliquots of UHP were spiked with either HCl or sulphite to achieve final concentrations of 0.005 and 0.015 M HCl and 100 and 300 μM S(IV) respectively. Standard additions of Fe(II) standard (0 – 0.5 nM) were made to the aliquots. The HCl blanks was quantified as the difference between the x-intercept of the linear plots, the sulphite blank was measured as half of the difference between the x-intercepts. The combined HCL and sulphite blanks were typically <20 pM.

Table 2.6. Analytical figures of merit for dissolved iron determination

Parameter		Figures of Merit
Blank		56 ± 24 pM $(n=59)$
Detection Limit		17 ± 9 pM $(n = 59)$
Precision, RSD (%)*	Range	0.96 – 21.2
	Mean	8.0 ± 3.0 $(n = 17)$
Sensitivity (calibration slope)	Range	1.23 – 3.80 mV nM^{-1}
	Mean	2.33 ± 0.67 $(n = 17)$
Linear Range		0.1 - 10 nM
Sample Throughput		~7 h^{-1}

* The precision is calculated as the percent relative standard deviation (%RSD) and based on repeatability between replicate measurements of standard additions (0-100 nM).

Contributions to the blank signal were minimised though the use of clean acids (distilled HCl, trace metal grade acetic acid) and bases (isopiestic distilled ammonia), and through the use of clean protocols. Similarly, the passing of the luminol reagent through a Chelex column prior to use reduced background CL signal. Additional 8-HQ columns placed in the UHP water rinse and buffer solution lines of the manifold (Figure 2.4), also contributed to reducing impurity additions from these solutions, lowering both the blank and limit of detection.

2.3.3 Accuracy and Precision

There is no appropriate certified reference material for sub-nanomolar concentrations of iron. The dissolved iron in the National Research Council of Canada NASS-5 solution contains 3.71 ± 0.63 nM Fe, a concentration that is at least tenfold greater than most open ocean concentrations. The accuracy of the method was therefore tested by determining dFe in seawater samples collected as part of two separate analytical intercomparison exercises and was performed using the automated analyser with pre-concentration column.

A bulk volume of seawater was collected from the Atlantic in a SCOR-IUPAC sponsored exercise led by the University of Plymouth. From a dataset of 45 results, compiled from thirty-one laboratories in eleven different countries, the mean dFe in this bulk seawater sample (IRONAGES) was reported as 0.59 ± 0.21 nM (Bowie et al., 2006). During a second intercomparison exercise, Sampling and Analysis of Fe (SAFe) sponsored by U.S. NSF, two bulk samples of North Pacific seawater were collected; one from the surface (approximately 10 m) and one from depth (1000 m). Thirty-two scientists from eight countries participated (including the author representing the University of Plymouth) and consigned dFe concentrations in the surface and deep water samples of 0.097 ± 0.043 nM (S1) and 0.91 ± 0.17 nM (D2) respectively (Johnson et al. 2007).

Analysis of an IRONAGES sample, performed by the author at sea, gave a mean dFe concentration of 0.72 ± 0.06 nM ($n = 5$). Further analyses performed by the author in the laboratory of an IRONAGES sample from a different bottle determined a value of 0.58 ± 0.06 nM ($n = 2$). Both of these determined values are within the range (0.59 ± 0.21 nM) reported by Bowie et al. (2006), and are comparable to a previous comparison exercise using the IRONAGES samples where dFe concentrations of 0.76 ± 0.18 nM and 0.75 ± 0.29 nM were reported (Bowie et al., 2004). The values reported for this study are also consistent with

data presented in a 3-laboratory blind intercomparison using two different analytical techniques (FI-CL and isotope dilution ICP-MS) where a mean dFe concentration of 0.535 ± 0.028 nM (n = 15) was reported for the five IRONAGES samples analysed (Bowie et al., 2007).
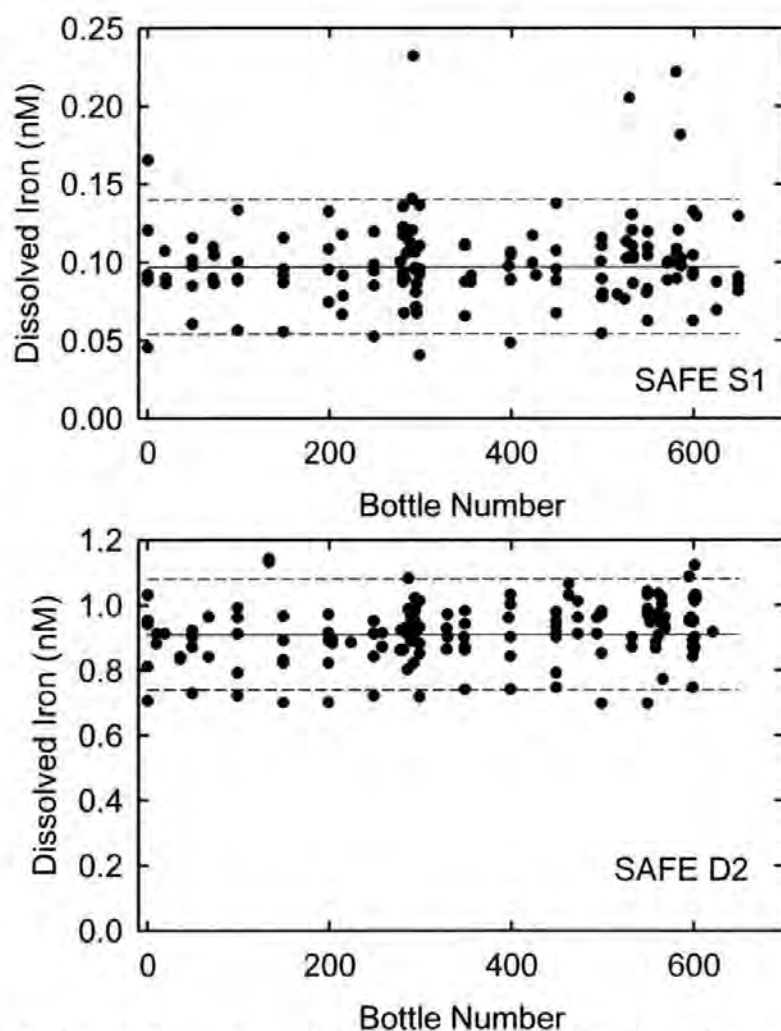
Figure 2.16 Results from the analysis of SAFe samples. Surface (S1) and deepwater (D2) seawater samples from 32 scientists who took part in the SAFe inter-comparison (Johnson et al. 2007).

The analysis of the SAFe samples by the author, involving replicate (n = 4) analysis of samples from the surface (S1) and deep (D2) seawater, resulted in mean values of 0.22 ± 0.02 nM (S1, n = 3) and 0.94 ± 0.11 nM (D2, n = 4). The result for D2 is within the range (0.91 ± 0.17 nM) of the consensus value assigned for the dFe concentration of this sample. The determined concentration for S1, however, is higher than the assigned consensus value (0.097

± 0.043 nM). The compiled results from the overall analyses of all the surface (S1) and deepwater (D2) samples for SAFe intercomparison are illustrated in Figure 2.16 and include the results of the author (Johnson et al. 2007). The community results for the S1 surface sample show a wide spread in dFe concentrations from <0.05 nM to ~0.24 nM, the results from this study fall in the higher range.

The method has demonstrated good agreement for the Atlantic IRONAGES sample and for the deep Pacific SAFe sample. Furthermore, comparable dFe results have been observed between samples analysed using the pre-concentration method described here and an isotope dilution ICP-MS (Petrov et al. 2007). However, at the low concentrations observed in the surface waters of the Pacific, differences in method and operationally defined fractions appear to exist. This is an area which requires further investigation by the iron community.

2.4 Conclusions

The analytical figures of merit (Table 2.6) for the FI-CL pre-concentration method demonstrate that this is an adequate and sensitive technique for determining iron. The low detection limits (~ 17 pM) ensure that this method can be employed for the investigations carried out during this Ph.D, including the detection of the low sub-nanomolar concentrations of iron encountered in the open ocean seawater environment and also employed in the investigation of the potential generation of low levels of Fe(II) by phytoplankton.

Overall, the results presented here, from the analyses of the IRONAGES and SAFe samples and from intercomparison studies, provide the confidence in using this analytical technique for the studies carried out during this Ph.D.

Chapter 3

A Dissolution Study of Iron and Aluminium from Six

Dusts in North Atlantic Ocean Seawater

3.1 Introduction

Atmospheric transport of aeolian dust forms an important source of nutrients, such as nitrogen and phosphorus, and trace metals, including the micro-nutrient iron, to the marine environment (Duce and Tindale, 1991; Jickells et al., 2005). While regional processes such as upwelling can be highly significant, atmospheric transport is considered the principle external source of soluble iron to the surface waters of remote oceans (Jickells and Spokes, 2001). This transport pathway may play a significant role in enhancing primary production (Mills et al., 2004) or influencing phytoplankton community structure (Marchetti et al., 2006).

The solubility of iron from aerosols in seawater is a subject of debate and uncertainty and is a key area in our understanding of the cycling of this nutrient in ocean systems. Using different experimental protocols and analytical techniques, previous studies report a wide range of aerosol iron solubility from 0.001 – 87 % (Bonnet and Guieu, 2004; Hand et al., 2004; Jickells and Spokes, 2001; Zhuang et al., 1990). The use of sieved soils generally resulted in lower solubilities (Bonnet and Guieu, 2004) than those reported for atmospheric aerosols (Baker et al., 2006b; Zhuang et al., 1990). It has been reported that chemical and/or photochemical reactions during atmospheric transport are responsible for the higher solubility observed for atmospheric aerosols (Spokes and Jickells, 1996), although field and modelling studies have not shown that transport processes had any significant effect on iron solubility (Baker et al., 2006a; Baker et al., 2006b; Hand et al., 2004; Luo et al., 2005).

The use of crustal Al / Fe ratios in combination with known dissolved aluminium concentrations has allowed estimates of aeolian deposition of iron to surface waters to be

estimated (Measures and Brown, 1996; Measures and Vink, 1999; Measures and Vink, 2000). Through the known concentrations of dissolved aluminium in the surface layer of the oceans, Measures and Brown (1996) suggested that these could be used to indirectly estimate dust deposition fluxes. From this, the amount of iron (based on the crustal ratio) could also be estimated. In principal, aluminium is an ideal tracer of mineral dust inputs to the surface oceans as it exists in continental materials at a relatively constant concentration of around 8 % (Wedepohl, 1995). It has no complicating redox chemistry and is removed from surface waters with little biological recycling (Hydes and Liss, 1977). In regions with low atmospheric inputs, the concentration of aluminium in surface seawaters is low (< 1 nM). The relatively short (3 - 6.5 years) residence time of aluminium in the surface ocean contributes to the low concentrations observed (Jickells et al., 1994; Orians and Bruland, 1986).

Aeolian inputs to the oceans are highly spatially and temporally variable and the location of land and desert regions are important factors in dust distribution. The North Atlantic is a region with high dust input, receiving a third of the global aeolian input from the Sahara desert (Duce and Tindale, 1991; Jickells and Spokes, 2001). This atmospheric transport of Saharan dust is a major source of dissolved iron to the tropical North Atlantic (Gao et al. 2001), however, even in this region of high dust input, iron has been known to limit primary production and co-limit N_2 fixation (Mills et al., 2004; Moore et al., 2006).

In order to gain further understanding of iron solubility in North Atlantic seawater, and to investigate whether using aluminium/iron ratios are a good proxy for estimating dust deposition events, a dissolution study was carried out using six dusts from diverse regions and with differing compositions. The dissolution was performed using particle concentrations down to 0.1 mg L^{-1} and a contact time of 24 h and 8 days, representative of the contact time between atmospheric particles and seawater. While the particle concentrations used were

relatively high in comparison to those encountered in the natural environment, these could be accurately weighed and transferred during the experiment. This study was undertaken with the following objectives:

1. Determine the release from dusts of dissolved iron(II + III) (dFe) and dissolved aluminium (dAl) into seawater.

2. Establish the solubility of iron and aluminium in North Atlantic seawater.

3. Assess the use of iron / aluminium ratios as a proxy for iron (in dust) deposition to oceans.

3.2 Experimental

The experimental approach of this study was to expose six different dusts, consisting of 5 sieved soils (4 African, 1 Asian) and 1 aerosol dust (collected in Turkey), to filtered North Atlantic seawater in shipboard incubation experiments. The natural aerosol dust collected in Turkey had therefore undergone atmospheric processing (wet and dry cloud cycling) and is referred to as the Turkish atmospherically processed dust to distinguish it from the sieved soils. The dusts were provided by four different institutions (Table 3.1) and different exposure conditions (Table 3.1) were used in order to assess the solubility of iron in a homogeneous batch of surface North Atlantic seawater.

Measurements of the dissolved iron(II + III) (dFe) fraction (< 0.2 μm filtered) were made at sea whilst on board ship. For the analyses of aluminium, stored filtered sub-samples from the shipboard experiments were transported back to a land based laboratory and

analysed for dissolved aluminium (dAl) concentrations.

To investigate the solubility of iron in seawater, a sensitive analytical technique capable of sub-nanomolar detection limits was required. Flow injection using luminol chemiluminescence is among the most sensitive ship-board FI-CL methods, capable of determining picomolar concentrations of dissolved iron in seawater (Achterberg et al., 2001). During this study, the measurement of dFe concentrations in the seawater samples was carried out using a fully automated and portable flow injection instrument with chemiluminescence detection (FI-CL).

Table 3.1 Source of dust and experimental parameters for the dust dissolution study.

Dust Source	Provider of Dust		
Turkish Atmospherically Processed Dust	University of Plymouth		
Gobi	University of East Anglia		
Moroccan	University of East Anglia		
Namibia	Royal Netherlands Institute for Sea Research		
Mauritanian	Royal Netherlands Institute for Sea Research		
South Algerian	University of Brest		
Experimental parameters			
Particle concentration (mg L^{-1})	0.1	2	10
Exposure time	24 h		8 days

A fluorimetric method using the complex of aluminium and lumogallion has been widely used for the determination of dissolved aluminium in seawater (Hydes, 1983; Measures, 1995). For the aluminium measurements performed during this study, a modified version of this method (Ren et al., 2001) was used.

All work for the analyses of both metals was conducted using trace metal clean techniques. For the shipboard experiments all sample handling, manipulation and analytical work was carried out in clean container with a class-100 laminar flow hood, for the land based aluminium analyses all sample handling and manipulation was carried out in a class-100 laminar flow hood.

3.2.1 Reagents and Solutions

All chemicals were obtained from Sigma-Aldrich unless otherwise stated and prepared in ultra high purity (UHP) water (Millipore, 18 MΩ cm^{-1}). For shipboard dFe analyses, reagent solutions were prepared as detailed in chapter two. These include the chemiluminescent reagent luminol (1 x 10^{-5} M, pH 11.8), ammonium acetate (0.4 M) for the in-line buffering of samples and 0.05 M Q-HCl as the eluent. An iron(III) reducing agent, sodium sulphite (0.04 M, Na$_2$SO$_3$) was added to standards and samples to achieve a final concentration of 100 μM. Low iron seawater (LISW), previously obtained from surface waters of the open ocean and stored in the dark, was used for all calibrations. For iron calibration, stock solutions of 0.02 M ammonium ferrous (Fe(II)) sulphate (99.997 %, Aldrich) were prepared weekly and stored in a refrigerator ($\sim$4 °C). The working solutions of 40 μM and 200 nM were prepared immediately prior to analysis.

For the shore based analyses of dAl, a 0.02 % lumogallion (TCI Europe) solution was prepared by dissolving 0.02 g in 100 mL of UHP water. Samples were buffered using ammonium acetate (2 M) and adjusted to pH 5.5 with acetic acid. The surfactant Brij-35 (Aldrich) was prepared by dissolving 125 g in 500 mL (25 % solution) overnight in UHP water. For calibration, a 0.05 M stock solution of aluminium potassium sulphate (AnalaR, VWR) was prepared by diluting 0.2372 g in 100 mL in acidified (0.5 M, Q-HCl) UHP water. Working solutions of 40 μM (in 0.05 M HCl) and 200 nM were prepared daily by serial

dilution and used immediately.

3.2.2 Sample Collection and Preparation

Sampling took place during the Meteor 60 cruise (M60/5) on-board the German research vessel FS Meteor (9th March and 15th April 2004). The cruise track followed an east-west transect of the North Atlantic from 63°W to 26°W at 21-41°N (Figure 3.1).
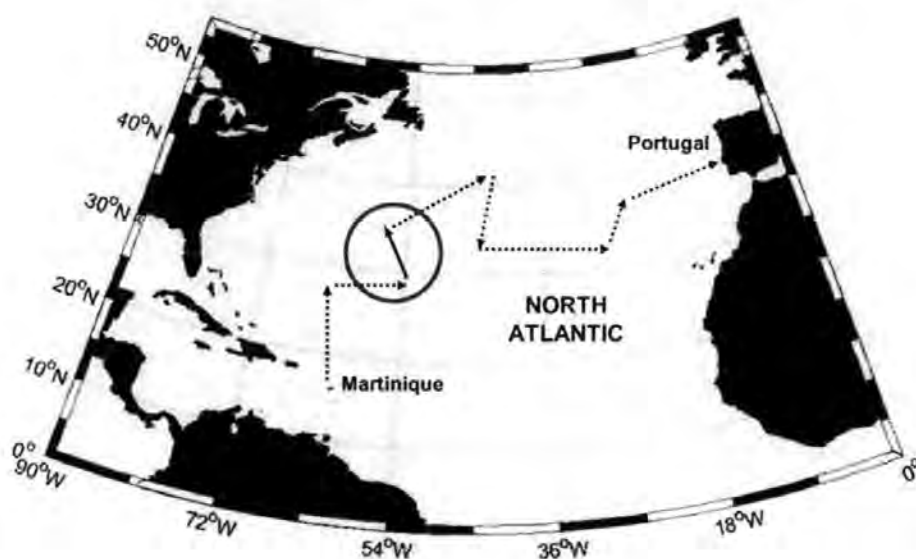
Figure 3.1 Cruise track for the Meteor 60/5 cruise from Martinique to Portugal. The surface sampling for the dust dissolution experiment took place during the third transect of the cruise (red circle).

The main objective of the cruise was to investigate the nutrient requirements of the in-situ phytoplankton community, this was carried out through ship-board bioassay experiments. In addition, the North Atlantic is a region noted for its high dust input as a result of dust transport from the Sahara, it was therefore an ideal opportunity to investigate this crucial source of the essential nutrient iron through dust dissolution studies in these waters.

For the dissolution experiment, surface seawater (1-2 m) was collected using a torpedo shaped tow-fish fitted with acid cleaned PVC tubing, during a transect of the cruise (Figure 3.1, circled area). The seawater was pumped (~2 L min^{-1}) using a PTFE diaphragm pump (Verder Air, Almatech-A15) fitted with PTFE and silicone pump tubing and filtered in-line through a Sartobran-P (Sartorius) polypropylene cartridge containing a 0.45 μm and 0.2 μm cellulose acetate pre-filter and final filter membrane respectively. The seawater from the tow-fish was collected over a short period of time (<1 h), fed into the clean container and filtered directly into a 60 L clean polycarbonate carboy (Nalgene). This homogeneous filtered surface seawater (FSW) was then sub-sampled for the dissolution experiment (see below). The dissolved iron concentration for this FSW was 0.30 ± 0.02 nM.

Initiation of dissolution experiment and sub-sampling for analyses

Five sieved soils (four African, one Asian) and one atmospherically processed dust (collected in Turkey) were used in the dissolution experiment. Each dust was homogenised in 10 L of the FSW in clean 20 L polycarbonate carboys (Nalgene) to create a mother solution with a particle concentration of 10 mg L^{-1}. The mother solutions were then diluted where necessary, using the FSW control, into duplicate 1 L polycarbonate (Nalgene) incubation bottles so as to achieve three final particle concentrations of 0.1, 2 and 10 mg L^{-1}, Figure 3.2 illustrates the processes followed during these steps.

The process time for the transfer was minimal (1 – 2 min) so as to minimise partitioning between dissolved and particulate fractions. The bottles were placed in on-deck incubators (Figure 3.3) with circulating surface seawater, this continual circulation maintained comparable
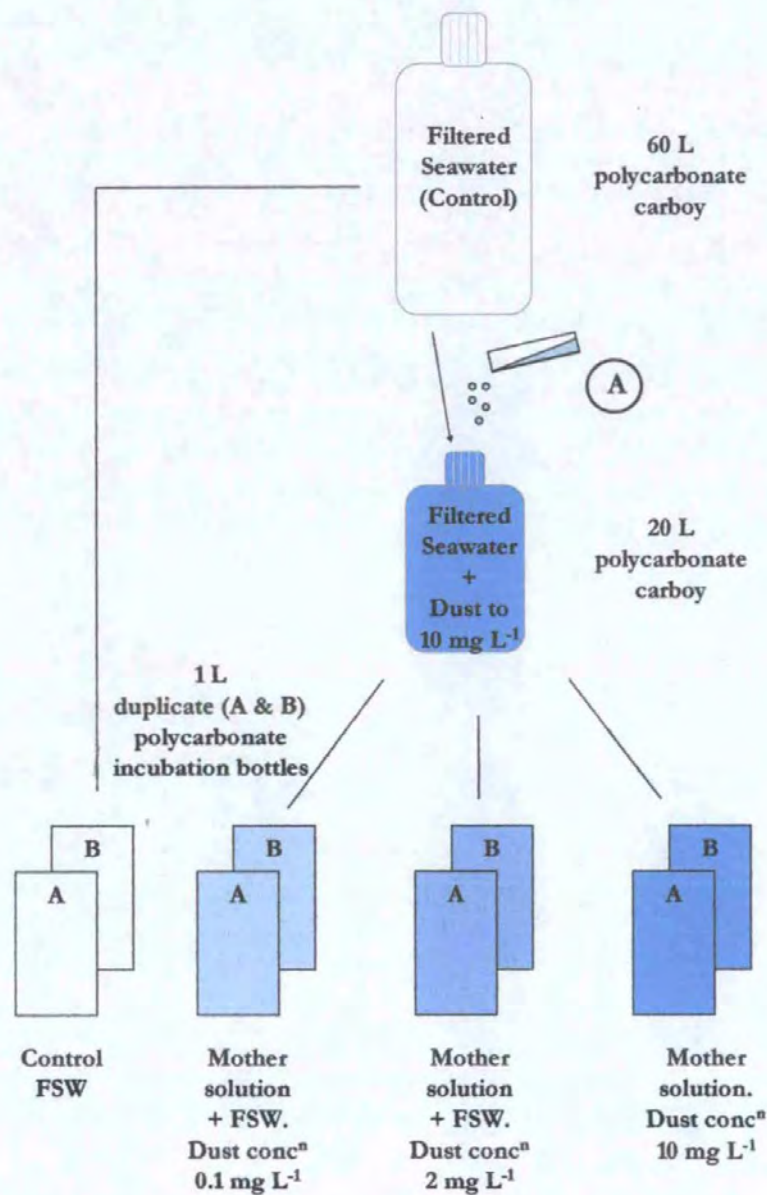
Figure 3.2. Design of dust dissolution experiment. Dust was added to 20 L polycarbonate carboys (A) to achieve a particle concentration of 10 mg L^{-1}. This mother solution was then transferred and diluted using filtered seawater (also control) into 1 L polycarbonate bottle to achieve final particle concentrations of 0.1, 2 and 10 mg L^{-1}. This final step was carried out in duplicate.

temperatures in the incubators with that of surface seawater. A control (filtered seawater without addition of dust) was incubated for the same time periods. The ship's motion ensured mixing of the dust and seawater. Light was attenuated to 20% of incident surface values with blue filters, as described by Mills et al. (2004).

The bottles were then sealed and incubated for two time periods; 24 h and 8 days. The time periods were chosen to investigate instantaneous dissolved iron fraction (24 h) and compare this with a longer residence time (8 days). Bonnet and Guieu (2004) used similar exposure times which are representative of the contact time between atmospheric particles and seawater during the particle residence time in the surface mixed layer of the ocean (Ridame and Guieu, 2002).

Figure 3.3 On deck incubator tanks used during dissolution studies. Light was attenuated to 20% of incident surface values using blue filters.

Following the two incubation times (24 h and 8 days), sub-samples were collected for analyses from both the duplicate incubation bottles (represented as bottles A and B in Figure 3.2). These were sampled into trace metal clean, 60 mL low density polyethylene (LDPE) bottles (Nalgene) and filtered into duplicate clean LDPE bottles using 25 mm Gelman syringe filters (0.2 μm, PTFE membrane). The filters were previously treated with methanol (Romil, UpS™) to activate the membrane, acid washed (0.5 M hydrochloric acid (HCl)) and rinsed with UHP water and sample prior to use. Two sets of sub-samples were collected, one for the shipboard dFe analyses and the other for land based aluminium analyses.

3.2.3 Method

DFe concentrations were determined using FI-CL (Bowie et al., 1998; Bowie et al., 2002) as detailed in chapter two. The FI instrument was set-up as illustrated in Figure 2.4 (section 2.2.4, chapter two) and cleaned with 0.5 M Q-HCl for a minimum of 4 h prior to use on board ship, this was followed by flushing with UHP water. Prior to all experimental analyses, the system was operational with reagents flowing for at least 1 h to conditions sample lines and ensure baseline stability. Sub-samples, collected and filtered (as described above), were acidified to pH 2 (HCl, Ultrapur Merck) and then the reducing agent sodium sulphite was added to achieve a final concentration of 100 μM in the sample. Separate 12 hour acidification and 12 hour reduction steps were performed off-line.

Stored sub-samples were analysed in a shore based laboratory for dissolved aluminium by Dr A. Fisher, using micelle-enhanced fluorimetric detection of the aluminium-lumogallion complex (Ren et al., 2001). Briefly, samples were buffered to pH 5.0 using ammonium acetate and the fluorescent reagent lumogallion added to achieve a final concentration of 0.5 μM, the samples were then left overnight to react. Following the reaction time, the samples were

analysed using a fluorescence spectrophotometer (Hitachi F-4500) at wavelengths of 504 nm (excitation) and 554 nm (emission) after the addition of the surfactant Brij-35 (1% v/v).

Additionally, in order to calculate the solubility of iron and aluminium in seawater, the total composition of each metal in the dusts was required. This was determined, by Dr A. Fisher, following a hydrofluoric acid digest (Thomson and Banerjee, 1991). Dust samples (~ 0.0500 g) were weighed into pre-cleaned Teflon bombs and nitric acid (2 mL, Primar, Fisher Chemicals) added. The bombs were sealed and placed in an aluminium block on a hotplate where they were boiled at 120°C for 2 days. After cooling, the bombs were opened and hydrofluoric acid (1 mL) added. The bombs were then re-sealed and heated at 120°C for a further 24 hours. After the elapsed time, the lids were removed from the bombs and the acid contents allowed to evaporate to dryness. The residues were taken up by a mixture of 1 mL nitric acid and 0.5 mL hydrochloric acid (Primar, Fisher Chemicals), transferred quantitatively to clean tubes, diluted and spiked with indium to a concentration of 100 ng mL^{-1}. A certified reference material (NIST 2711) was digested and analysed in the same way.

Furthermore, after a shore based review of literature, an ammonium acetate leach (pH 4.7) was performed to mimic wet deposition processes. Metals were extracted from dust samples (~0.0500 g) using ammonium acetate leach (1 M, pH 4.7) for 1 – 2 h .

The digests and ammonium acetate leaches were analysed using either inductively coupled plasma – optical emission spectrometry (Thermo Jarrel Ash Atomscan 16), inductively coupled plasma – mass spectrometry (Thermo ElemantalPQ2 + Turbo), or flame atomic absorption spectrophotometry (GBC 902) depending on the concentration of the analyte being determined.

3.2.4 Calibration and Blanks

Dissolved iron(II + III)

The FI instrument was calibrated daily using LISW which was treated in the same way as the pre-treatment of the samples, i.e. acidified to pH 2.0 using Q-HCl and then sodium sulphite added. Standard additions of iron(II) working stock were made to the treated LISW in the range 0.2 - 1.0 nM, equating to 20 – 100 μL addition to 20 mL samples, immediately analysed and used to generate calibration graphs.

The blank was defined as the signal obtained for an analytical cycle with the loading of the buffer solution (ammonium acetate) only, without a sample, onto the 8-HQ column. This was analysed in the same manner as samples and standards and includes any signal associated with the reagents and the manifold. A procedural blank, associated with the contribution to the signal from the addition of Q-HCl and sulphite to samples, was obtained using standard additions of each solution to UHP water and immediately analysing. The contribution from all blank signals were calculated during the calibration process and subtracted from the final sample concentrations.

Dissolved aluminium

The fluorometer was calibrated daily using the method of standard additions and used to generate a calibration graph. The standard additions were performed on an experimental sample from each particle concentration (0.1, 2 and 10 mg L^{-1}) and varied over the 5 –300 nM. The standard additions were prepared at the same time as the samples themselves and left to react overnight with the lumogallion complex prior to fluorometric analyses. The calibration graphs generated were used to calculate the concentrations of Al in all samples.

The blank was defined as the signal arising from the reagents used, lumogallion and ammonium acetate buffer, when added to UHP water. The blank was treated in the same manner as the samples, left overnight to react and analysed at the same time as standards and samples. As with the dFe analyses, the contribution from the blank signal was calculated during the calibration process and subtracted from the final sample concentrations.

3.3 Results and Discussion

3.3.1 Analytical Figures of Merit

The standard graphs generated for iron and aluminium displayed excellent linearity, with correlation coefficients (r^2) typically >0.98, and were used to calculate the concentrations of each metal in the respective analyses.

For the shipboard iron calibrations, the mean repeatability and standard deviation for the standard additions performed (4 replicates) was 8.4 $\pm$ 2.7 % (n = 17). The mean iron blank signal produced for these analyses was 47 $\pm$ 25 pM (n = 10) resulting in a mean limit of detection (defined as three times the standard deviation of the blank) of 14 $\pm$ 7 pM (n= 3). These figures are consistent with those previously reported by Bowie et al. (2004).

Similarly, the repeatability of 5 replicate analyses of standard additions performed for an aluminium calibration were typically in the range 2 – 13 % (n = 18). The blank signal for aluminium was typically 12 $\pm$ 3 nM (n = 8) resulting in a limit of detection 0.44 nM.

The contributions to the blank signal for both iron and aluminium arise from the impurities contained in the solutions and reagents used during the analyses of samples, e.g. the luminol and lumogallion reagents, the ammonium acetate buffer used for both analyses, HCl and sulphite used in sample pre-treatment for iron analyses. Where possible, these contributions were minimised through the use of clean acids and reagents and additional cleaning of solutions prior to use (as detailed in chapter two, section 2.2.2).

During the analyses of the particle digest samples, a standard reference material (NIST 2711) was also analysed. The results from the NIST 2711 (certified values in mg kg^{-1} in parenthesis) were copper 118 $\pm$ 1 mg kg^{-1} (114 $\pm$ 2), zinc 330 $\pm$ 3.3 mg kg^{-1} (350 $\pm$ 4.8), iron 26600 $\pm$ 266 mg kg^{-1} (28900 $\pm$ 600) and lead 1110 $\pm$ 11 mg kg^{-1} (1162 $\pm$ 31) (confidence intervals for the measured values represent $\pm$ 1 % of the instrument variability (n = 3)). The percentage recovery for the metals (92 – 104 %) was within the target range of 90 – 110 %. These results are based on one digestion of the reference material, and, in order to maintain the same digestion protocol between the reference material and the six dusts, a similar quantity ($\sim$50 mg) was analysed. The largest source of error in the overall procedure is likely to be the acid digestion step, but this was not quantified due to insufficient dust being available. It was also observed that at the end of the digestion period for the dusts a small residue remained in the Teflon bombs leading to slightly low recovery. In addition, the reference material was not completely dried prior to use and may still have contained moisture, this would account for up to 5 % of the difference between determined and certified values. Taking these sources of error into account, the determined results for the reference material show reasonable agreement with the certified values.

3.3.2 Dust Composition

The mean crustal abundances of iron and aluminium are $\sim$3.5 % (Duce and Tindale,

1991) and ~ 8 % (Wedepohl, 1995) respectively, although the proportion of metals in rocks and soils is known to vary from place to place depending on the mineralogy of the source rock (e.g. 2.9 to 4.8 % for iron (Taylor and McClennan, 1985)).

For the dusts used in this experiment the iron and aluminium content are shown in Table 3.2. Due to insufficient quantity of dust, replicate digestions were not performed and these results are based on the digestion and analysis of one sample (~50 mg) of each dust. As discussed in section 3.3.1, the digestion process has inherent sources of error which must also be considered when interpreting these results.

Table 3.2. Percentage of iron and aluminium (% mass fraction) in each dust determined after hydrofluoric digestion and the subsequent aluminium / iron mass ratios.

	Iron	Aluminium	Fe / Al Ratio
Mauritanian	1.65	4.36	0.38
Moroccan	1.72	3.66	0.46
Namibian	5.05	8.38	0.60
Gobi	3.04	5.58	0.54
S. Algerian	4.84	7.40	0.65
Turkish*	2.88	4.08	0.70

* Atmospherically processed
These results are from the digestion and analyses of one sample of dust.

The percentage mass fraction of iron and aluminium in each dust varied from 1.65 to 4.84 % and 3.66 to 8.38 % in weight respectively, giving mean values of 3.2 % for iron and 5.6 % for aluminium. This resulted in iron/aluminium mass ratios (Table 3.2) ranging from 0.30 to 0.70 (mean 0.57) equating to an average molar ratio of 0.28. This molar ratio matches that reported by Arimoto et al. (2004) for aerosol samples collected in China (0.28), but is lower

than the average molar ratio (0.53) reported by Buck et al. (2006) for aerosol samples collected in the Northwest Pacific. While the average molar ratio observed for this study (0.28) is similar to published data (Arimoto et al. 2004), overall all of these values (previously reported and in this study) demonstrate the wide range in iron and aluminium dust composition, these uncertainties should be considered when interpreting dust and/or iron fluxes based on average values.

3.3.3 Dissolved Iron and Aluminium Concentrations

The dFe concentrations after 24 h and 8 days of incubation are shown in Figure 3.4. The results have been normalised to the control (filtered seawater) and represent the difference in iron concentration (ΔdFe), where ΔdFe = $[dFe]_{after\ contact\ time}$ - $[dFe]_{initial}$, for the three particle concentrations (0.1, 2 and 10 mg L^{-1}).

After 24 h contact time between the seawater and dusts, an increase in dFe was observed for the atmospherically processed Turkish dust, typically the sieved soils showed either no increase or a loss of iron. Values of ΔdFe for the Turkish dust were ~0.06 and ~ 0.18 nM at particle concentrations of 2 and 10 mg L^{-1}, respectively.

After 8 days of contact time, the Namibian and Gobi dusts showed little change from the control regardless of particle concentration (Anova P values > 0.05 at 95% confidence interval). For the remaining four dusts, values of ΔdFe increased with particle concentration ranging from 0.01 to 0.44 nM. The highest value of ΔdFe (~0.44 nM) was produced by the Turkish, atmospherically processed dust. Comparing this data to the total iron content of the dusts (Table 3.2), the highest percentage of iron is contained in the Namibian dust (5.05 %), however lowest concentrations of ΔdFe were observed for this dust (<0 nM). The highest
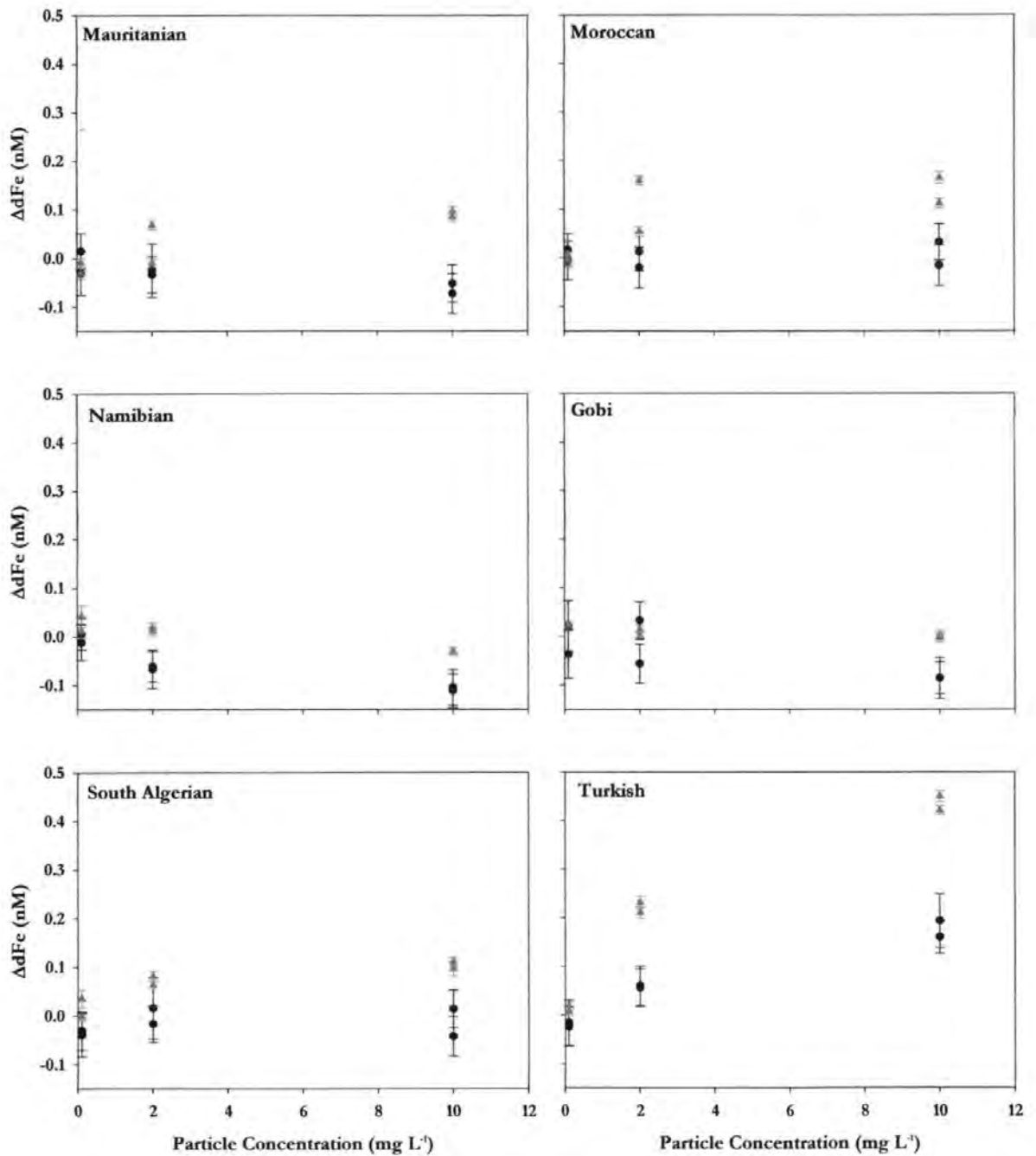
Figure 3.4 ΔDFe, from duplicate experiments, as a function of particle concentration. (●) 24 h and (▲) 8 days contact time with seawater. (Error bars represent 1 standard deviation).
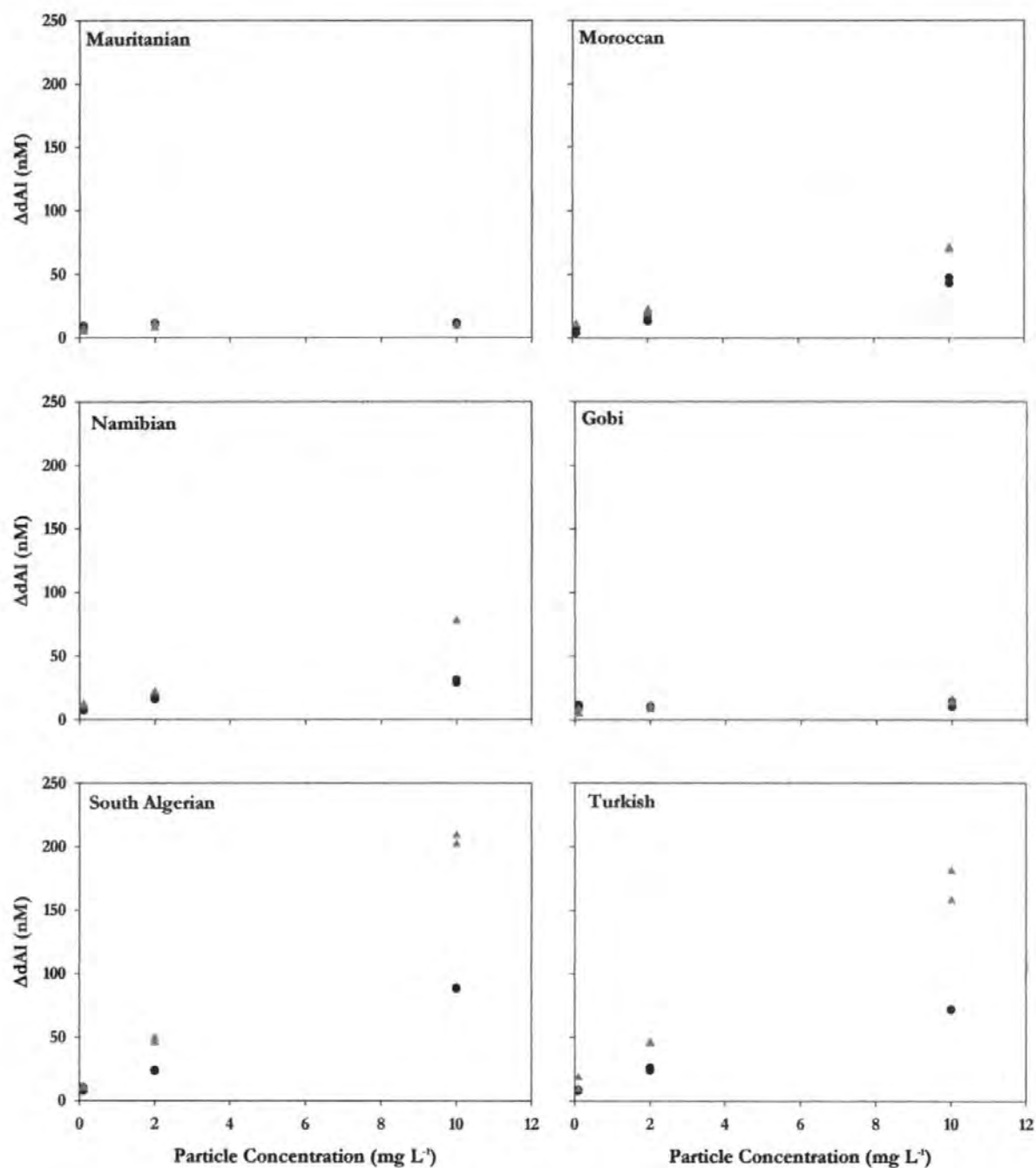
Figure 3.5. ΔDAl, from duplicate experiments, as a function of particle concentration. (●) 24 h and (▲) 8 days contact time with seawater.

AdFe values were observed for the Turkish dust, yet this dust contains nearly half the iron content (2.88 %) of the Namibian. These results indicate that particle iron concentration is a minor factor in the dissolution of the metal and that solubility is governed by other variables.

The dAl concentrations (Figure 3.5) were also normalised to the control and represent the difference in aluminium concentration (ΔdAl), where ΔdAl = $[dAl]_{after\ contact\ time}$ - $[dAl]_{initial}$, plotted against the three particle concentrations. In contrast to the results for dFe, the ΔdAl values increased for all dusts after 24 h of contact time with the seawater. The values for ΔdAl were found to be a function of particle concentration, typically increasing as particle concentration increased. After 7 days of incubation, the values of ΔdAl increased further (ranging from 5.7 to 205.5 nM) for all dusts except the Mauritanian and Gobi. Lower aluminium dissolution was observed from dusts containing a high total aluminium concentration. Consequently, as with iron, the aluminium dissolution is governed by factors other than total metal concentration.

3.3.4 Estimates of Iron and Aluminium Solubility

The percentage of iron and aluminium released from each dust in seawater is detailed in Table 3.3 and was calculated using the following equation.

$$\%dMe = \frac{(dMe - dMe_{Init}) \times relative\ atomic\ mass\ of\ metal \times 100}{(Me_p \times Pc \times 0.001)}$$

where;

dMe = dissolved metal concentration after contact time (nM)

dMe_{Init} = initial dissolved metal concentration (nM)

79

$$Me_p \quad = \text{concentration of metal in each dust (\% - taken from Table 3.1)}$$

$$Pc \quad = \text{amount of particles introduced (mg } L^{-1})$$

After 24 h incubation, the only increase in ΔdFe was for the Turkish atmospherically processed dust. The calculations are therefore based on the dissolved metal concentrations after 8 days of incubation. The percentage of iron released into seawater was extremely low (0.001 to 0.04 %) and in some cases, due to apparent negative ΔdFe concentrations (see Figure 3.4), estimates of solubility could not be calculated and were therefore excluded from the data in Table 3.3. The percentage of aluminium released ranged from 0.06 to 9.0%.

Table 3.3. Percentage solubility[§] of iron and aluminium as a function of particle concentration after 8 days of incubation

Dust Conc^n (mg L^{-1})	Iron Solubility (%)			Aluminium Solubility (%)		
	0.1	2	10	0.1	2	10
Mauritanian	-	0.005	0.003	3.8	0.30	0.06
Moroccan	0.002	0.019	0.004	7.8	0.76	0.51
Namibian	0.03	0.001	-	3.7	0.35	0.25
Gobi	0.04	0.001	-	3.3	0.23	0.07
S. Algerian	0.02	0.004	0.001	3.9	0.87	0.70
Turkish*	0.03	0.022	0.008	9.0	1.5	1.12

* Atmospherically processed
[§] Results calculated from the mean of duplicate experiments

The solubility of the two metals varied depending on the particle concentration, resulting in lower solubilities at higher dust concentrations and vice versa. Figure 3.6 demonstrates the trends using the South Algerian and Turkish dusts as examples. The graphs illustrate that a particle affect is evident, and at even lower particle concentrations the percentage release of each metal would be much higher.
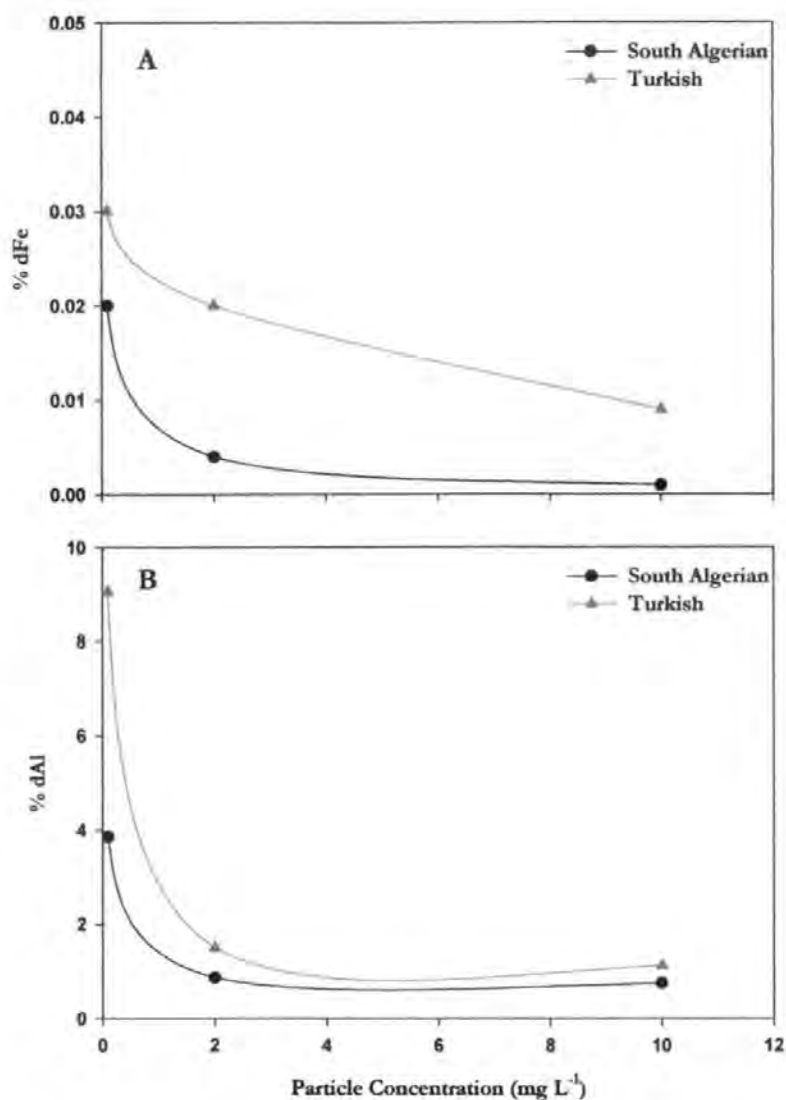
Figure 3.6. (A) Dissolved iron and (B) dissolved aluminium solubility as a function of particle concentration. (♦) South Algerian and (▲) Turkish dusts introduced into seawater for a contact time of 8 days.

Particle scavenging in the ocean environment is a removal pathway for both metals. When aerosol particles enter seawater partial dissolution occurs, however, at high particulate loadings the particles can act as adsorption substrates and both dissolved iron and aluminium can re-adsorb to the particle surfaces, removing the dissolved metals from the seawater (Chester et al., 1993; Zhuang and Duce, 1993). The solubility data presented here (Figure 3.6) demonstrates this process. Similarly, previous studies have also reported that the percentage

dissolution of iron decreases as particulate load increases (Bonnet and Guieu, 2004; Zhuang et al., 1990). Bonnet and Guieu (2004) observed higher iron dissolution values, up to 1.6 %, for a Saharan sieved soil similar to the South Algerian sieved soil used in this study using a lower, wider particle concentration range to this study of 0.01 to 10 mg L^{-1}. The use, however, of such low particle concentrations (0.01 mg L^{-1}), which are more realistic of dust deposition events, presents handling problems and potential sources of error which need to be considered.

In addition to particle scavenging, there is also the possibility of metal adsorption to the surface of the walls of the incubation bottle. In the same manner that metals can re-adsorb to particles, the clean walls of incubation bottles can also act as adsorption substrates again removing the metal from solution. However, Vasconelos et al. (2002), using similar polycarbonate incubation bottles that were used in this study, measured metal concentrations in algae (extracellular adsorption plus intracellular uptake) and found that the metal concentration in the algae balanced the metal lost from seawater, thus indicating negligible adsorption onto container walls. The low ΔdFe observed after 24 h of contact time with the seawater (Figure 3.4) could therefore be a result of two processes. Either low dissolution was observed for the six dusts, or the results indicate that iron is more particle reactive than aluminium and that after 24 h, scavenging may have been equal to dissolution.

The results presented here, using filtered seawater and relatively high particle concentrations of 0.1 - 10 mg L^{-1}, are comparable with previous estimates of iron and aluminium solubility in seawater dissolution studies (Bonnet and Guieu, 2004; Chester et al., 1993; Maring and Duce, 1987; Prospero et al., 1987). It has been suggested that atmospheric (photo)chemical processing enhances aerosol iron solubility (Spokes and Jickells, 1996; Desboeufs et al. 1999) through wet and dry cloud cycling and the presence of acid species (SO_4^{2-}) in the dust particles. While these processes were not investigated here, the dissolution of iron from the atmospherically processed dust used in this study was not significantly

different to the other dusts used. At the lowest particle concentration of 0.1 mg L⁻¹ there was little difference in the iron solubility (0.01 – 0.04 %) observed for the six dusts, and the highest value was produced by the Gobi dust (0.04 %) and not the atmospherically processed Turkish dust (0.03 %). However, at the lower particle concentration (0.1 mg L⁻¹), the dissolution of aluminium attached to atmospherically processed particles was higher (9 %) than to the dusts from sieved soils (3.3 – 7.8 %) suggesting aluminium in atmospherically processed particles is more soluble.

Recent studies have reported higher iron solubility during wet deposition events. Observed iron solubilities of up to ~ 40 % have been reported from precipitation samples (Table 3.4). The lower pH encountered in rainwater (typically between pH 4 – 6) would have an impact on the sea surface micro-layer during wet deposition and therefore potentially increase the percentage of soluble iron delivered to the surface ocean. To simulate the lower pH experienced in rainwater, co-workers have utilised either an ammonium acetate leach (pH 4.7) or UHP water (pH 6) as a model for rainwater release (Baker et al., 2006a; 2006b; Buck et al., 2006; Guieu et al., 2002; Ridame and Guieu, 2002). In order to investigate this enhancement in iron solubility under rainwater conditions, an ammonium acetate leach (1 M, pH 4.7) was carried out using the six dusts to further assess the release of iron from them. The results of the ammonium acetate leach and the iron seawater solubility data from this study are presented in Table 3.4, this is compared with data from previous studies. The percentage release of iron from the ammonium acetate leach increased by two orders of magnitude from the seawater, ranging from 0.15 - 1.48 % (mean 0.63 %). The is comparable with reported values using a similar method (Bruland et al., 2001). In contrast to the seawater data, the largest release of iron was from the atmospherically processed Turkish dust (1.48 %) and the lowest being from the Gobi dust (0.15 %).

Table 3.4 Iron solubility data from sieved soils and aerosols. Solubilities are % soluble Fe as a fraction of total aerosol Fe.

Particle Source	% Dissolution	Reference
Seawater		
Mauritanian	-	
Moroccan	0.002	
Namibian	0.03	This
Gobi	0.04	study
South Algerian	0.02	
Turkish	0.03	
Saharan soil	~0.4	Guieu et al. (2001)
Saharan soil	0.05 – 1.6	Bonnet and Guieu (2004)
Marine aerosols	5 – 50	Zhuang et al. (1990)
Model rainwater leach		
Mauritanian	0.49	
Moroccan	0.48	
Namibian	0.70	This
Gobi	0.15	study
South Algerian	0.45	
Turkish	1.48	
Various aerosols	0.5– 7.9	Baker et al. (2006a; 2006b)
Marine aerosols	0 – 87	Hand et al. (2004)
Marine aerosols	46	(Buck et al., 2006)
Soluble iron collected in precipitation*		
Erdemli, Turkey	9.6	Ozsoy and Saydam (2001)
Wilimigton, USA	26	(Kieber et al., 2001b)
Dunedin, New Zealand	37.8	Keiber et al (2001a)

* Average values from several measurements (adapted from Ussher et al. (2004))

The range in observed iron solubility is large regardless of the dissolution media, 0 – 50 % (seawater), 0.15 – 46 % (rainwater model) and 9.6 -37.8 % (rainwater samples), though overall the lowest dissolution has been observed in seawater. Iron solubility is dependent on dust composition (Zhu et al., 1992) and the degree of cloud processing that the aerosol

undergoes (Jickells and Spokes, 2001). Aerosols therefore have different inherent characteristics and different dissolution results should be expected. In addition, laboratory protocols relating to dissolution media (leaching conditions), particle size and concentration, and the time between collection and analysis make it difficult to compare results. However, the results presented in this study are within the range of previously reported studies. Particle size is known to be an important influence on iron solubility and generally higher releases of iron have been observed from the fine mode of aerosol particles as opposed to the course mode (Baker et al., 2006b; Hand et al., 2004) . In future studies, these factors need to be addressed to further our understanding of iron solubility.

3.4 Conclusions

The aim of this study was to gain further insight into iron and aluminium solubility in North Atlantic waters. This was achieved and solubility estimates of 0.001 to 0.04 % for iron and 0.06 to 9.0 % for aluminium in seawater were determined. For iron the estimated solubility increased, ranging from 0.15 to 1.48 %, for a model rainwater (ammonium acetate) leach. These results are within the range of previously reported solubility estimates performed using similar media.

Wet and dry dust deposition fluxes of 61×10^{12} g y^{1} (modified from Duce et al. 1991; Jickells and Spokes 2001) and 160×10^{12} g y^{1} (Duce et al. 1991) respectively have been estimated for the North Atlantic. Based on the average iron content (3.2 %) for the six dusts used in this study, this would result in an iron input ranging from $0.035 - 0.092 \times 10^{12}$ mol y^{1}. Using the range of solubilities from the seawater and ammonium acetate leach (0.002 – 1.48 %) observed for the six dusts, this would result in a soluble iron input to the North Atlantic of

0.02 – 5.2 x 10^8 mol y^{-1}. Although dry deposition is two to three times higher (160 x 10^{12} g y^{-1}) the resulting range of soluble iron (0.02 – 0.37 x 10^8 mol y^{-1}) would be lower than the release from wet deposition (0.05 – 5.2 x 10^8 mol y^{-1}), a reflection of the higher solubility observed for the ammonium acetate leach.

Previous studies have indicated that iron availability is a significant determinant of phytoplankton productivity in the North Atlantic (Martin et al., 1993; Mills et al., 2004; Moore et al., 2006). Although the solubility of iron from the dusts in this study are very low (0.001 – 0.04 %), the residence time of particles in the surface mixed layer has been estimated to be ~ 20 days (Jickells 1999). Bonnet and Guieu (2004) have shown that the dust particles can release significant quantities of dissolved iron (0.07 – 1 nM) due to the long residence time in the mixed layer. In a recent incubation study, the addition of two dusts (which were used in this study; South Algerian sieved soil and a Turkish Atmospherically processed dust) stimulated a similar growth response to nutrient additions (N, P and Fe) in the natural phytoplankton community (Moore et al. 2006). This illustrates the importance of iron solubility from aerosols as a source of nutrients to the North Atlantic and hence controls primary productivity in this region.

The average iron/aluminium molar ratio (0.28) for the six dusts is comparable with reported data and appears to be a good proxy for use in estimating iron release from dust deposition events. However, the range in the iron/aluminium data presented demonstrates the need for caution when interpreting these values and it is therefore better to determine dissolved iron concentrations directly, following and/or during a dust storm. For a more complete picture, these measurements should be carried out at sea and, if possible, combined with atmospheric deposition measurements as demonstrated by Baker et al. (2006a; 2006b) and Buck et al. (2006). Shipboard experiments, however, are not always possible and dust events are sporadic, in addition, performing dissolution experiments at sea presents additional challenges, e.g. maintaining trace metal clean procedures. It is also extremely difficult to

mimic the processes which occur in the sea surface micro layer. Laboratory based experiments are therefore needed to elucidate iron solubility further. Environmental variables such as particle size and concentration, plus temperature and movement need to be constrained and the kinetics of iron release over time needs further, more detailed investigation. The use of UV seawater without the presence of ligands and with ligands added could be used to aid these studies.

Iron plays a critical role as a limiting nutrient for primary productivity in the world's oceans and there are still issues which need to be addressed in order to increase our knowledge of the marine biogeochemistry of this essential element. For instance, iron solubilities from aeolian sources needs further investigation in order to resolve the disparity in results. In addition, a broader understanding of the biogeochemical interactions and feedback mechanisms which occur in and across the air-sea interface can only be achieved through combined study of the ocean and atmosphere. The results from laboratory based experiments (as detailed above) in combination with field studies will provide more detailed information on the cycling of iron and other metals and nutrients in the marine environment. Collaborative initiatives such as SOLAS (Surface Ocean – Lower Atmosphere Study), will enhance global understanding concerning the deposition of nutrients that control marine biological activity and the cycling of atmospherically important trace gases.

Chapter 4

Determination of Hydrogen Peroxide in Laboratory
Cultures and Natural Surface Seawater using Flow
Injection with Chemiluminescence Detection

4.1 Introduction

Reactive oxygen species (ROS) are ubiquitous in the surface waters of the oceans and include oxygen ions, free radicals and peroxides, of which hydrogen peroxide (H_2O_2) is one of the principal species. As a key chemical species in redox reactions, H_2O_2 has the potential to affect the cycling of trace metals and organic compounds. The concentration, sources and sinks of this species in seawater is therefore an important area of study.

Previously, studies concerning H_2O_2 in oceanic waters have mainly focused on either photochemical production (Cooper et al., 1988; Millero, 2006; Yocis et al., 2000) or the atmospheric deposition of peroxides (Cooper et al., 1987; Croot et al., 2004a; Gerringa et al., 2004; Yuan and Shiller, 2000). However, relatively little is known about the biological contribution to the ROS pool in surface waters. Phytoplankton are known to generate ROS (including H_2O_2) and recent studies have suggested that biological production of H_2O_2 may be significant (Wolfe-Simon et al., 2005; Yuan and Shiller, 2005). In order to elucidate the importance of oceanic biological H_2O_2 generation, a better understanding of the underlying biological processes is required. The aim of the work described in this chapter was therefore to develop an analytical technique for the sensitive (nM detection limits) and real time detection of H_2O_2 in order to address the following objectives:

1. Investigate the biological contribution to H_2O_2 concentrations in seawater during naturally occuring phytoplankton blooms.

2. Investigate real-time H_2O_2 production in phytoplankton cultures in the dark and in response to light.

A flow injection-chemiluminescence method was used to fulfil these aims and

determine H_2O_2 concentrations in both seawater samples and in laboratory based assay experiments involving diatom cultures. The optimisation of this method is described and field results from two very different oceanic regions are presented; the coastal shelf region of the English Channel, chosen specifically due to the presence of a phytoplankton bloom, and the open waters of the Ross Sea, an oceanic region known for experiencing large phytoplankton blooms (Arrigo et al., 2000; Arrigo and van Dijken, 2003; Smith et al., 2000). The biological influence on peroxide concentrations in the water column in these two contrasting climates with very different ambient conditions is discussed. The adaptation of the analytical method to specifically examine H_2O_2 production by diatoms is also described, the versatility of the technique is illustrated using results from assays experiments in which diatom cells were exposed to varying irradiance levels to investigate the relationship between H_2O_2 production and exposure to light.

4.2 Experimental

As detailed in chapter two, flow injection with chemiluminescence detection provides high sensitivity and rapid sample throughput, necessary parameters for the determination of transient reactive species. The oxidation of luminol (5-amino-2,3-dihydro-1,4-phthalazinedione) by H_2O_2 in the presence of a catalyst in alkaline solution has been widely used for the determination of H_2O_2 (Rose and Waite, 2006; Yuan and Shiller, 1999). The most sensitive inorganic catalyst for the luminol-H_2O_2 reaction is Cobalt(II), a metal which has been used previously with success both in laboratory and shipboard studies for the analyses of H_2O_2 in seawater (Price et al., 1994; Yuan and Shiller, 1999).

In this study, the determination of H_2O_2 was carried out using the Co(II) catalyzed

oxidation of luminol adapted from Price et al. (1994). Modifications were made to the original method; the sample injection loop was reduced to 60 μL and the previously separate reagents mixed to a single combined luminol / Co(II) reagent solution, thereby simplifying reagent preparation and improving mixing and sensitivity. To facilitate investigations into H_2O_2 production by phytoplankton, an in-line transparent filter unit was incorporated into the FI manifold to immobilise phytoplankton cells upstream of the detector system. This system allows the cell to be constantly flushed with flowing media and the environmental conditions of the cells to be manipulated without interfering with downstream detection of H_2O_2 in the filtrate solution. This method is described in detail below.

4.2.1 Reagents and Solutions

All reagents were obtained from Sigma-Aldrich unless otherwise stated and prepared with ultra high purity (UHP, Millipore, 18 MΩ cm^{-1}) water. Stock solutions of 0.03 M luminol and 0.05 M Co(NO$_3$)$_2$.6H$_2$O (Fluka) were prepared in 0.1 M NaCO$_3$ and left for 24 h. These stock solutions were stored at 4 - 7 °C where they were stable for three months. From these stock solutions, a working mixed reagent solution of luminol / Co(II) (3×10^{-5} M / 5×10^{-4} M) was prepared in 0.1 M NaCO$_3$ buffer and the pH adjusted to 10.8 with HCl (12 M, AnalaR, Fisher Scientific). This solution was left for 24 h to ensure complete dissolution.

Primary solutions of H_2O_2 were prepared daily in filtered seawater (FSW) by serial dilution to concentrations of 10 mM and 50 μM from a stock solution of H_2O_2 (30 %, AnalaR, Fisher Scientific). These were prepared immediately prior to analysis.

For the laboratory based bioassay experiments, 60 L of seawater from the English Channel (50° 09.55 N 04° 14.66 W) was collected from a depth of 65.5 m using a CTD rosette frame and Go-Flo bottles. This seawater was filtered (0.2 μm Sartobran P, Sartorius) and aged at room temperature in the dark for at least two weeks. This aged FSW was used for all

experimental assays (with and without cells), standard solutions and calibrations. To demonstrate the specificity of the FI-CL H_2O_2 signal, the H_2O_2 scavenging enzyme catalase (bovine liver) was added to yield a final concentration of $1 - 3$ U mL^{-1} (1 unit of enzyme decomposes ~ 1 μM of H_2O_2 per mL).

4.2.2 Sample Collection and Preparation

Coastal Seawater Samples

Coastal seawater samples were collected on two separate occasions, both during a coccolithophore bloom, off the South-west coast of England in August 2005 and July 2006. A map of the sampling location is shown in Figure 4.1 along with satellite images of the two blooms (dated 7th August 2005 and 27th July 2006).
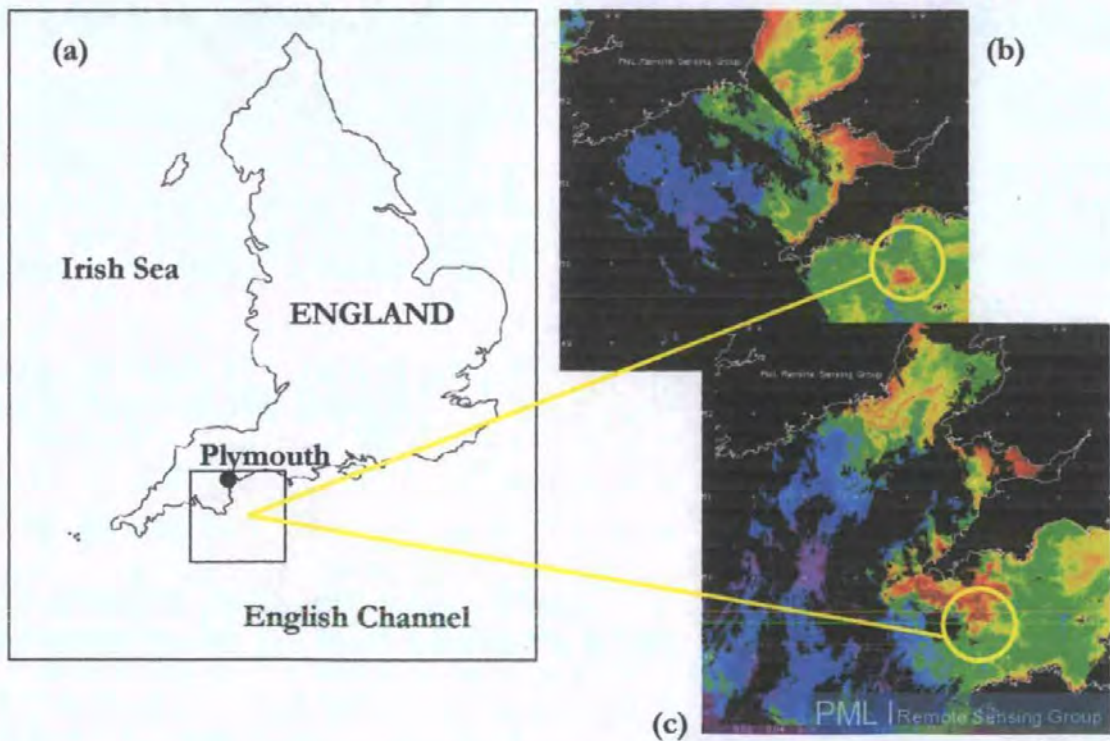
Figure 4.1 Location of sampling (a) off the South-west of England. Satellite images of the coccolithophore bloom in (b) August 2005 and (c) July 2006, red indicates regions of high chlorophyll and the area sampled is circled in yellow
(http://www.npm.ac.uk/rsdas/data/browse/file_info.php?image=MODIS/pace/2005/08/07).

Using a CTD rosette frame and Go-Flo bottles, on board the R.V. Plymouth Quest, samples were collected from varying depths (maximum of 40 m) in order to profile H_2O_2 concentrations within the water column at two separate locations; outside the bloom and from the centre of the bloom. The samples were immediately filtered (sterile cellulose acetate membrane, 0.2 μm, Nalgene) directly into clean, acid washed 250 mL low density polyethylene (LDPE) bottles (Nalgene). The samples were stored for ~6 – 7 h in the dark and kept cold prior to analysis in a land based laboratory.

Open Ocean Seawater Samples

Open ocean sampling took place during a research cruise in the Ross Sea (Figure 4.2) between 1st November and 16th December 2006. The investigation into H_2O_2 concentrations in the water column was part of a wider scientific initiative as part of the CORSACS II (Controls on Ross Sea Algal Community Structure, http://www.whoi.edu/sbl/liteSite.do?litesiteid=2530) cruise on board the research vessel Nathaniel B. Palmer. All sample handling, manipulation and analytical work was carried out in a class-100 clean air container.
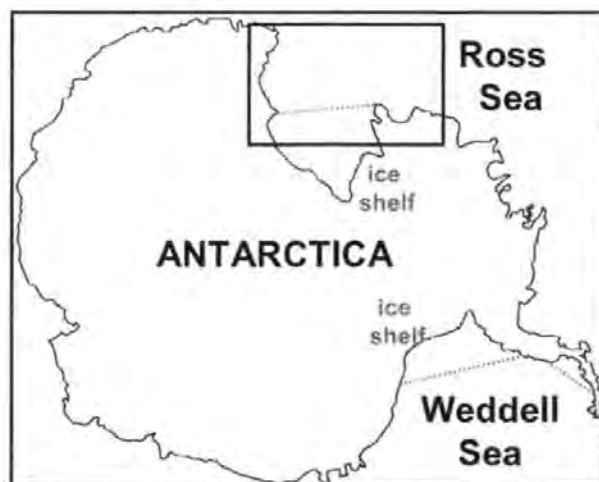
Figure 4.2 Location of the Ross Sea, Antarctica.

Seawater profiles were collected from varying depths (to a maximum of 400 m) by hydrocast using 5 L trace metal clean Niskin bottles suspended on a Kevlar line. The Niskin bottles were pressurised using 0.2 μm filtered, high purity nitrogen gas in order to filter sub-samples of the collected seawater. Samples were filtered through acid cleaned polypropylene cartridges (Sartorius) containing sequential 0.45 μm and 0.2 μm cellulose acetate filter membranes directly into 60 mL acid washed LDPE bottles (Nalgene). Samples were stored in a dark cool box for approximately 3 – 4 h prior to analysis.

Phytoplankton Cultures for Assay Experiments

Cultures of *Thalassiosira weissflogii* were incubated at 15 °C, 150 μmol photons m^{-2} s^{-1}, 12:12 light / dark cycle in filtered seawater supplemented with 500 μM NaNO$_3$, 32 μM K$_2$HPO$_4$, 100 μM Na$_2$SiO$_3$, and Guillard's F/2 vitamins and a trace metal solution containing 3.8 μM Na$_2$-EDTA, 1 μM FeCl$_3$, 80 nM ZnSO$_4$, 460 nM MnCl$_2$, 50 nM CoCl$_2$, 20 nM CuSO$_4$, 2 μM Na$_2$MoO$_4$, and 200 nM H$_2$SeO$_3$. Cultures were maintained in mid to late log phase by routine subculture or dilution. Cell counts were determined using a haemocytometer (Improved Neubauer slide), samples were either counted immediately or preserved by the addition of Lugols solution (100 : 1 v/v culture : lugols) and counted within 5 days.

4.2.3 Instrumentation

All measurements were carried out using a flow injection system and a schematic diagram of the manifold with flow rate is illustrated in Figure 4.3. The system consisted of a peristaltic pump (Gilson Minipuls, Anachem), a 6-port 2-position rotary injection valve (Anachem) with a 60 μL sample loop for manual sample injection and an end-window photomultiplier Tube (PMT, Thorn EMI 9789QA) which housed a coiled quartz flow cell.

All tubing for the manifold was PTFE (0.75 mm i.d., Fisher Scientific), with the exception of a mixing baffle (silicone, Elkay) and the peristaltic pump tubing (flow rated silicone, Elkay). High power voltage was supplied to the PMT using a 1.1 kV power supply (PM 28B, Thorn EMI). The continuous PMT voltage output was amplified and filtered (LPF-100A, Low Pass Bessel Filter 4 Pole, Warner Instrument Corp.) and then digitised (Minidigi 1A, Axon Instruments). Peak detection and offline analysis was performed using Axoscope 9.0 and Clampfit 9.0 software (Axon Instruments).
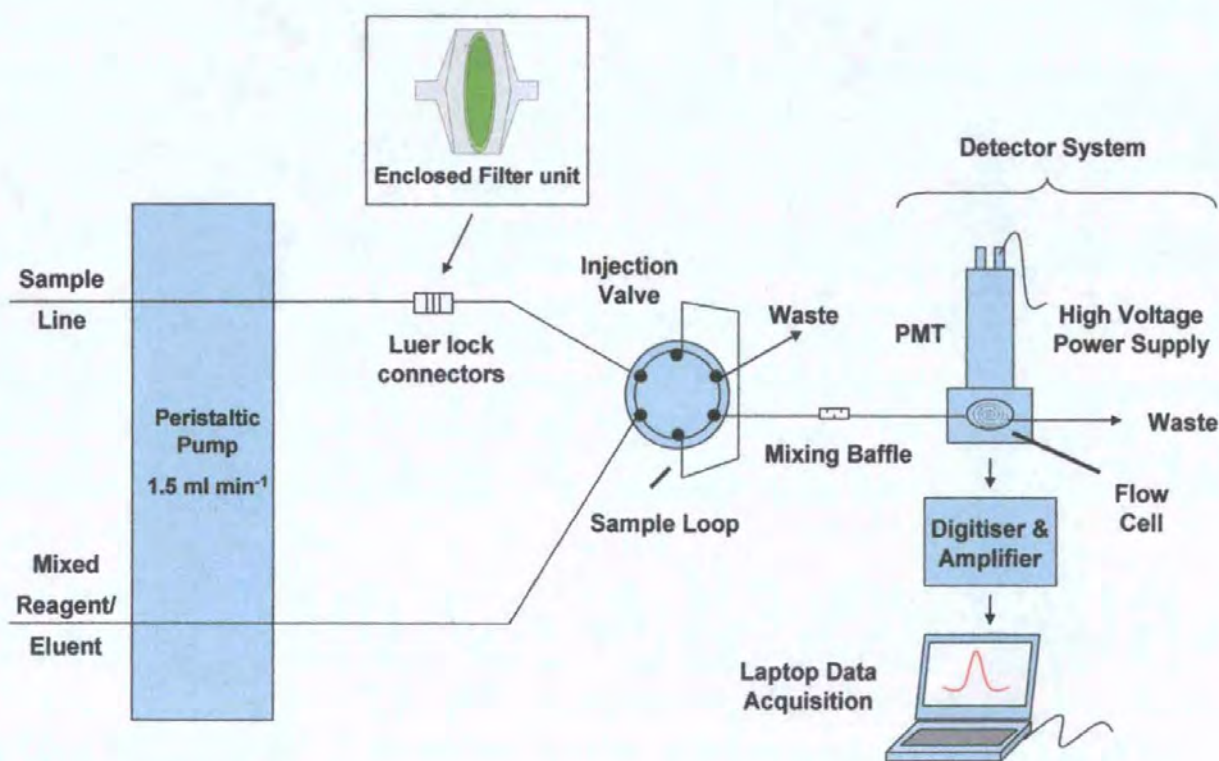
Figure 4.3 Flow Injection manifold for the determination of H_2O_2. For phytoplankton assays a 25 mm enclosed acrylic filter unit (inset) was placed in the sample line using luer lock connectors and FSW continually pumped through the sample line.

For the phytoplankton assay experiments, diatom cells were supported within a clear acrylic 25 mm in-line filter holder (2.5 mL volume, Sartorius) attached to the sample lines using luer lock connectors (Cole Parmer) (see inset in Figure 4.3). Photosynthetically active radiation was provided using a fibre optic lamp (Schott Mainz, K450B) directed onto the cells. This set-up allowed for manipulation of the microenvironment of immobilised cells during experimental assays, both in terms of nutrient availability in the flowing media as well as exposure to light and / or varying temperatures, all of which have been reported to affect the production of reactive oxygen species (Evans et al. 2006).

4.2.4 Method

H_2O_2 concentrations were determined using an FI method adapted from Price et al. (1994). The same method was used for both the analyses of discrete seawater samples and for the phytoplankton assays. However, in addition to the analytical procedure required for discrete sample analyses, e.g. cleaning and preparation of the manifold prior to experiments and workings of the injection valve, additional steps were necessary in order to perform the assay experiments. These additional procedures, involving the collection and placement of phytoplankton cells within the FI manifold, are described separately.

Analytical Procedure for Discrete Sample Analyses

The FI manifold (Figure 4.3) was cleaned prior to the start and at the end of each experiment with 0.5 M HCl for 30 min, this was followed by flushing with UHP water for another 30 min. Prior to all experimental runs, the system was operational with reagents and FSW flowing for at least 30 min to ensure baseline stability and condition sample lines.

On initiation of an analytical cycle, the injection valve was placed in the load position (Figure 4.4 (a)) and discrete seawater samples, previously collected and stored in the cold and

dark, were pumped via the sample line into the sample loop (60 μL). After a load time of ~ 10 s, the valve was manually switched to the elute position, the sample was eluted in the reverse position with the mixed reagent (Figure 4.4 (b)) and delivered to the detector after 2.4 sec. This combined reagent - sample solution was then pumped to the flow cell housed in the detector system. The photons produced from the subsequent chemiluminescence reaction generated a signal in the form of a narrow peak. Each injection was completed in ~ 1 min and each sample was analysed four times. One analytical cycle for an individual sample was therefore completed in ~ 4 min, and the mean of the four peaks from each injection was taken as the H_2O_2 concentration.
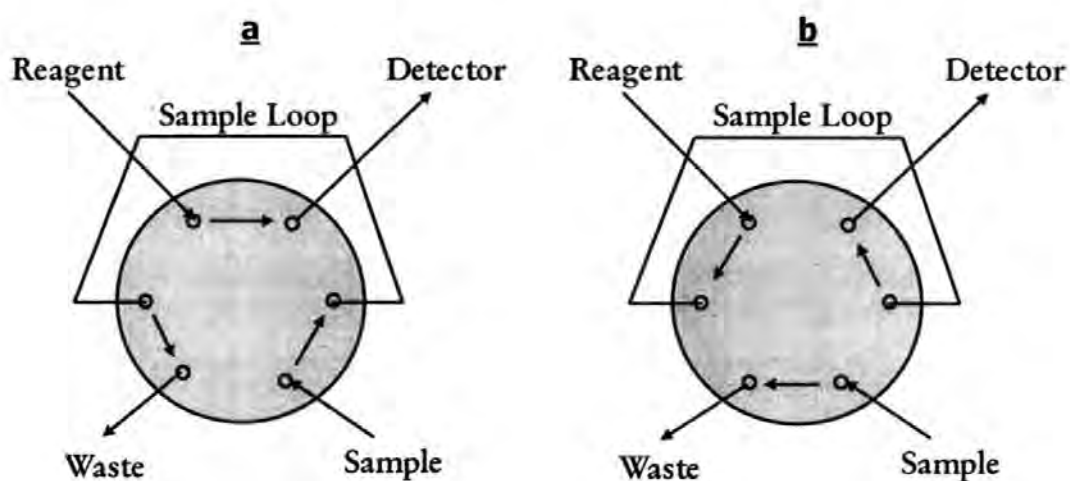
Figure 4.4 Manual injection valve showing (a) load and (b) elute positions.

Procedure for investigating H_2O_2 production by phytoplankton

The same procedures relating to cleaning, preparation and sample injection, as described above, were applied in conjunction with the following four additional steps (Figure 4.5). (1) Cells from cultures of *T. weissflogii* were harvested and concentrated by filtration (3 μm polycarbonate, 47 mm, Whatman Cyclopore™ Track Etched) and (2) washed and re-suspended in FSW. Re-suspended cells were transferred to clean containers and acclimated in the dark for at least 20 min before use in experiments. (3) From the cell suspension, a fixed

volume was transferred, by syringe, onto a 25 mm diameter (0.4 µm Whatman Cyclopore™) filter membrane which was supported in the transparent filter holder. (4) The filter unit was placed in the sample line of the manifold using the luer lock connectors. Cells were flushed continually with FSW in the dark for 15 min before the start of assays at a flow rate of 1.5 mL min^{-1}, this was maintained throughout the experiments.

Assays typically lasted 1 - 2 h, during which time the immobilised cells were intermittently exposed to varying light levels (30 – 500 µmol photons m^{-2} s^{-1}) and the filtrate analysed. Between each light period the immobilised cells were returned to the dark until the H$_2$O$_2$ signal returned to a consistent value, typically close to the baseline. Similar to discrete sample analyses, manual injections of the FSW filtrate were performed (~ one injection min^{-1}) to determine the H$_2$O$_2$ generated by the cells. Prior to calibration, the filter unit was by-passed and standards injected through the sample line.
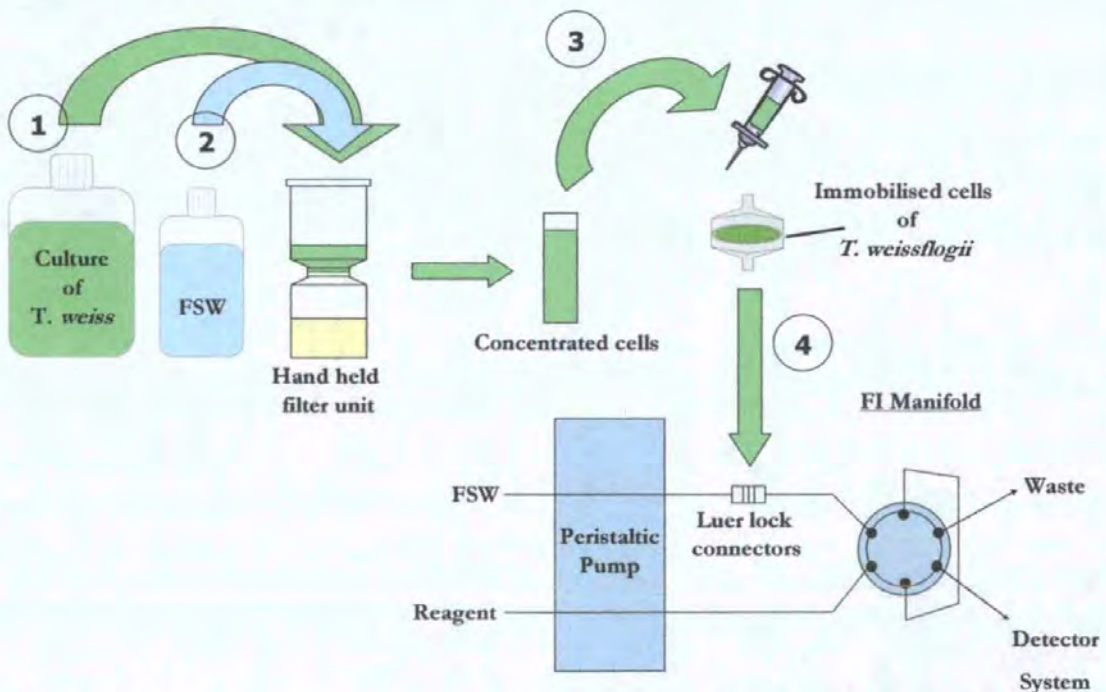
Figure 4.5 The key stages in preparing for an assay experiment to determine H$_2$O$_2$ production by phytoplankton. (1) Filtration and concentration of diatom cells using a hand held filtration unit, then (2) washing and re-suspending the cells in FSW before collection of the concentrated cells into a clean plastic vial. (3) The transfer of a fixed volume of the concentrated cells into the filter unit using a sterile syringe, and (4) placement of the filter unit within the FI manifold using the luer lock connectors.

Control experiments to determine the extent of any abiotic or photochemical generation of H_2O_2 in the absence of biomass was conducted using the same apparatus without micro-algal cells. Additionally, to demonstrate the specificity of the FI-CL H_2O_2 signal, the H_2O_2 scavenging enzyme, catalase, was added to the FSW flowing over the cells.

4.2.5 Calibration and blanks

Calibrations were performed in a matrix to match the respective study area or experiment. In fields studies carried out in the English Channel and Southern Ocean, this constituted seawater from the deepest cast, representing the lowest in H_2O_2 concentration. For the phytoplankton assays, the previously collected and aged FSW was used. Standard additions of H_2O_2 were made in the range 10 – 200 nM, equating to 10 – 200 μL additions from a 50 μM standard stock to 50 mL of respective seawater. The standards were immediately analysed and used to generate standard curves. The H_2O_2 system was calibrated before and after each experimental run to account for any change in sensitivity.

In order to ensure accurate calibrations over the period of the study, the concentration of the stock solutions of H_2O_2 were periodically determined using potassium permanganate. This is based on the following reaction which occurs when $KMnO_4$ is added to H_2O_2 solution acidified with H_2SO_4:

$$2MnO_4^- + 5H_2O_2 + 6H^+ = 2Mn^{2+} + 5O_2 + 8H_2O$$
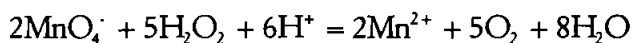
The full procedure relating to standardisation is detailed in Vogel (1989), but briefly, dilute solutions of stock H_2O_2 (30%) were acidified with dilute H_2SO_4 (1 : 5 v/v H_2SO_4 : UHP water) and titrated with standard potassium permanganate (0.02 M) until the persistence of a faint purple colour signified the end point.

The blank was determined using either seawater from the deepest cast (field studies) or FSW (assays), this was analysed in the same manner as the standards and includes any signal associated with the reagents and the manifold. The contribution of this blank signal was calculated during the calibration process and subtracted from the final sample concentrations.

4.3 Results and Discussion

4.3.1 Optimisation of Analytical Parameters

The method taken from Price et al. (1994) was modified to improve mixing and sensitivity. The two separate reagent streams previously used were combined to a single reagent solution and the instrumental apparatus altered accordingly. In the new instrument configuration, the combined solution became both reagent and sample eluent. The addition of a mixing baffle prior to the combined sample-eluent solution entering the quartz flow cell (Figure 4.3) was to ensure complete mixing of the sample and reagent.

To establish and confirm the optimum conditions for the improved method, the two main analytical parameters affecting the chemiluminescence signal were investigated; the pH of the reaction and the system flow rate.

pH dependency of chemiluminescence

The chemiluminescence reaction (quantum efficiency) of the chemiluminescent dye, luminol, is highly pH sensitive. To establish the optimum pH of the mixed luminol / Co(II) reagent, five solutions with pH varying from 9.2 – 11.5 were prepared. The reagent was
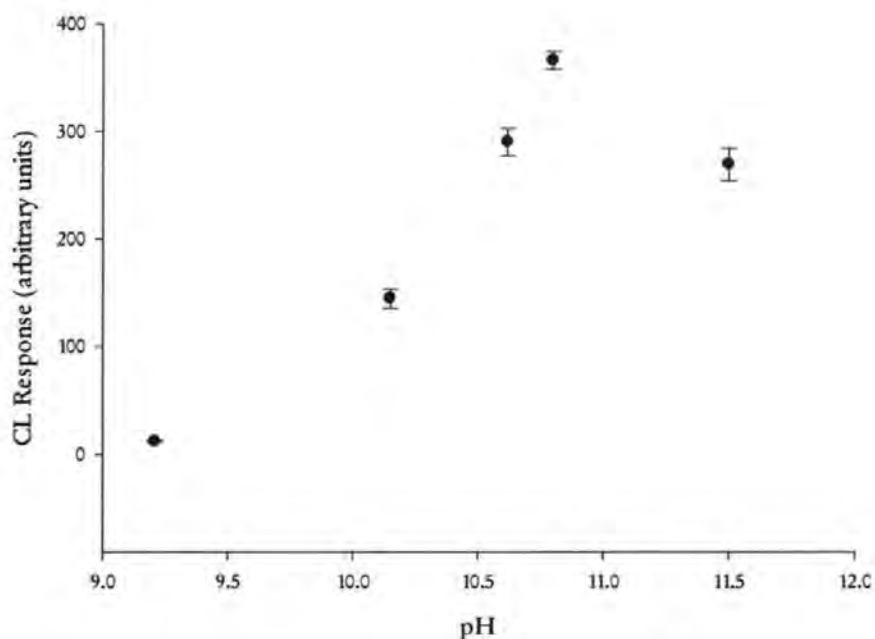
Figure 4.6 Optimum pH of the mixed luminol-Co(II) reagent corresponding to replicate injections of a 100 nM H_2O_2 standard ($n = 3$) prepared in FSW. (Error bars represent one standard deviation).
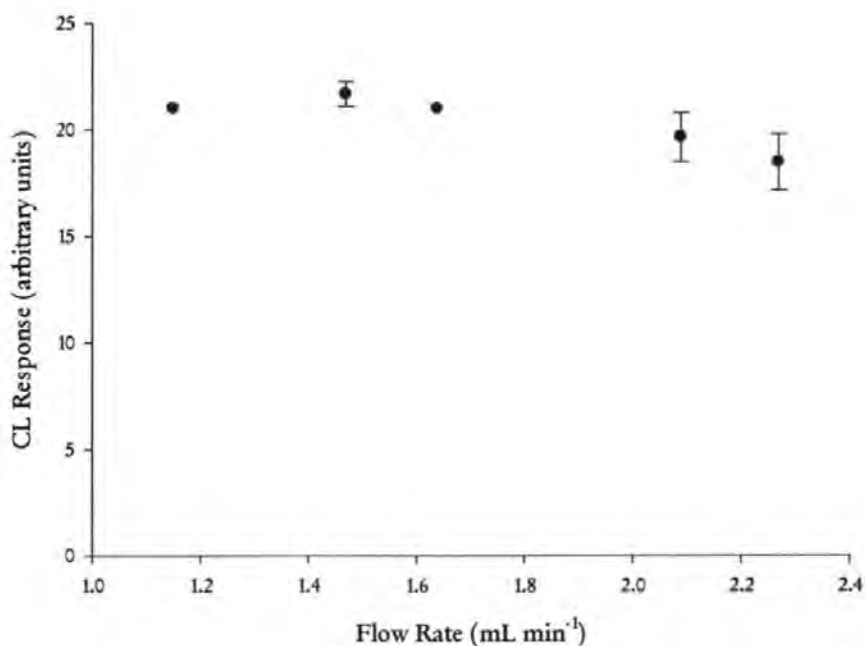
Figure 4.7 Optimal flow rate for the mixed luminol-Co(II) reagent system corresponding to replicate injections of a 50 nM H_2O_2 standard ($n = 3$) prepared in FSW. (Error bars represent one standard deviation).

buffered with 0.1 M Na₂CO₃ and the pH adjusted through the addition of concentrated HCl. The optimum chemiluminescence response of a 100 nM H_2O_2 standard prepared in FSW was recorded at pH 10.8 (Figure 4.6). This confirmed the pH reported by Price et al (1998; 1994) using a system with separate luminol and Co(II) reagent streams.

Flow rate

While a range of flow rates from 1.1 to 2.3 ml min-1 gave excellent peak detection, the optimal flow rate for the system was determined as 1.5 mL min⁻¹ (Figure 4.7), this corresponded to the maximum peak response from replicate injections ($n = 3$) of a 50 nM standard prepared in FSW. This flow rate was also considered to be feasible for maintaining the integrity of the diatom cells contained within the filter unit when carrying out phytoplankton assay experiments (Dr. M. Davey, personal communication), this flow rate was therefore maintained for all experimental analyses. This was similar to Price et al (1998; 1994) where a flow rate of 1.6 mL min⁻¹ was used.

4.3.2 Calibration and blanks

Using the optimum conditions described, replicate analyses ($n = 4$) were performed for all standard solutions when calibrating the system. The standard graphs generated were used to calculate the concentration of H_2O_2 in respective experiments. For the calibrations carried out during coastal field studies in the English Channel and in the laboratory based phytoplankton assays, the standard graphs were typically linear in response (Figure 4.8). In the Ross Sea of the Southern Ocean however, calibration graph tended to be parabolic (Figure 4.9), even at the low concentration range under study, and required a parabolic least-squares fit. A typical trace for standard additions of 10 – 50 nM for the two calibrations are shown in Figures 4.8 and 4.9, the mean repeatability and standard deviations for four replicate analyses

over this range are shown and compared in Table 4.1. In both instances, the correlation coefficients (r^2) for the calibration curves generated were better than 0.98 (and typically > 0.99).

Table 4.1. Analytical figures of merit for H_2O_2 determination*

	Laboratory Analyses	Shipboard Analyses
Blank	3.7 ± 1.1	1.0 ± 0.6
Detection Limit	1.3 ± 1.1 ·	0.4 ± 0.3
Precision, RSD (%)§	1.8 ($n = 4$)	1.1 ($n = 3$)
Sensitivity (mV nM[-1])	3.9 ± 1.9 ($n = 9$)	4.6 ± 3.6 (n = 9)
Linear Range	10 – 200	Dynamic
Sample Throughput	~60 h^{-1}	~60 h^{-1}

* All data given in nM (unless otherwise indicated). Error bounds indicate ± one standard deviation. The figures represent the mean of all data gathered during experiments.
§The precision is calculated as the percent relative standard deviation (%RSD) and based on repeatability between replicate measurements of a 50 nM standard.

The blank contribution to the H_2O_2 method arises from three sources; the manifold, the seawater used for the blank analysis and the reagents. The contribution from the luminol-Co(II) reagent was minimised by using a mixed reagent system, which not only simplified the preparation but also led to the removal of residual traces of hydrogen peroxide. The mixing of luminol and Co(II) at the optimum pH (described above) produces a chemiluminescence reaction with any H_2O_2 present in the solution (Yuan and Shiller, 1999). Leaving the mixture overnight, not only ensured complete dissolution of the luminol and Co(II) reagents, but also ensured that residual H_2O_2 was removed by decay. To minimise the chemiluminescence signal produced from the seawater used for blank analysis, and to account for the signal associated with the mixed reagent and also the manifold, seawater collected from depth and stored in the dark was used. H_2O_2 concentrations typically show a distinct exponential profile (Croot et al., 2004b; Yuan and Shiller, 2001) with maximum concentrations in surface waters which decrease with depth. In addition, even though H_2O_2 is the most stable of the reactive oxygen

species, it still dissipates over time with a reported half-life ranging from hours to days (Cooper et al., 1994; Petasne and Zika, 1997; Yuan and Shiller, 2001; 2005). The signal, therefore, produced from stored deep seawater should be lower then surface water concentrations and was used in all blank measurements and calibrations.
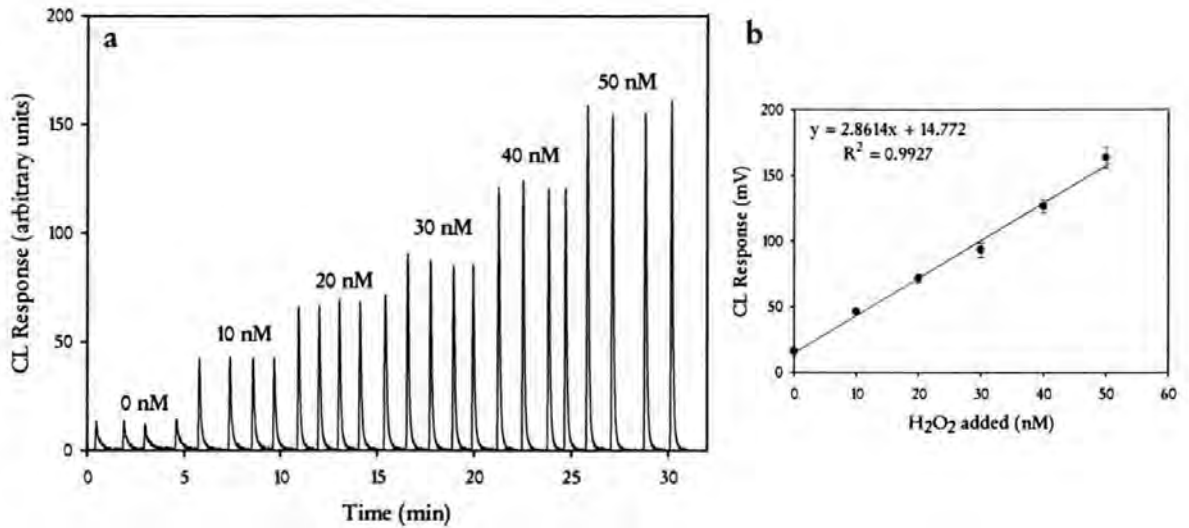
Figure 4.8 (a) Calibration peaks and (b) corresponding standard addition for H_2O_2 over the range 10 – 50 nM in FSW for land based analysis. Error bars represent 2 standard deviations.
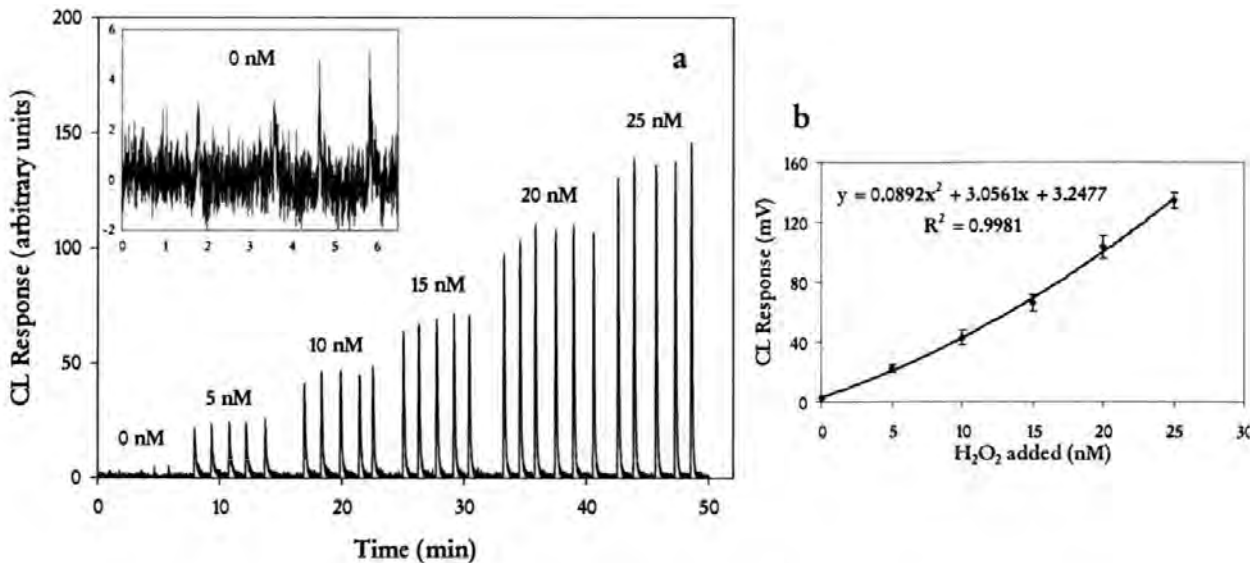
Figure 4.9 (a) Calibration peaks and (b) corresponding standard addition for H_2O_2 over the range 10 – 50 nM in deep seawater for analysis carried out in the Ross Sea. The signal for the blank (0 nM) is further highlighted (inset). Error bars represent 2 standard deviations.

The analytical figures of merit for the operation of the system at sea and in the laboratory are listed in Table 4.1. The mean blank signal produced during land based (coastal samples and assay studies) and shipboard (Ross Sea) analyses was 3.7 ± 1.1 nM, ($n = 28$) and 1.0 ± 0.6 nM, ($n = 35$) respectively, resulting in respective limits of detection of 1.3 nM and 0.4 nM (defined as three times the standard deviation on replicate analyses of the blank ($n = 4$)). Though the deep water used for calibrations in the Ross Sea was stored for a short period of time (typically < 1 day), the lower blank signal and corresponding detection limit are indicative of the lower H_2O_2 concentrations found in general in the water column of the Ross Sea region, but particularly at depth. The sampling limitations of the coastal bloom study and for the FSW used in the phytoplankton assays resulted in seawater being collected from a maximum depth of 60 m. In contrast, the seawater used for blank measurement and calibrations in the Ross Sea was collected from a minimum depth of 300 m where H_2O_2 concentrations were typically < 1 nM.

4.3.3 Field results from the English Channel and Southern Ocean

The results from field studies carried out in the coastal shelf region of the English Channel and the Ross Sea region of the Southern Ocean are detailed below.

Profiles from the English Channel

While there have been previous laboratory based studies investigating the generation of H_2O_2 and / or O_2^- by a number of phytoplankton, particularly species which cause seawater discolouration also known as red tide e.g. *Heterosigma carterae*, *Chattonella marina*, (Asai et al., 1999; Kustka et al., 2005; Lee et al., 1995; Oda et al., 1997) few, if any, have investigated this phenomenon in the field. The regular seasonal occurrence of a summer coccolithophore (phylum Haptophyta) bloom dominated by *Emiliania huxleyi* provided an opportunity to

undertake a study in the English Channel. In order to investigate the influence that biological ROS production may have on H_2O_2 concentrations in the water column, depth profiles were conducted in two locations (inside and outside the bloom) during two separate bloom events in August 2005 and July 2006.

The depth profile results from both August 2005 and July 2006 (Figure 4.10) show enhanced H_2O_2 concentrations in surface waters, and a reduction to near detection limits at depth. The concentrations are consistent with previously reported open ocean profiles for H_2O_2 (Croot et al., 2004b; Yuan and Shiller, 2001). Upper surface waters, particularly in coastal regions, typically exhibit higher hydrogen peroxide concentrations. The elevated levels of dissolved organic matter (DOM) and light penetration in the upper water column, components involved in the photochemical formation of H_2O_2 (Cooper et al., 1988; Millero, 2006; Yocis et al., 2000), are two factors that influence the concentration changes through the water column (chapter one provides a more detailed explanation of this H_2O_2 production pathway).

From the profiles shown here (Figure 4.10) it is evident that, in both years, the surface (< 20 m) concentrations of H_2O_2 inside the bloom, ~ 150 nM (2005) and ~ 85 nM (2006), were higher than those determined outside, ~ 100 nM (2005) and ~ 45 nM (2006) and supports the hypothesis of phytoplankton mediated ROS production. However, samples were not collected at the same light period in each year and therefore this may contribute to the differences observed.

Overall, the concentrations in 2005 (> 100 nM) were higher than those in 2006 (< 100 nM). This difference in surface concentrations may be related to the growth stage of the bloom. In 2005 the coccolithophore bloom was nearing the end of its growth cycle, whereas in 2006 the bloom was in a mid to late growth stage. However, other factors also need to be considered. Photochemical production is a major pathway for the formation of H_2O_2 in

surface waters, therefore the time of day samples are collected will play a factor in the concentrations observed (Miller and Kester, 1994; Yuan and Shiller, 2001; 2005; Zika et al., 1985). In addition weather conditions, such as cloud cover, wind, turbulence of waters and temperature, can influence either photochemical production and / or mixing of surface waters and hence the surface water mixed layer.
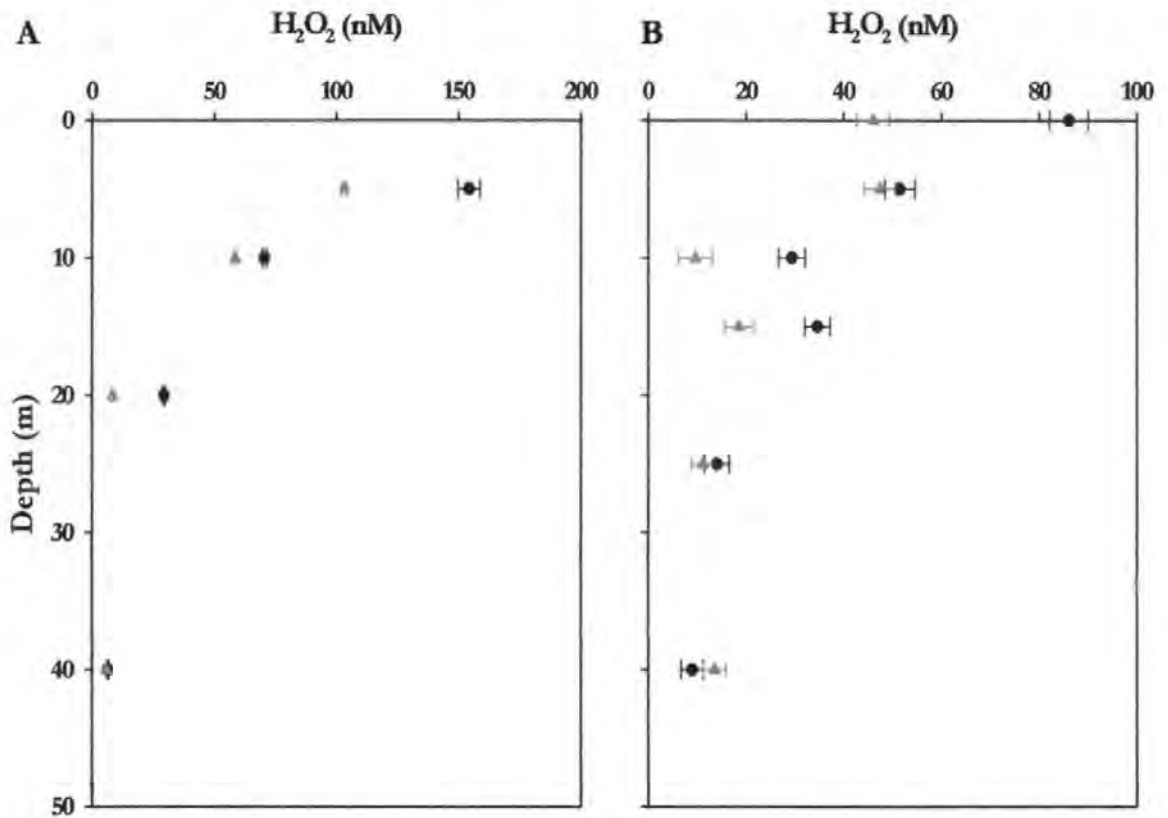
Figure 4.10 Depth profiles from samples collected inside (●) and outside (▲) the *Emiliania huxleyi* blooms. (A) August 2005 and (B) July 2006.

The H_2O_2 profiles presented here are the result of an opportunistic investigation and, although they compare profiles from only two locations (inside and outside the coccolithophore bloom), they provide an indication of the potential affect this massive bloom-forming phytoplankton species can have on peroxide concentrations in surface waters. From the higher H_2O_2 concentrations observed within the bloom, it is possible to interpret H_2O_2 production by this species. Further intensive field studies (including complete transects and time series analyses over diel cycles) would need to be undertaken to confirm the observations

of this study. However, these exploratory investigations provided the impetus for the laboratory based study of H_2O_2 production involving a different algal species discussed in section 4.3.4.

Profiles from the Ross Sea, Antarctica

Substantial rates of primary production have been associated with the coastal polynyas (an area of open water surrounded by ice) located over the Antarctic coastal shelf (Arrigo and van Dijken, 2003). The Ross Sea polynya is the Antarctic's most productive where the colonial haptophyte *Phaeocystis antarctica* blooms profusely in weakly stratified waters (Arrigo et al., 2000; Arrigo and van Dijken, 2003; Smith et al., 2000). There are no data available on viral lysis on P. Antarctica in the Ross Sea, and losses due to grazing are low (Caron et al., 2000). The period of sampling (November to early-December) was characterised by substantial ice cover, low irradiance (though 24 h sunlight had been reached) and small periods of extreme winds which reduced air temperatures to ~-40 °C.

In contrast to the coastal environment, and to most open ocean regions, Antarctic waters are noted for their low H_2O_2 concentrations (Croot et al., 2005; Sarthou et al., 1997). The low incidence of solar radiation combined with ice cover result in the lower concentrations of this reactive species. The H_2O_2 measurements carried out in the Ross Sea were part of a scientific study investigating a range of parameters, including nutrients and trace metals, in the water column and relating these to the growth and taxonomic species of the resident algal community. To complement the initial field investigations carried out in the English Channel, and to contrast with results from a different climate and different planktonic species, the H_2O_2 results were related to shipboard hydrographical measurements (such as fluorescence) to examine the hypothesis of biological H_2O_2 production. While discreet chlorophyll measurements were performed during the cruise, fluorescence can also be used as an indication of biomass and was used for comparative purposes.
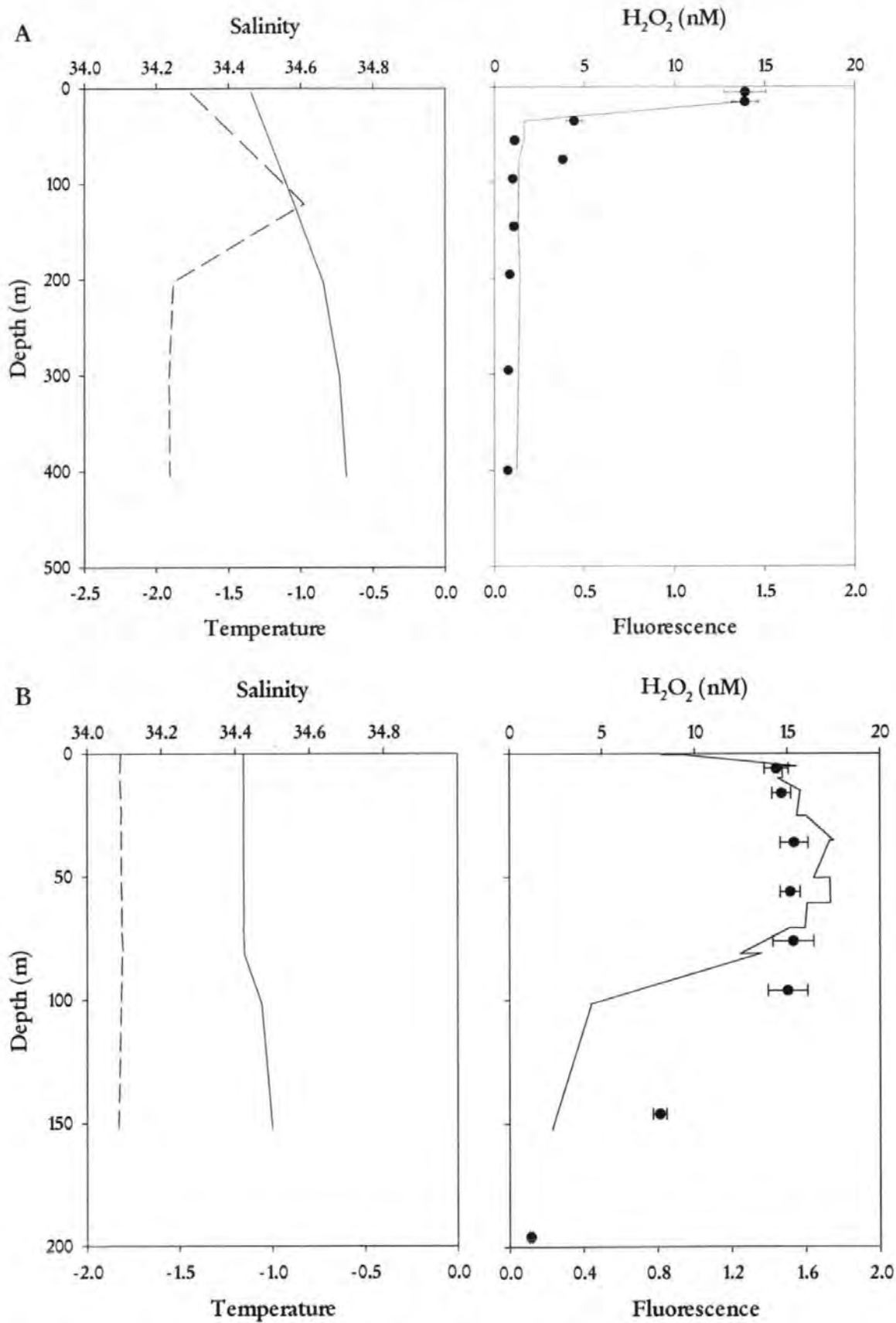
Figure 4.11 Profiles of H_2O_2 obtained from two stations (A) NX-13 and (B) NX-14 in the Ross Sea. (●) fluorescence (solid black line), salinity (solid blue line) and temperature (dotted black line). The location of the profiles is shown in Figure 4.12.
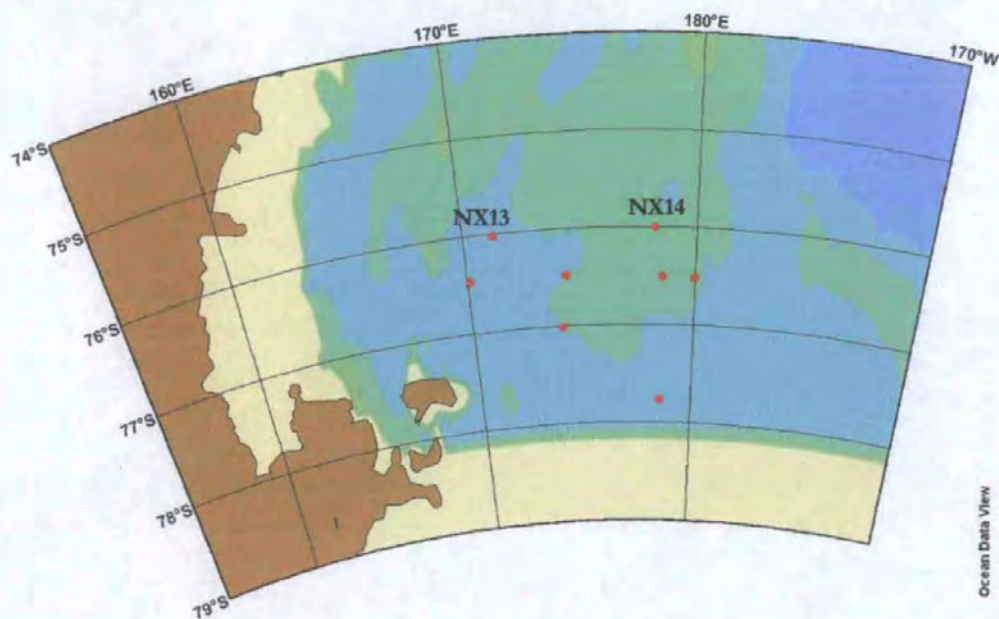
Figure 4.12 Location of sampling stations in the Ross Sea, NX-13 and NX-14 are highlighted.

Table 4.2 details the concentrations of H_2O_2 observed during the field campaigns undertaken during this study, also included are data from previously reported studies. The H_2O_2 profiles from the Ross Sea (Figure 4.11) are consistent with previously reported H_2O_2 data (Sarthou et al., 1997) and are typical of the profiles observed during the CORSACS cruise. Data from two stations are presented, NX-13 and NX-14 (Figure 4.12), to illustrate results from areas with different water masses. At station NX-13 (Figure 4.11 (A)), H_2O_2 concentrations decreased sharply with depth from ~ 14 nM to sub-nanomolar levels in the first 50 m. Additionally, a change in the water column dynamics is evident, salinity and temperature changed during the first 200 m, although these changes did not affect H_2O_2 concentrations. In contrast, for station NX-14 (Figure 4.11 (B)), H_2O_2 concentrations were sustained at ~ 15 nM to a depth of 100 m before gradually decreasing to ~ 1.0 nM. For both stations, the vertical variations of H_2O_2 correlated with the changes in fluorescence in the water column.

Table 4.2 A compilation of H_2O_2 concentrations observed in surface seawater[*].

Study Location		H_2O_2	Reference
Coastal:	English Channel – inside coccolithophore bloom	85 - 150	This study
	English Channel – outside coccolithophore bloom	45 - 100	This study
Polar:	Ross Sea	·15 - 20	This study
	Southern Ocean	5 - 20	Sarthou et al. 1997
Temperate	Equatorial Atlantic Ocean	24 - 300	Yuan and Shiller 2001
	Mediterranean	25 – 125 16 - 154	Johnson et al. 1987 Price et al. 1998
	Northwest Pacific	<10 – 250	Yuan and Shiller 2005
	Northeast Gulf of Mexico	100 – 200	Zika et al. 1985a
	Peru upwelling region	8 – 50	Zika et al. 1985b

[*] All data presented in nM.

The low hydrogen peroxide concentrations determined for the two profiles presented (<20 nM) are typical of values recorded at all stations during the cruise. These concentrations are consistent with other studies in the Southern Ocean where a range of <LOD to 30 nM have been reported (Croot et al., 2005; Sarthou et al., 1997). In both instances, the H_2O_2 concentrations observed at the two stations followed fluorescence data and provides further more substantial evidence of a biological contribution to the concentrations of this reactive species in the surface of the ocean.

4.3.4 Results from Phytoplankton Assay Experiments

The data above supports the hypothesis that phytoplankton metabolism may directly contribute to the concentration of H_2O_2 in surface waters. Such biological production of H_2O_2 arises as a metabolic by-product of aerobic respiration and oxygenic photosynthesis (Falkowski and Raven, 1997; Fridovich, 1998). Both processes leak approximately 1 – 4 % of

their electrons internally to O_2 (Halliwell, 1982), producing O_2^- and subsequently H_2O_2 inside the phytoplankton cell. Additionally, H_2O_2 can be produced extracellularly by reduction of O_2 at the cell surface. There is evidence to support similar NADPH oxidase-like cell surface enzyme activity that can transfer electrons across the plasma membrane to external O_2 thus generating superoxide in the extracellular medium at the surface of the cell (Kim et al., 1999; Twiner and Trick, 2000). This generation of ROS has been associated as a physiological response to abiotic and biotic stress (Bolwell, 1999). A schematic representation of these processes is shown in Figure 4.13.
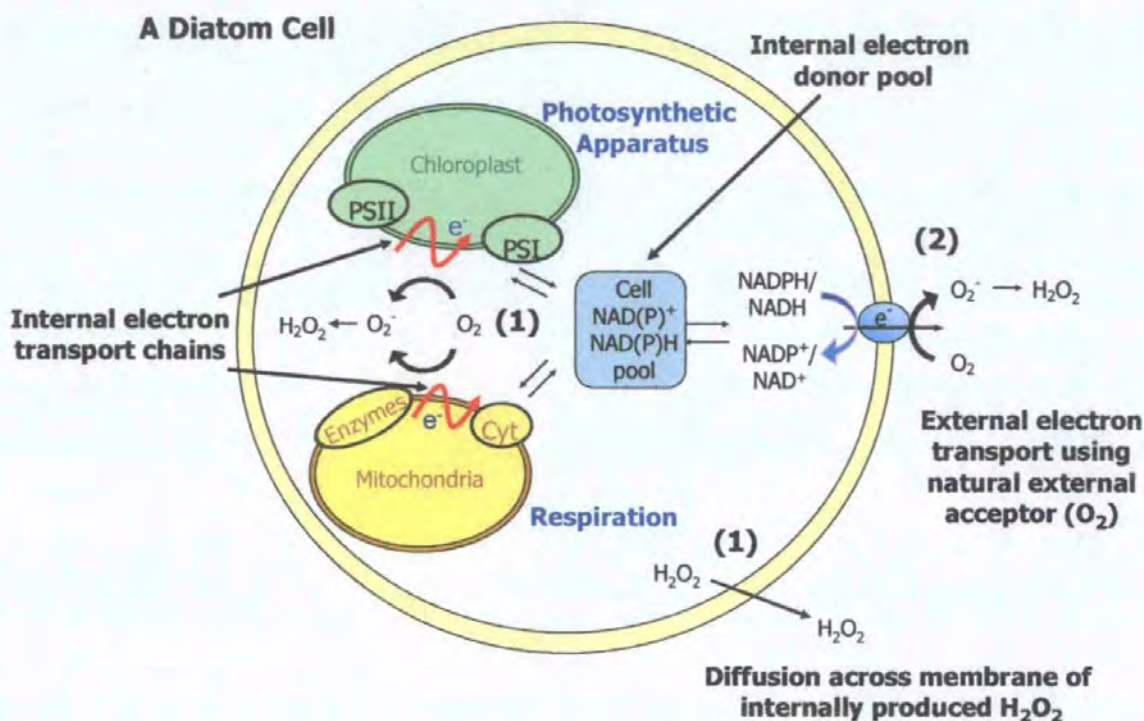
Figure 4.13 A schematic figure of H_2O_2 production by a diatom. (1) Internally produced H_2O_2, arise as a result of reduction of O_2 and subsequent dismutation to H_2O_2. This is known to occur via electron leakage from the electron transport processes of the mitochondria and chloroplast. H_2O_2 is membrane permeable and if not quenched by intracellular antioxidant mechanisms may diffuse across the outer plasma membrane. (2) Externally produced H_2O_2, following the disproportionation of O_2^-, through the cell surface reduction of O_2, the natural terminal electron acceptor.

Diatoms, unicellular algae of the class Bacillariophyta, are noted as being widespread bloom-forming organisms. During single cell experiments, it was demonstrated that photosynthetic metabolism interacts with constitutive plasma membrane electron transport activity in marine diatoms in the presence of artificial electron acceptors (Davey et al., 2003). Diatoms have also demonstrated a high capacity for plasma membrane electron transport (Taylor and Chow, 2001). For the assay experiments performed during this study, diatoms cells of the species *T. weissflogii* were used to investigate plasma membrane electron transport activity in the presence of a natural electron acceptor (O_2) and hence production of ROS. During the assay experiments different light regimes were adopted with the goal of stimulating the cells internal metabolic processes, any subsequent H_2O_2 production produced as a result of this stimulation was determined in the cell filtrate and monitored continually during the assays.

The production of H_2O_2 by diatoms was investigated through the incorporation of an in-line transparent filter unit to immobilise phytoplankton cells upstream of the FI-CL detector system. This system allowed the cells to be constantly flushed with flowing media and the environmental conditions to be manipulated without interfering with downstream detection of H_2O_2 in the filtrate solution. The coastal diatom *Thalassiosira weissflogii* was used in the preliminary assay experiments to determine H_2O_2 production and how this may be influenced by light. The compact transparent filter holders could be readily illuminated or shielded during light and dark exposures. The small volume of the filter holder (2.5 mL) and the flow rate used resulted in a relatively short residence time (~ 1.7 min), ensuring minimal loss of signal. During the assays, immobilised cells were exposed to three different light intensities, 30, 150 and 500 μM photons m^{-2} s^{-1}, using a non-UV irradiating source. The light intensity was calibrated using a photon counter, light from the source was passed through the filter unit and the required intensity recorded.

Initially control experiments were performed, in the absence of cells, to account for any abiotic photochemical generation of H_2O_2 in FSW. Increases in the chemiluminescence signal were observed at irradiances above 150 μM photons m^{-2} s^{-1} (Figure 4.14). When the experiments were repeated with cells in the filter chamber, larger light-dependent H_2O_2 signals were observed within seconds of light exposure (Figure 4.14). The small, gradual background signals generated represented < 10 % of the signal in the presence of the cells, which was instantaneous and evident at all light intensities. These assay experiments demonstrated that it is possible to monitor, in real-time, with great sensitivity the effect of light exposure on the production of H_2O_2 by *T. weissflogii*. To further demonstrate the specificity of the H_2O_2 production by *T. weissflogii*, catalase (a H_2O_2 scavenging enzyme) was added to the FSW flowing over the cells. The rapid and complete quenching of the signal upon addition of the enzyme is shown in Figure 4.15

Typically the H_2O_2 signal generated by the diatoms when exposed to the increasing light intensities (between 4 – 33 nM, Figure 4.14) corresponded to production rates ranging from 1.1 – 6.6 x 10^{-16} mol H_2O_2 $cell^{-1}$ h^{-1}. These rates were calculated by taking into account the flow rate of the system and the cell numbers (calculated as described in the section *Phytoplankton Cultures for Assay Experiments*) contained in the filter unit using the following equation;

$$\frac{H_2O_2 \text{ (nM)} * \text{Flow Rate (L min}^{-1}\text{)}}{\text{Cell Numbers}}$$

The calculated rates are comparable to previous laboratory based assays performed using another H_2O_2 fluorogenic probe Amplex Red™ (3.1 x 10^{-16} mol H_2O_2 h^{-1}, M. Davey, personal communication). During dark periods, the average production rate was an order of magnitude lower, 5.8 x 10^{-17} mol H_2O_2 $cell^{-1}$ h^{-1}, based on a H_2O_2 signal generated by the diatoms of between 1.7 – 3 nM (Figure 4.14).

114
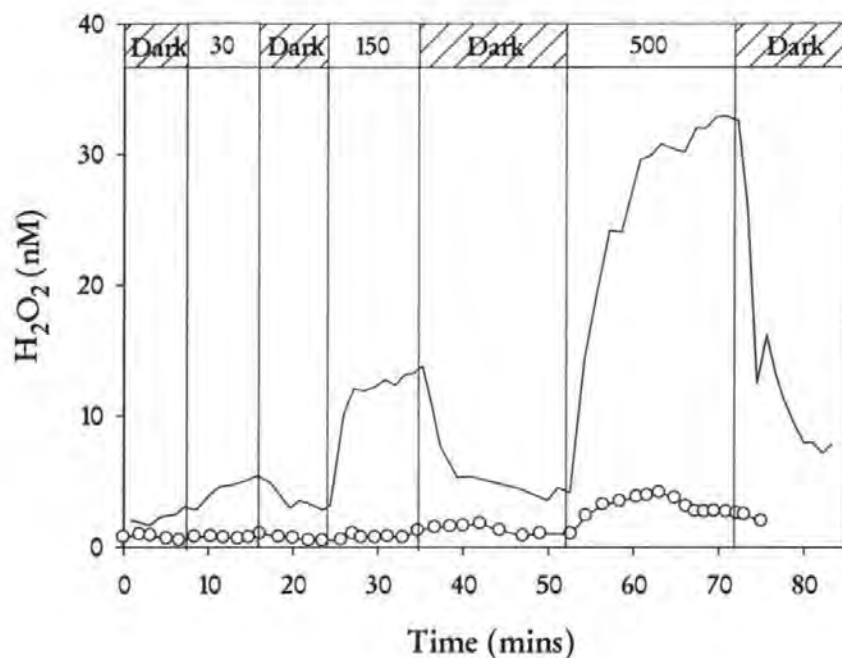
Figure 4.14 Light dependent H_2O_2 production by *T.weissflogii*. Typical light response data are shown for the production of H_2O_2 when the in-line filter unit was loaded with *T. weissflogii* (–) and without cells (-o-) and exposed to periods of light (μmol photons m^{-1} s^{-1}) as indicted in the bar at the top of the graph.
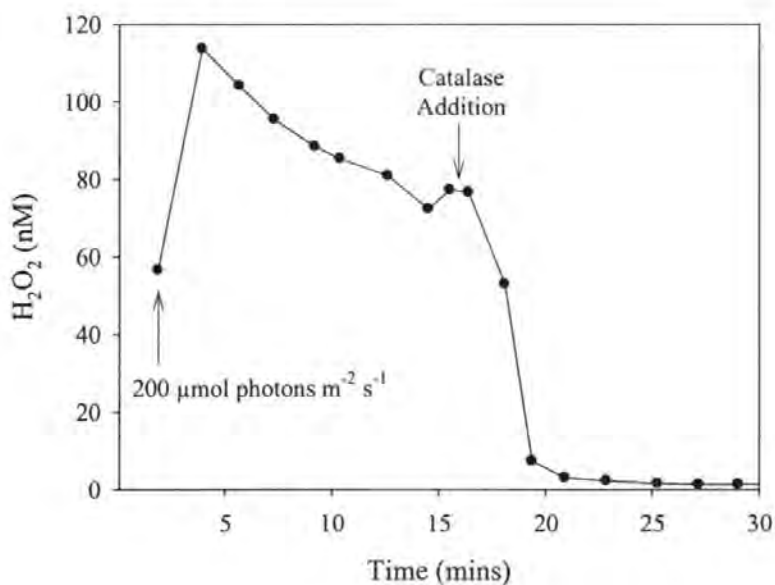
Figure 4.15 Specificity of H_2O_2 production and detection. A representative trace showing that in the presence of *T.weissflogii* cells light-stimulated increase in luminol signal was completely quenched by 1 – 3 U mL^{-1} of the H_2O_2 scavenging enzyme catalase.

Finally, it was predicted that biological production of H_2O_2 would be proportional to the biomass present. This was examined by conducting experiments in which increasing numbers of cells were immobilised on a filter within the filter holder and exposed to a fixed irradiance level. In these experiments H_2O_2 production was clearly proportional to the biomass present on the filter (Figure 4.16).
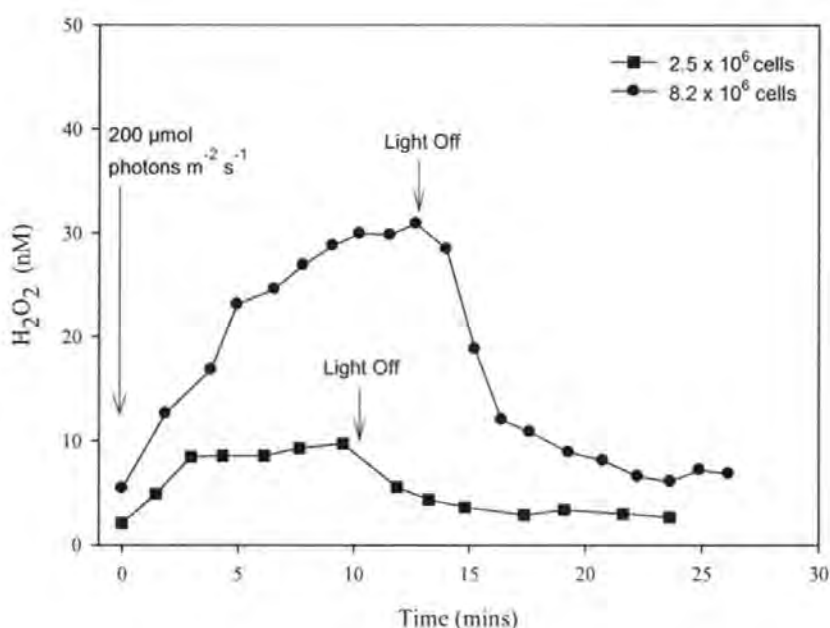
Figure 4.16 Effect of phytoplankton biomass on H_2O_2 production. The cell density supported by the in-line filter unit was increased and light-stimulated H_2O_2 production monitored for each biomass level.

4.4 Conclusions

The overall aims and objectives of this study have been accomplished. A versatile and adaptable FI system has been developed, with low detection limits (< 1 nM), excellent precision (1.1 – 1.8 %RSD) and capable of sensitive real-time determination of H_2O_2 concentrations over a dynamic concentration range. This system has been utilised both in the

116

field, enabling H_2O_2 concentrations from different oceanic regions to be compared, and adapted for the direct analysis of phytoplankton H_2O_2 production under varying light regimes.

The H_2O_2 profile data collected in the English Channel and the Ross Sea, is indicative of a relationship between H_2O_2 concentrations and phytoplankton. This is particularly evident from the Ross Sea data, where a direct correlation between fluorescence and H_2O_2 concentrations was observed. This relationship was investigated in laboratory studies and the production of H_2O_2 by the diatom species, *T. weissflogii* demonstrated.

The technique described here for the determination of diatom H_2O_2 production should be applicable to a wide range of studies where high sensitivity, real-time analysis of biological H_2O_2 production is required. The technique can be used to further investigate H_2O_2 production in a range of phytoplankton species and, because the abiotic environmental conditions can be readily manipulated, how this production may be affected by nutrient limitation and / or light. The method may also be used in field studies to estimate biological H_2O_2 production of natural populations in surface waters.

The results presented for H_2O_2 production by the diatom *T. weissflogii* are a measure of gross cellular ROS production. The H_2O_2 measurements include any signal that would have been associated with O_2^-, following its rapid disproportionation to H_2O_2 (due to a reported half life of seconds to minutes (Zafirou 1990; Millero 2006)), and also include intracellular production due to the membrane permeability of H_2O_2 (Figure 4.13) which can readily diffuse out of the cell. For a more comprehensive understanding of ROS production, and to resolve extracellular from gross cellular production, O_2^- production also needs to be accounted for. A method based on the techniques described here has been developed in order to measure both O_2^- in parallel with H_2O_2 to achieve this (Milne et al. submitted). In combination, the two assay methods can provide simultaneous real-time data on intra and extra-cellular ROS

production based on the differing permeability properties of H_2O_2 and O_2^-.

In summary, the method described has the potential to contribute to our understanding of the role phytoplankton ROS production plays in nutrient acquisition such as iron. Recently, Kustka et al. (2005) determined O_2^- (the pre-cursor to H_2O_2) generation by *T. weissflogii* grown under constant light, and concluded that whilst iron(III) could be reduced by O_2^-, this mechanism was responsible for only transient generation of iron(II) and unlikely to play a major role in iron assimilation in this organism. In contrast, Rose et al. (2005) suggest that O_2^- production by the coastal cyanobacterium *Lyngbya majuscule* facilitates increased iron uptake and speculated that this is a reasonably widespread process. The redox reaction involving both H_2O_2 and O_2^-, affects the speciation of iron. The role that phytoplankton may play in this iron cycle is poorly understood, in order to address this issue the filter unit apparatus was incorporated into a system for flow injection-chemiluminescence detection of iron(II) (Bowie et al., 1998; 2002), and is described in the following chapter.

Chapter 5

The Impact of Diatom Redox Activity on Model Iron-Chelates in Seawater

5.1 Introduction

It is known that the growth of phytoplankton is limited by the availability of iron in several oceanic regions, particularly in HNLC areas (Boyd et al., 2000; Martin et al., 1994). The availability of this essential nutrient is hindered by its low solubility in seawater and removal by scavenging processes. The presence of strong organic ligands which complex iron (>99 %) in the surface waters of the ocean, increase iron solubility and reduce its removal (Rue and Bruland, 1995; Wells, 2003). However, the availability of organically complexed Fe(III) to marine organisms is poorly understood and how phytoplankton acquire iron for growth is an area of great interest and debate.

Under iron-limiting conditions, heterotrophic and phototrophic marine bacteria (e.g *Psuedomonas*), like their terrestrial counterparts, secrete siderophores to complex iron (Granger and Price, 1999; Reid et al., 1993; Trick and Wilhelm, 1995). In addition to increasing the solubility of iron, siderophores also accelerate iron oxide dissolution (Kraemer et al., 2004; Yoshida et al., 2002). Marine bacteria can access iron from multiple siderophores, produced by different organisms, which are thought to be internalized within the cell via high-affinity iron membrane transporters which scavenge siderophore bound iron (Granger and Price, 1999; Hutchins et al., 1999; Trick and Wilhelm, 1995). In contrast, siderophore production by marine eukaryotic phytoplankton has been demonstrated in only one study (Trick, 1983). However, the high-affinity, siderophore mediated, iron-transport system (used by bacteria) has been demonstrated in green micro-algal species grown under iron deficient conditions (Benderliev and Ivanova, 1994). Siderophores are thought to form a major component of the strong iron binding ligand pool due to the similarity in the binding constants determined from marine siderophores grown in laboratory based cultures (e.g $K_{Fe'L,Fe} = 10^{11.5} - 10^{12.5}$ M^{-1}, (Lewis et al., 1995; Macrellis et al., 2001)) with those determined in the field (e.g $K_{Fe'L,L} = 10^{12}$

and 10^{11} M^{-1}, (Rue and Bruland, 1997) where the constant is calculated from all inorganic iron species (Fe') rather than free Fe^{3+}).

An alternative mechanism to the secretion and uptake of iron-bound complexes is through the direct reduction of Fe(III) complexes (Weger et al., 2002). This reduction is mediated by redox enzymes in the plasma membrane that can transfer an electron from an internal donor to the complexed extracellular Fe(III). Such plasma membrane oxidoreductases have been widely reported in animal, plant and algal cells (De Silva 1996; Schmidt, 1999). Recent studies have demonstrated that the diatom species, *Thalssiosira oceanica*, possess reductases at the cell surface that mediate the reduction of organically bound Fe(III) (Maldonado and Price, 2001). The subsequent increase in concentrations of inorganic labile Fe(II), following dissociation from the ligand, are available for uptake via metal transport proteins at the cell surface. There is widespread occurrence of plasma membrane bound oxidoreductases and high plasma membrane redox activity has been detected in diatoms (Davey et al., 2003; Taylor and Chow, 2001), though to what extent these enzymes are specifically involved with iron acquisition remains unknown.

Data presented in chapter four and elsewhere (Rose et al., 2005; Salmon et al., 2006; Shaked et al., 2004) demonstrated that the diatom species, *Thalassiosira weisflogii*, likely utilises oxygen as an external electron acceptor for the constitutive plasma membrane oxidoreductases. The result is the production of reactive oxygen species, such as H_2O_2 (chapter 4), which is also dependent on a number of environmental factors such as light. Hence, not only do the plasma membrane bound redox enzymes have the potential to directly reduce extracellular iron but the ROS species produced by the reduction of molecular oxygen may indirectly influence iron speciation at the cell surface and subsequent uptake by metal transport proteins. In a study by Kustka et al. (2005), O_2^- generation by *T. weissflogii* grown under constant light was demonstrated, however, it was concluded that whilst iron(III) could

be reduced by O_2^- this mechanism was unlikely to play a major role in iron assimilation in this organism. In contrast, Rose et al. (2005) have suggested that the production of O_2^- by the coastal cyanobacterium *Lyngbya majuscule* facilitates increased iron uptake and speculated that this is a reasonably widespread process.

The overall aim of the work presented in this chapter was to develop a method to determine Fe(II) in order to assess the potential role of membrane bound reductases and diatom produced ROS on the bioavailability of organically complexed iron. In order to achieve this aim, the following objectives were addressed;

1. Verify the stability of Fe(II) in physiologically relevant media suitable for continuous in-line measurements.

2. Determine Fe(II) complexation by ligands.

3. Demonstrate Fe(III) complexation with selected model ligands and assess the potential interference on the pre-concentration method.

4. Using the developed system, assess the generation of Fe(II) by diatom cells using FI-CL.

5.1.2 Background

Iron in seawater is predominantly in the Fe(III) redox state and has been found to be > 99 % complexed by strong organic ligands (Bruland and Wells, 1995; Gledhill and Vandenberg, 1994; Powell and Donat, 2001; Wu and Luther, 1995). The ability of a ligand to complex iron under ambient conditions is expressed using stability constants, $K_{Fe'L}$, defined from the following equation

$$[Fe'] + [L] \xleftarrow{\quad k \quad} [FeL]$$
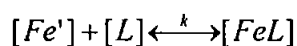
$$K_{Fe'} = \frac{[FeL]}{[Fe'][L]}$$

where [Fe'] represents the sum of all inorganic iron species (Fe(III)' and Fe(II)') and [FeL] represents the sum of the organically bound fraction. Due to the rapid oxidation of Fe(II) in seawater, the term Fe' often refers to Fe(III)'. For conditional stability constants, which can refer to the affinity of the ligand to complex with either Fe(II) or Fe(III), the value of $K'_{Fe^{3+}L}$ or $K'_{Fe^{2+}L}$ is conditional upon the solution composition and the inorganic side reaction co-efficient $(\alpha_{Fe'})$. Both thermodynamic and conditional stability constants are referred to in literature.

An organism's ability to access complexed iron is not well understood. Stability constants, redox potentials and the molecular structure of the ligand are all factors that may affect the ability of an organism to acquire iron from the surrounding medium. In this study four ligands (ethylenediaminetetraacetic acid (EDTA), citrate, desferrioxamine B (DFB) and protoporphyrin IX) were used, each with different physicochemical properties (Table 5.1) and chemical structures (Figure 5.1). The ligands were chosen to represent the variety of compounds with different iron binding functionalities which may be found in the ocean. The range of different physicochemical properties displayed by the ligands (Table 5.1), also facilitates the assessment into whether ligands are preferentially reduced based on the redox potential.

Important classes of siderophores which have been identified include hydroxamates and catecholates (Wilhelm et al., 1998). The siderophore DFB, a hydroxamate, was chosen to

(a)

Desferrioxamine B (DFB)

(b)

Protoporphyrin IX

(c)

Ethylenediaminetetraacetic acid (EDTA)

(d)
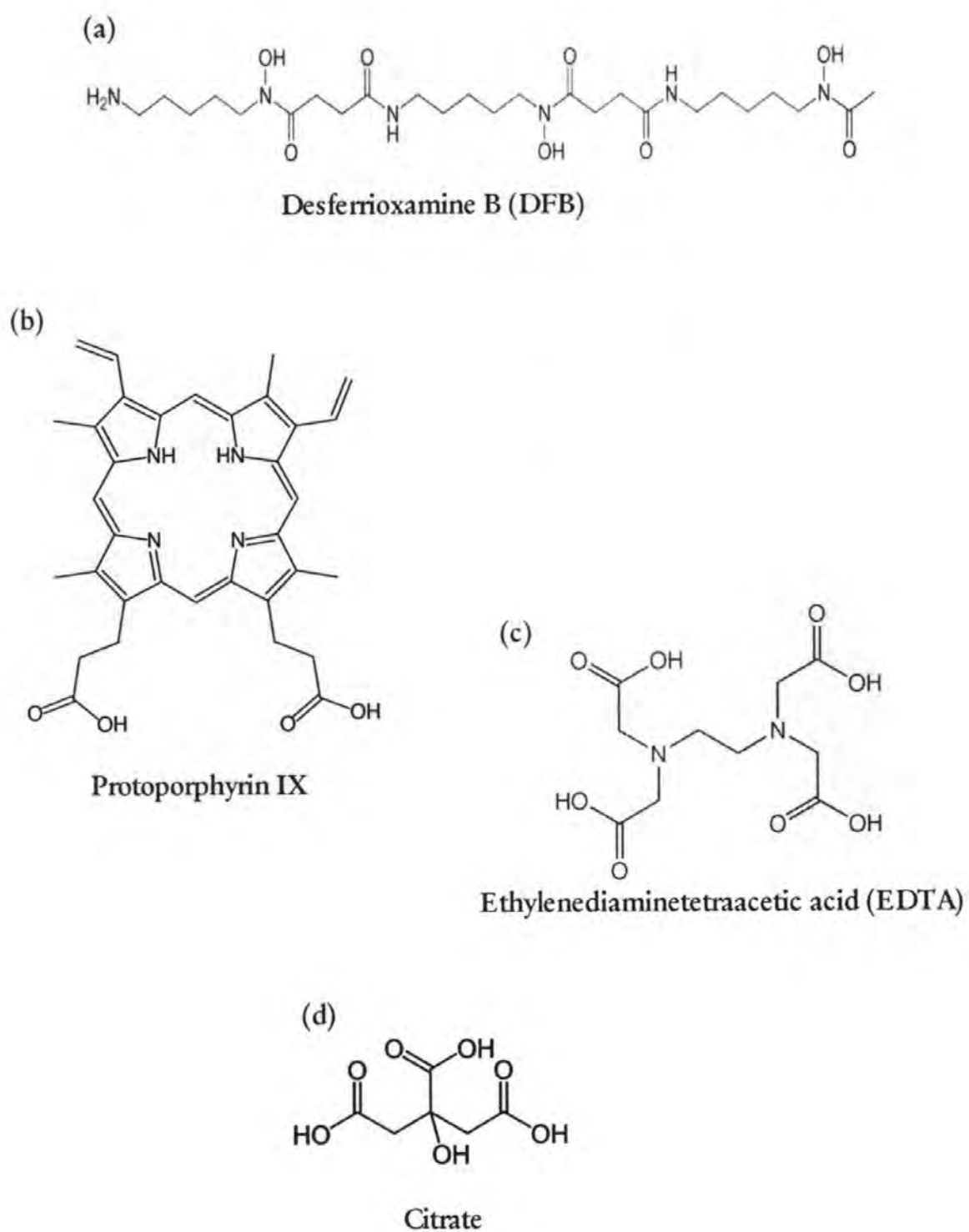
Citrate

Figure 5.1. Molecular representations of the model ligands used in this study. (a) desferrioxamine B (DFB), (b) Protoporphyrin IX, (c) ethylenediaminetetraacetic acid (EDTA) and (d) citrate.

represent this structural group (Figure 5.1 (a)). Phytoplankton cells contain porphyrin complexes which bind iron internally, e.g cytochrome a. These porphyrin complexes can be released into seawater following cell lysis as a result of viral attack or grazing. This group is represented by protoporphyrin IX, a square planar molecule with carboxylic side chains (Figure 5.1 (b)). The synthetic metal chelator, EDTA, has been used in a number of experiments investigating iron availability to organisms (Anderson and Morel, 1982; Gerringa et al., 2000; Soriadengg and Horstmann, 1995). Though not iron specific, the properties of EDTA are well documented (Herring and Morel, 1993; Rue and Bruland, 1995) and therefore this ligand was included in the study as an iron-chelator of moderate redox potential (Figure 5.1 (c)). The inclusion of citrate (Figure 5.1 (d)), a weak iron binding ligand, was based on the results of a recent study investigating iron uptake in the cyanobacterium *Lyngbya majuscule*. Salmon and co-workers (2006) reported the highest iron uptake from Fe(III)-citrate in their study of ten model ligands.

Table 5.1 Physicochemical parameters for the model ligands used in this study. Detailed are the measured stability constants for the Fe(III) complexes versus thermodynamic stability constants for the Fe(II) complexes with the four model ligands.

Ligand	*Log $K_{Fe^{3+}L}$	§Log $K_{Fe^{2+}L}$	¥E° (mV)
DFB	21.6[a]	20.32[d]	- 460[f]
EDTA	17.35[b]	18.35[e]	- 200[g,h]
Protoporphyrin IX	22.4[a]	-	- 100[h]
Citrate	10.36[c]	8.81[c]	+ 170[i]

[a] Witter et al. (2000)
[b] Sunda et al. (2005)
[c] Konigsberger et al. (2000)
[d] Hering and Morel (1993)
[e] Delgado et al. (1997)
[f] Maldonado et al. (2005)

[g] Dhungana and Crumbliss (2005)
[h] Ussher et al. (2005)
[i] Gibbs (1976)
* Conditional stability constants
§ Thermodynamic stability constants
¥ Redox potentials relative to a standard hydrogen electrode

The nutrient status of an organism can influence its mechanisms of nutrient acquisition, e.g. the production of siderophores under iron stress (Granger and Price, 1999; Reid et al., 1993; Trick and Wilhelm, 1995) and different iron uptake rates observed for diatom cells grown under either iron replete or limited conditions (Maldonado and Price,

2001). To investigate whether iron stress influences the potential role of membrane bound reductases and ROS production in diatoms, cells grown under iron replete and iron starved conditions were utilised in the assay experiments.

5.2 Experimental

The overall aim of the work presented in this chapter was to investigate the ability of diatoms to reduce $Fe(III)$ bound to ligands of different redox potential by determining the $Fe(II)$ produced. To achieve that aim a number of preliminary investigations had to be performed to investigate and optimise the $Fe(II)$ pre-concentration method being used. All the data presented in this chapter therefore relates solely to the determination of $Fe(II)$ and not total dFe (fractions previously defined in section 2.2.1.).

All experimental work and analysis was conducted using trace metal cleaning procedures, including the preparation of plasticware, clean acids, buffer and reagents used in the experiments, these are described in more detail in chapter two. All sample handling, manipulation and analytical work was carried out in either a class-100 clean room, or in a class-100 laminar flow hood.

5.2.1 Reagents, Solutions and Media Preparation

Reagents

All chemicals were obtained from Sigma-Aldrich unless otherwise stated and prepared in ultra high purity (UHP) water (Millipore, 18 MΩ cm^{-1}). For $Fe(II)$ analyses reagent

solutions were prepared as detailed in chapter two (section 2.2.3). This included a 1×10^{-5} M working solution of luminol mixed in 0.14 M Na_2CO_3 buffer (pH 11.8). UHP water (DI method) and 0.05 M Q-HCl (pre-concentration method) were used as eluents. Additionally, for the pre-concentration method, samples were buffered using 0.4 M ammonium acetate (pH 5.5).

For calibration, stock solutions of 0.02 M ammonium ferrous (Fe(II)) sulphate (Aldrich) were prepared weekly. The stock was acidified (0.1 M, Q-HCl), spiked with sodium sulphite (100 μM) and stored in a refrigerator (~ 4 °C). Working standard solutions of 80 μM and 200 nM were prepared immediately prior to analysis. The iron(III) reducing agent, sodium sulphite (0.04 M, Na_2SO_3), was added to standards to achieve a final concentration of 100 μM in order to stabilise the redox state of the Fe(II) solution. Fe(II) working solutions were prepared by serial dilution from this stock and used in the interference experiments, this included solutions of 12 and 1.2 μM, 600 and 400 nM, which were prepared by serial dilution.

Solutions

The four model ligands examined were EDTA, citrate, DFB and protoporphyrin IX, and were used without further purification. Stock solutions of each ligand were prepared as follows: EDTA (0.1 M) was prepared by diluting 1.4621 g in 8 mL NaOH (2 M) and made up to 50 mL with UHP water; Citrate (0.1 M) was prepared by diluting 1.4716 g in 50 mL of UHP water; DFB 0.0001 M (100 μM) solution of DFB was prepared by diluting 0.06658 g in 10 mL of methanol and making up to 1 L with UHP water and Protoporphyrin IX (0.001 M) was prepared by diluting 0.02828 g in 50 mL acidified (0.01 M, HCl) methanol (ROMIL, UpS). All stock solutions were prepared monthly and refrigerated (~ 4 °C). Working solutions of 100 μM (not necessary for DFB) were prepared daily prior to experiments.

A 0.005 M stock solution of ammonium iron(III) sulphate (AnalaR; VWR) was

127

prepared by diluting 0.24109 g in 100 mL UHP water. The solution was left for 2 h to ensure complete oxidation of iron and then acidified (0.1 M, Q-HCl). Working solutions of 1 and 10 μM in 0.01 M Q-HCL were prepared by serial dilution prior to use.

Filtered coastal seawater was collected on board the R.V. Plymouth Quest using the ships underway system. This seawater was UV irradiated and cleaned (UV-FSW) as described in chapter two (section 2.2.3). The UV-FSW seawater was used in preliminary studies, for the preparation of the Fe(III)-ligand solutions used for the assay experiments and for the calibrations performed.

Culture preparation for phytoplankton assays

Cultures of *T. weissflogii* were prepared for use in the assay experiments, these were grown under either iron replete or iron starved conditions. Under iron replete conditions, cultures were incubated at 15 °C, 150 μmol photons m^{-2} s^{-1}, 12:12 light / dark cycle in filtered seawater supplemented with 500 μM NaNO$_3$, 32 μM K$_2$HPO$_4$, 100 μM Na$_2$SiO$_3$, and Guillard's F/2 vitamins and a trace metal solution containing 3.8 μM Na$_2$-EDTA, 1 μM FeCl$_3$, 80 nM ZnSO$_4$, 460 nM MnCl$_2$, 50 nM CoCl$_2$, 20 nM CuSO$_4$, 2 μM Na$_2$MoO$_4$, and 200 nM H$_2$SeO$_3$. Cultures were maintained in mid to late log phase by routine subculture or dilution. For iron starvation, iron-deplete media (media without the addition of FeCl$_3$) was inoculated (1:40 v:v) with cells from iron replete cultures. These were sub-cultured at least three times and were harvested for use in assays if the growth rate was significantly lower than cells grown in replete media.

Confirmation of iron limitation in cultures

Iron limitation was confirmed by nutrient (with and without iron) addition bioassays that were carried out on sub-samples of the cultures. The response of the subcultures to

nutrient additions was monitored and iron stress confirmed if growth was significantly stimulated by the addition of iron compared to controls without iron (nutrients only). Cell counts were determined using a haemocytometer (improved Neubauer slide), samples were either counted immediately or preserved by the addition of Lugol's solution (100 : 1 v/v culture : Lugol's).

5.2.2 Instrumentation

Measurements were carried out using two FI systems, the instrumentation for each of these has been described in previous chapters. The instrumentation for the DI method used in the study of Fe(II) complexation is detailed and illustrated in chapter two (section 2.2.5) and was used as described without change.
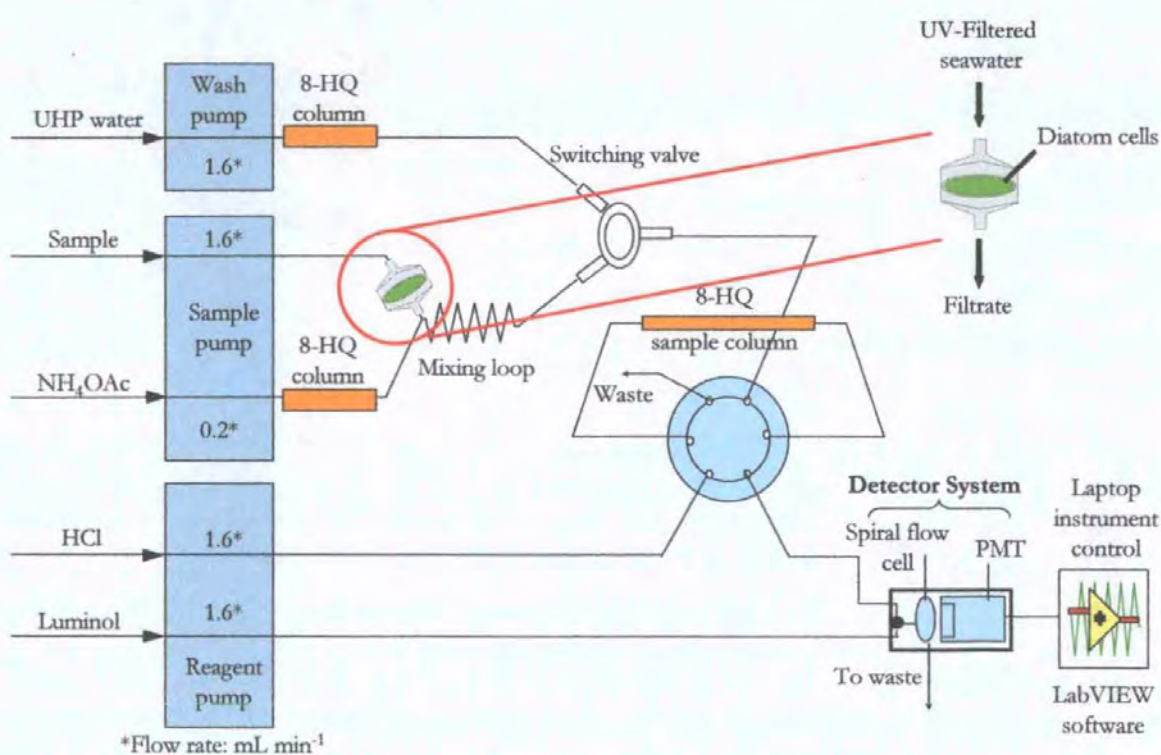
Figure 5.2 Schematic of FI-CL manifold for the automated determination of iron(II). The placement of the filter unit in the sample line is highlighted

The instrumentation for the pre-concentration of Fe(II) was also detailed in chapter two (section 2.2.5), however this was adapted in a similar manner to the H_2O_2 instrumentation (described in chapter 4) in order to facilitate the phytoplankton assay experiments. In addition to the instrumentation previously detailed for Fe(II) determination, diatom cells were supported within a clear acrylic 25 mm in-line filter holder (2.5 mL volume, Sartorius) attached to the sample lines using luer lock connectors (Cole Parmer). Figure 5.2 illustrates the manifold with the placement of the filter unit. Photosynthetically active radiation was provided using a fibre optic lamp (Schott Mainz, K450B) directed onto the cells.

5.2.3 Sample Preparation Procedures

A series of separate experiments were performed in order to establish and verify the constraints of the FI-CL method to determine Fe(II) generation by diatoms. This section describes the preparation of the samples used in the separate experiments and also the procedures followed for the phytoplankton assays. The method and analytical analysis of the samples is detailed later (section 5.2.4).

Stability of Fe(II) in solution

The purpose of these experiments was to investigate and verify the stability of Fe(II) in solution over time. This would provide further information on the oxidation of Fe(II) when performing the assay experiments. In addition, by creating an environment where Fe(II) was relatively stable, it would be possible to investigate Fe(II) complexation with the model ligands. This in turn would provide information into the potential for re-complexation of Fe(II) during the assay experiments. To facilitate this study, and also to reduce the oxidation of Fe(II) to Fe(III), the DI method was used in a de-oxygenated environment.

The stability of the Fe(II) was investigated, initially in UHP water and then in UV-FSW. In these studies, 20 nM Fe(II) standard was added to 30 mL (either UHP water or UV FSW) samples under de-oxygenated conditions and the Fe(II) signal monitored over time.

Complexation of Fe(II) with model ligands

There have been few studies investigating the complexation of Fe(II) with ligands (Lin and Kester, 1992; Rijkenberg et al., 2006). To complement the proposed assay experiments, it was essential to establish to what extent Fe(II) binds to any of the chosen model ligands (EDTA, citrate, DFB and protoporphyrin IX). It was also important to confirm that the method was specific to Fe(II) and did not detect Fe(II) bound to ligands. An equilibration approach, between Fe(II) and the ligands, was not undertaken. For the future phytoplankton assay studies, it would be the dynamics of instantaneous complexation with any labile Fe(II) generated (as a consequence of Fe(III)-ligand reduction) that would be of interest. Therefore, in this instance, samples were analysed immediately after the addition of the Fe(II) standard. The study was performed using the DI method in a de-oxygenated environment.

Experiments were initially performed in UHP water and repeated in UV-FSW in order to compare the response in each media. 30 mL aliquots (UHP water / UV–FSW) were each spiked with 60 μL from one of the ligand stock solutions (100 μM) to achieve a final concentration of 200 nM. To each of these solutions 20 nM Fe(II) standard was added and the solution immediately analysed. A solution of 20nM Fe(II) was used as a control during each experiment. The timing of these experiments (t = 0) began from the addition of the Fe(II) standard and the procedure was performed in a de-oxygenated environment.

Complexation of Fe(III) with the model ligands

The four model ligands were complexed with Fe(III) in preparation for use in the

131

phytoplankton assays. Total complexation was verified using the pre-concentration method. These experiments were carried out in an aerobic environment using the automated analyser with pre-concentration column.

Individual stock solutions of 20 μM Fe(III) + ligand (EDTA, citrate, DFB and protoporphyrin IX) were prepared in UHP water using a 1:1 ratio. Prior to use the solutions were left for > 24 h to equilibrate. From these individual pre-complexed stocks, individual solutions of 20 nM Fe(III)-ligand in UV-FSW were prepared. Each solution was analysed and the results compared with UV-FSW without added ligand to verify complexation.

Procedure for phytoplankton assays

For all assay experiments, Fe(II) was determined using the automated pre-concentration method with an adapted manifold (Figure 5.2).

Individual stock solutions of 20 μM Fe(III) + ligand (in UHP water), and pre-complexed solutions of 20 nM Fe(III)-ligand (in UV-FSW), for the four model ligands were prepared as previously detailed (*Complexation of Fe(III) with model ligands*). The individual solutions of 20 nM Fe(III)-ligand in UV-FSW were prepared 12 h prior to experimental runs. Main stock solutions were stored at ~4 °C and a fresh stock prepared after one week.

Cells from either iron replete or iron starved cultures of *T. weissflogii* were harvested and concentrated by filtration (3 μm polycarbonate, 47 mm, Whatman Cyclopore™) following the same procedure as detailed in chapter four (Figure 4.5, section 4.2.4). The cells were harvested in the dark and at the same time each day to avoid any variation due to diel growth cycles. Following filtration, the cells were washed and re-suspended in either fresh F/2 or iron deplete F/2 media for iron replete and iron starved culture respectively. The re-suspended cells were transferred to clean containers and kept cool and in the dark before use.

For each experiment, a fixed volume of cells was transferred by syringe onto a 25 mm diameter (0.4 μm Whatman Cyclopore™) filter membrane which was supported in the transparent filter unit. The filter unit was placed in the sample line of the manifold using luer lock fittings in a position immediately upstream of the sample/buffer mixing loop (Figure 5.2). Cells were flushed continually with one of the UV-FSW + Fe(III)-ligand solutions in the dark for 3 min before timing (t = 0) of the assays commenced. The assays lasted ~40 - 50 min and a flow rate of 1.6 mL min^{-1} was maintained throughout, including for control experiments.

To avoid possible cross-contamination, assays were performed for each Fe(III)-ligand using a dedicated filter unit. For each experiment the same volume of cells were harvested from the same batch of *T. weissflogii*. In previous studies using diatom cultures, higher plasma membrane reductase activity was observed in response to light (Davey et al., 2003), as was the increase in ROS production (Milne et al. submitted). It was therefore of interest to examine the effects of any light induced increase on the Fe(II) CL signal. During the assays the immobilised cells were therefore exposed to two alternating periods of dark and light (150 μmol photons m^{-2} s^{-1}) and the filtrate analysed. A control experiment, using the Fe(III)-ligand solutions, was performed for each assay in the absence of micro-algal cells. After each assay (including control), and prior to calibration, the filter unit was removed and the sample lines flushed with UV-FSW.

5.2.4 Method

Fe(II) concentrations were determined using two FI methods; a direct injection without pre-concentration (King et al., 1995; Ussher et al., 2005) and an automated analyser with sample pre-concentration (Bowie et al., 1998; 2002).

Prior to use, all tubing, fittings and connections of the FI manifold of each instrument were cleaned with 0.5 M Q-HCl followed by rinsing with UHP water for at least 4 h. Before

analyses, each system was operational with reagents flowing through for at least 1 h to ensure baseline stability and to condition sample lines.

Analytical procedure for direct injection analyses

The DI method was used to investigate the stability of Fe(II) and complexation of Fe(II) with the four model ligands. The FI instrument was set-up as illustrated in Figure 2.5 (chapter two, section 2.2.5) and the analytical procedure, described in chapter 2 (section 2.2.6), followed without further alteration.

Analytical procedure for pre-concentration analyses

The method for the automated analyses of Fe(II) was used for studies involving the analyses of Fe(III)-ligand solutions and in the assay experiments performed with the diatoms cultures. This method was previously described in chapter two (section 2.2.6) and used without further alteration. However, to maintain the viability of the diatom cells supported in the in-line filter unit (Figure 5.2), the software programming was adjusted to ensure continuous running of the sample pump and therefore keep media (Fe(III)-ligand solutions) flowing over the cells.

5.2.5 Calibration and blanks for the phytoplankton assays

Calibrations using UV-FSW were carried out daily when performing the phytoplankton assay experiments. The UV seawater was buffered off-line to pH 5.5, this was to prevent the loss of Fe(II) due to oxidation while the standards were pumped through the FI manifold prior pre-concentration on the 8-HQ column. Standard additions of iron(II) working stock (200 nM) in the range 0.2 - 1.0 nM (equating to 20 – 100 μL addition to 20 mL samples) were made to the buffered UV-FSW, immediately analysed and used to generate

134

calibration graphs.

An analytical blank, associated with the reagents and the manifold, was determined by performing an analytical cycle (i.e. loading of the 8-HQ column) of the FI system without the loading of a sample. In this manner, the CL signal associated with the ammonium acetate buffer solution, the rinse solution (UHP water), the HCl eluent and the manifold were accounted for. The contribution from the analytical blank signal was calculated during the calibration process and subtracted from the final sample concentrations.

For each assay performed with the diatoms, a control was also performed, i.e. same procedure but without the diatoms cells in the filter unit. This control accounted for any signal associated with the complexed Fe(III) solutions.

5.3 Results and Discussion

5.3.1 Analytical Figures of Merit

The standard calibration graphs generated before each bioassay, displayed excellent linearity, with correlation coefficients (r^2) typically >0.98, and were therefore used to calculate the concentrations of Fe(II) in the assay experiments. The mean repeatability and standard deviation of replicates of standard additions performed for the iron calibrations, generated during the assay experiments, was 6.3 ± 3.2 % ($n = 29$). The mean iron blank signal produced for these analyses was 25 ± 14 pM ($n = 22$) resulting in a mean limit of detection (defined as three times the standard deviation of the blank) of 11 ± 4 pM ($n = 5$).

5.3.2 Stability of Fe(II) in Solution

In order to determine the potential complexation of Fe(II) by the model ligands a study was first conducted to measure the loss of Fe(II) due to oxidation alone, this was followed and compared with the loss of Fe(II) when the ligand was added. These initial stability studies were first investigated using UHP water and then UV-FSW. To facilitate this, both studies (stability and complexation of Fe(II) with the ligands) were carried out under de-oxygenated conditions.
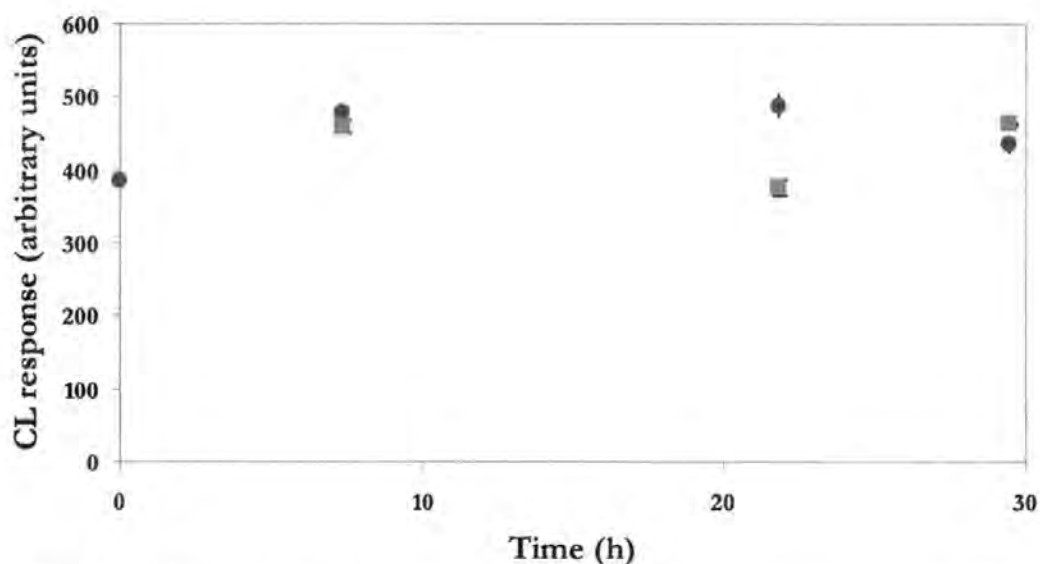
Figure 5.3 Stability of 20 nM Fe(II) in UHP water stored in a de-oxygenated environment and analysed over time. (●) Stored 20 nM Fe(II) compared to (■) freshly prepared 20 nM Fe(II) sample.

Figure 5.3 demonstrates the stability of Fe(II) in UHP water in an de-oxygenated environment over a time period of 30 h. Initial experiments using a large sample volume (250 mL) were unsuccessful at keeping the Fe(II) in solution (data not shown). This could have

been due to the larger surface area of sample which was exposed to the environment (even though in a bottle). Regular sampling over a period of time, as in the stability studies, removed solution from the bottle and increased the air gap above the remaining solution. Unsuccessful removal of all oxygen from the immediate environment would increase the chance of gas exchange over the larger exposed surface area of the sample, this would result in increased oxidation of the Fe(II) present. It was also observed that at low volume spikes ($<$ 50 μL) the solution in the pipette was not completely dispensed, possibly due to opposing pressure from the N_2 gas when inserted in the top of the LDPE bottle. The best stability was achieved using a 30 mL sample (in a 30 mL LDPE bottle) and using an Fe(II) spike of at least 50 μL.

The oxidation of Fe(II) in buffered UV-FSW (pH 5.7) under aerobic conditions was previously demonstrated (section 2.3.1, Figure 2.15) resulting in an half life of 10.4 min. Further comparison studies were performed in a de-oxygenated environment using the UV-FSW (buffered and non-buffered) and compared to a non-UV irradiated aged filtered seawater sample, previously collected from the North Pacific. The results from these are presented in Figure 5.4; (a) relates to the response observed for 12 nM Fe(II) added to North Pacific seawater, (b) corresponds to a 20 nM Fe(II) addition to UV-FSW, and (c) corresponds to the response observed for 20 nM Fe(II) addition to buffered UV-FSW.

The Fe(II) oxidation rates in these three samples was estimated using the same calculation procedure described in section 2.3.1. The pseudo first-order oxidation rates and corresponding Fe(II) half life for the different physical conditions investigated during this study (including data from the previous estimate detailed in Table 2.5) are displayed in Table 5.2.

Table 5.2 Rate constant and half life data for Fe(II) in the conditions used in this study.

Sample	Environment	pH	Rate constant (min^{-1})	Fe(II) half life (min)
UV-FSW	aerobic	5.7	0.0664	10.4
UV-FSW	de-oxygenated	~8.2	0.0516	13.4
UV-FSW	de-oxygenated	5.7	0.0058	119.5
Pacific FSW*	de-oxygenated	~8.2	0.3347	2.1

*Determined from data obtained after 10 min.

This data (Figure 5.4 and Table 5.2) illustrates the importance of pH and the presence of oxygen on the oxidation of Fe(II), and is in keeping with previous findings (Millero et al., 1987). The most interesting feature of the data is the rapid loss of Fe(II) in the untreated Pacific FSW. Though in a de-oxygenated environment, the half life of Fe(II) in the Pacific seawater (2.1 min) was 20 % of that observed for a buffered aerobic UV-FSW sample (10.4 min). The loss of the Fe(II) signal is therefore not purely through oxidation and the presence of excess organic ligands in the Pacific sample has potentially enhanced the removal of Fe(II) from the sample through complexation (in addition to oxidation to Fe(III)).

For assays experiments, the use of seawater at a physiological relevant pH is necessary for maintenance of viable cells and to represent the natural environment. This therefore negates the use of buffered seawater flowing over the diatom cells, however, the half-life of Fe(II) in seawater (Table 5.2) highlights the importance of buffering in-line immediately after the seawater has passed over the cells to reduce Fe(II) oxidation. The enhanced loss of Fe(II) in the Pacific seawater (Figure 5.4) endorses the use of UV-FSW for the studies with the model ligands and for the assay experiments, the use of this seawater in addition to the immediate in-line buffering of the sample will reduce the loss of Fe(II) during the experiments. It is also important to remove the natural organic ligands present in seawater through UV irradiation, as the competition between the natural and the model ligands is unknown.
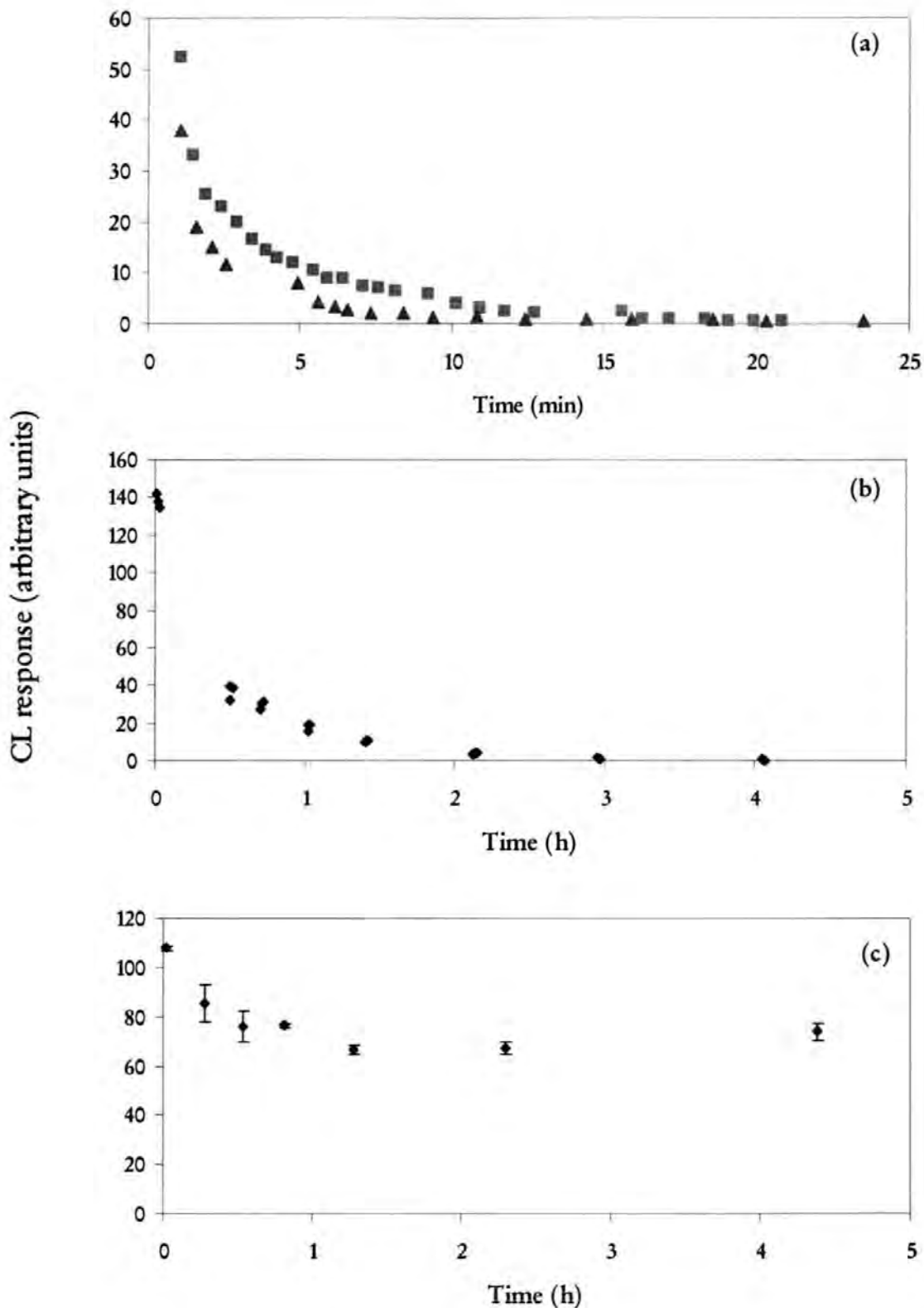
Figure 5.4 Relative Fe(II) CL signal in different seawater samples performed in a deoxygenated environment. (a) duplicate 12 nM Fe(II) in non-UV irradiated Pacific seawater, (b) 20 nM Fe(II) in UV FSW (pH 8), and (c) 20 nM Fe(II) in buffered UV FSW (pH 5.5). Graphs (a) and (b) show the analyses of duplicate samples whereas data on graph (c) is the mean of 4 injections of one sample (error bars represent 1 standard deviation).

5.3.3 Complexation of Fe(II) with Model Ligands

In order to accurately determine Fe(II) generated by the diatoms, it was necessary to examine if Fe(II) complexation occurred with the model ligands themselves. Complexation with Fe(II) would potentially cause an underestimation in the Fe(II) determined during the assays experiments. To address this, the first series of experiments were performed in UHP water with EDTA, citrate and DFB, and then repeated in UV-FSW with the same ligands and protoporphyrin IX. These studies were performed using the DI method in order to observe the affect on the CL signal directly without pre-buffering the solutions which would be necessary for pre-concentration method.

The results from the model ligand additions to UHP water are shown in Figure 5.5. In each graph a stored 20 nM Fe(II) standard (control) is shown. This was prepared at the same time as the Fe(II) + ligand samples (t=0) and kept in a de-oxygenated environment during the period of analysis (up to 25 h). At each sampling time point, the stored Fe(II) sample was analysed and compared to a freshly prepared and analysed 20 nM Fe(II) standard. This procedure demonstrated the persistence of Fe(II) in the UHP water samples and demonstrated the amount of complexation (rather than oxidation due to the environmental conditions) which occurred for the samples with Fe(II) + ligand.

The addition of EDTA (Figure 5.5 (a)) immediately complexed the Fe(II) in solution and no CL signal (0 %) was observed for the Fe(II)-EDTA complexed solution. The addition of DFB (Figure 5.5 (b)) reduced the Fe(II) CL signal by ~ 50 % after 5 h, relatively little change (~ 10 % further reduction) was observed over the remaining analysis period (25 h). The addition of citrate to 20 nM (Fe(II) (Figure 5.5 (c)) resulted in a minor reduction (~ 10 %) in the CL signal over the 25 h analyses period when compared to the initial 20 nM Fe(II)
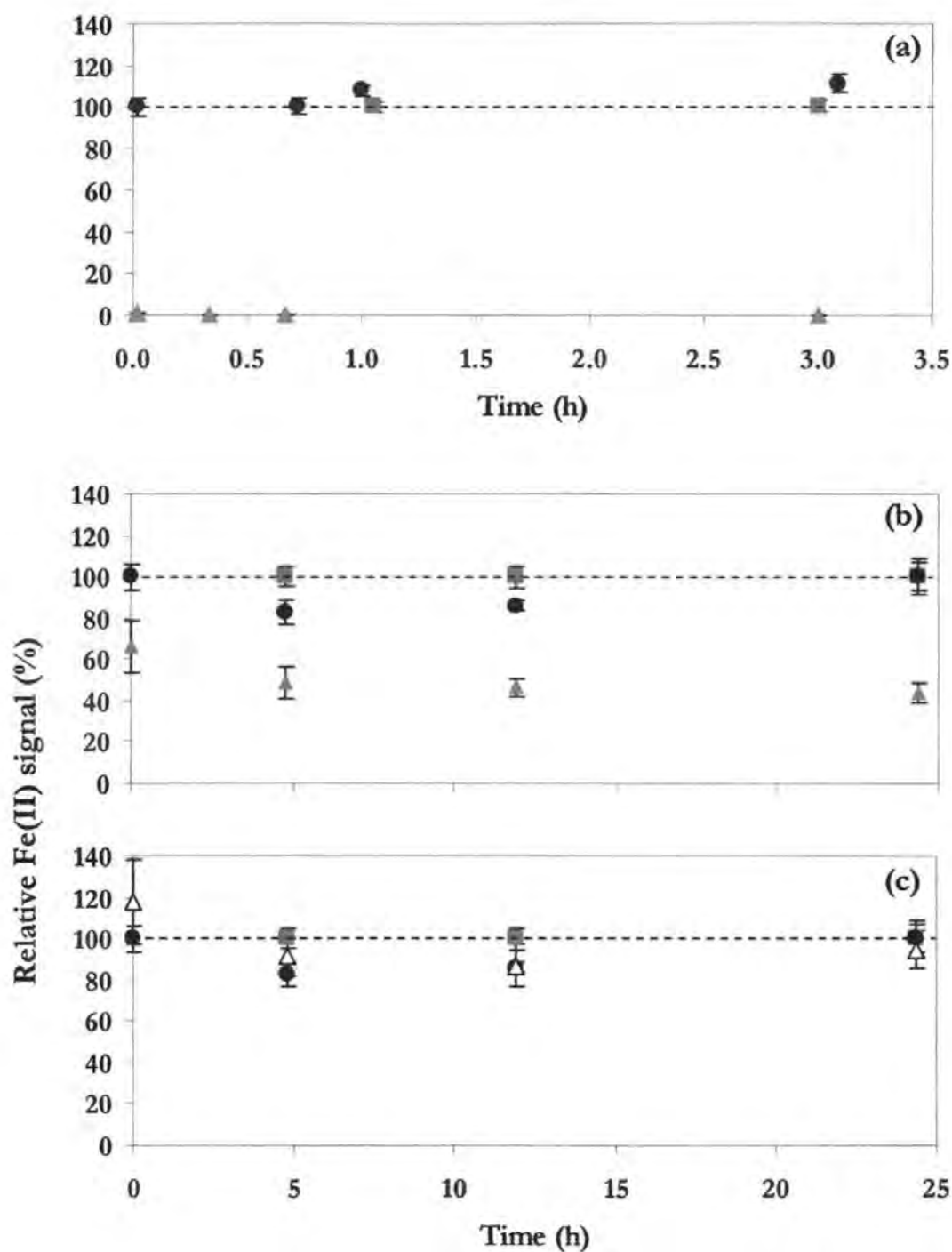
Figure 5.5 Complexation of model ligands with 20 nM Fe(II) in UHP water under de-oxygenated conditions. (●) Stored 20 nM Fe(II) standard measured over analysis time, compared to (■) a freshly prepared 20 nM Fe(II) standard to demonstrate stability of Fe(II). Addition of 200 nM ligand solution to 20 nM Fe(II) for (a) EDTA (▲), (b) DFB (▲), and (c) citrate (Δ). The data is displayed as a percentage of the freshly prepared Fe(II) standard (shown as 100% and highlighted by the dotted line). (Data presented is the mean of 4 replicate analyses of 3 samples ($n = 12$), error bars represent 1 standard deviation)

standard. These results would indicate that citrate and Fe(II) do not form a stable complex, EDTA forms a rapid complex with Fe(II) whereas there is less affinity between DFB and Fe(II). Based on the thermodynamic stability constants for Fe(II) (Table 5.1), citrate has the weakest stability constant out of the four ligands under study (Log $K_{Fe^{2+}L}$: 8.81) and the results suggest that the ligand was unable to form a stable complex with Fe(II) under the conditions of the study. While EDTA is a relatively non-selective complexing agent, used to buffer metal concentrations in culture media, it forms a stronger complex with Fe(II) (Log $K_{Fe^{2+}L}$ 20.32), the lack of competing cations in the UHP water sample have resulted in complete complexation of Fe(II). Siderophores have a high affinity for Fe(III) but can also form strong complexes with Fe(II) (DFB, Log $K_{Fe^{2+}L}$ 20.32). The negative redox potential for Fe(III)-siderophores complexes ($\sim$ -350 to -750 mV/ NHE (normal hydrogen electrode)) (Boukhalfa and Crumbliss, 2002) implies a strong tendency for siderophores to stabilise iron in the Fe(III) redox state, hence, in the presence of O_2, an Fe(II) siderophore will be readily oxidised to an Fe(III)-siderophore (Boukhalfa and Crumbliss, 2002; Dhungana and Crumbliss, 2005). This would also imply that the 50 % reduction in CL signal observed for this ligand (Figure 5.5 (b)) could have resulted from the binding of the Fe(II) present and immediate oxidation to Fe(III) in order to establish a stable complex, however, why there was incomplete removal of the Fe(II) signal is uncertain. Overall, these initial results in UHP water have demonstrated that the Fe(II) method is specific to the detection of labile Fe(II) and not complexed iron.

These same experiments were repeated using UV-FSW (Figure 5.6). A fourth ligand was also added to the investigation, protoporphyrin IX, to enhance the scope of the study. As Fe(II) oxidation is enhanced in seawater (see Table 5.2) a freshly prepared 20 nM Fe(II) standard was not used during these experiments. Instead the Fe(II) + ligand solutions were compared against the stored 20 nM Fe(II) control which was analysed during the period of study (up to 250 min) and treated in the same way as the samples throughout.
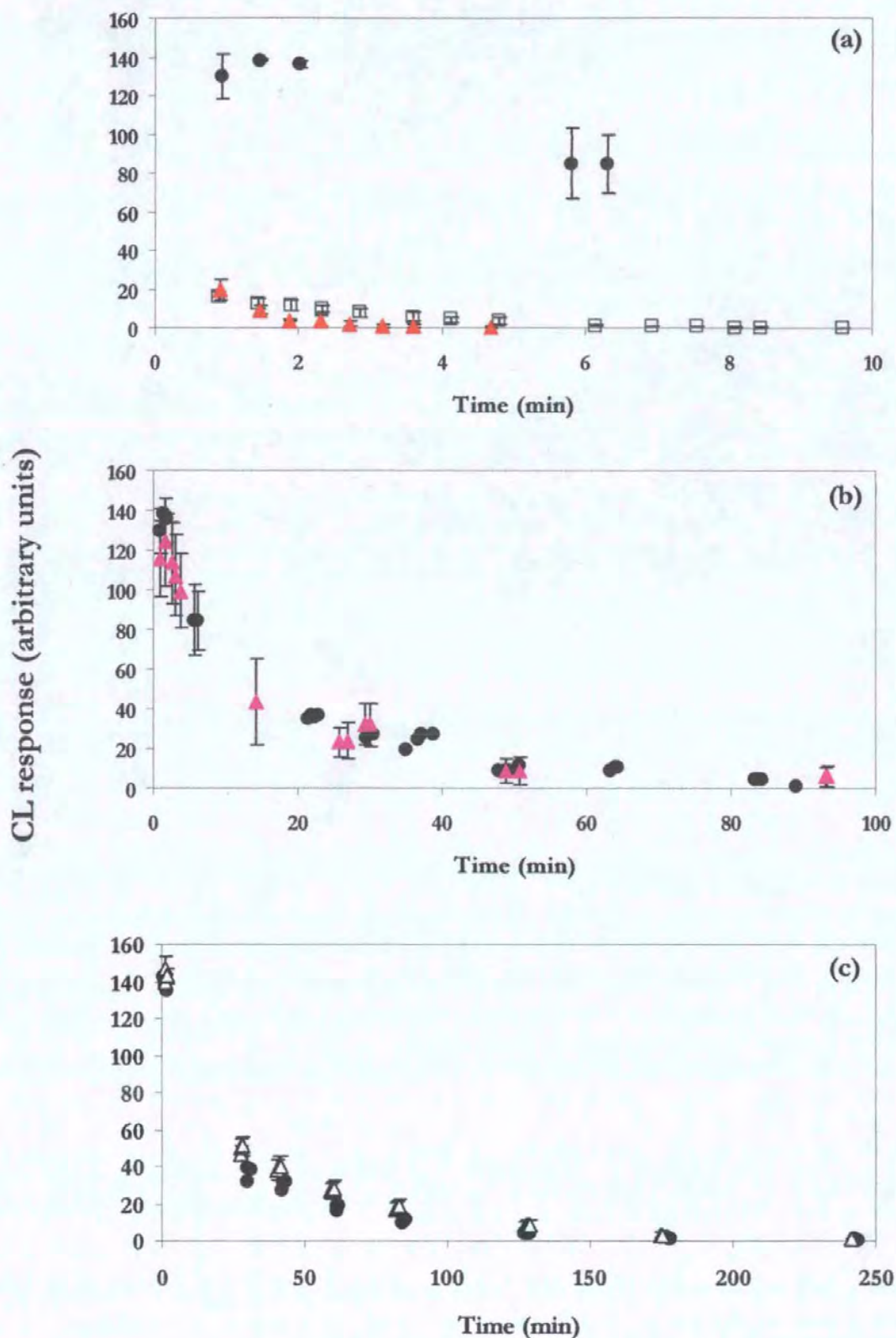
Figure 5.6 Complexation of model ligands with 20 nM Fe(II) in UV-FSW in a de-oxygenated environment. (●) Stored 20 nM Fe(II) sample measured over time, compared with 20 nM Fe(II) + 200 nM ligand in graph (a) DFB (▲) and protoporphyrin IX (□), graph (b) EDTA (▲), and graph (c) citrate (Δ). (Data presented is the mean of 3 samples ($n = 3$). Samples were analysed on the same day with the exception of EDTA where samples were analysed on 3 separate days. Error bars represent 1 standard deviation).

The results for the ligand additions to UV-FSW are presented in Figure 5.6. The addition of DFB and protoporphyrin IX (Figure 5.6 (a)) show rapid removal of Fe(II) prior to any noticeable oxidation, as illustrated by the persistence of the CL signal produced by the stored 20 nM Fe(II) control. The response of these two ligands, observed after 6 min, was negligible (<1 %) compared to the CL response of the stored Fe(II) control.

The response of DFB contrasted to that observed in UHP water (Figure 5.5 (b)) where the Fe(II) signal was reduced by 50 %. The reason for this difference in response is unclear, though it could result from the change in sample matrix, i.e. the pH of the sample solutions ($\sim$5 – 6 for UHP water over $\sim$8 for UV-FSW) and/or the additional constituents found in the UV-FSW matrix. As previously discussed, DFB can form a stable complex with Fe(II) (DFB, Log $K_{Fe^{2+}L}$ 20.32), however, a high affinity for Fe(III) implies a strong tendency to stabilise iron in the Fe(III) redox state. Whilst the results suggest the removal and complexation of Fe(II) by DFB, it is possible that rapid oxidation to Fe(III) occurs within the DFB-iron complex (Boukhalfa and Crumbliss, 2002).

Protoporphyrin IX, is utilised within cells (e.g. heme b) in the reduced Fe(II) form, though on exposure to O_2 oxidation occurs resulting in iron(III) protoporphyrin IX or hemin. There are no published stability constants for the protoporphyrin IX complex with Fe(II), however the results from this study under de-oxygenated conditions (Figure 5.6 (a)) suggest rapid binding and removal of Fe(II) from the UV-FSW sample.

In UV-FSW, EDTA was much slower to complex the Fe(II) and the data is similar to that of the stored 20 nM Fe(II) sample (Figure 5.6 (b)). In seawater, the competition from the abundant cations Mg^{2+} and Ca^{2+} results in inefficient complexation with free iron. The affinity of Mg^{2+} and Ca^{2+} for EDTA (Log K_{MgEDTA} 8.52 and Log K_{CaEDTA}: 10.46) (Martell and

Smith, 1997) is no stronger than that of Fe(II) but their predominance in solution and the immediate analysis of the sample prevent equilibration and exchange with EDTA. This was further investigated by increasing the concentration of EDTA added to a 20 nM Fe(II) solution. The results from this (Figure 5.7) demonstrate that under the conditions of this study (no equilibration), EDTA was required at a much higher concentration (200 μM) to achieve complete complexation with the 20 nM Fe(II) used in this study.
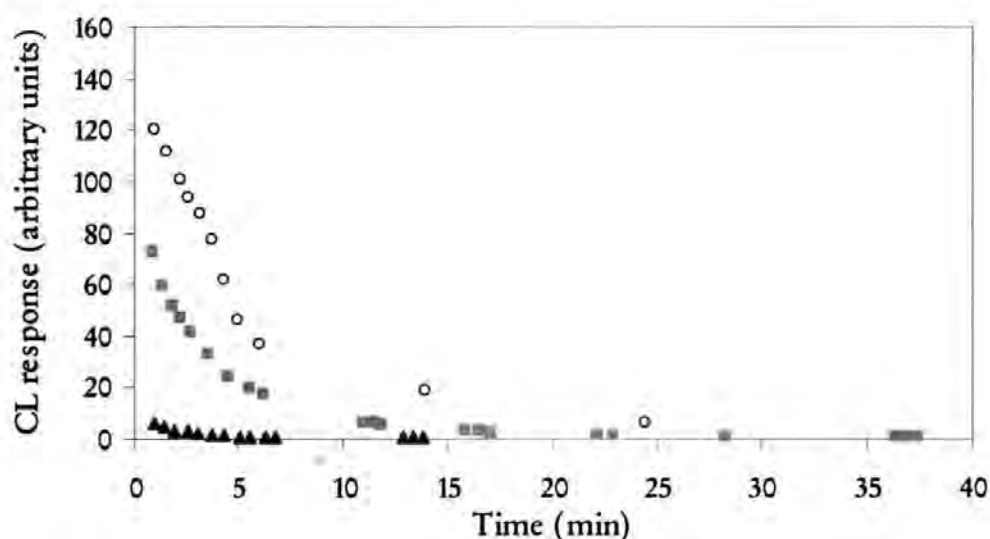
Figure 5.7 The affect of increasing concentrations of EDTA to 20 nM Fe(II) in UV-FSW under de-oxygenated conditions.. (○) 200 nM, (■) 20 μM and (▲) 200 μM

The addition of citrate to UV-FSW (Figure 5.6 (c)) produced a similar response to addition made to UHP water. The response mirrors the stored 20 nM Fe(II) sample. As previously stated, this demonstrates that citrate does not readily form a stable complex with Fe(II), either in UHP water or UV-FSW under the conditions used here.

These results have confirmed that the method being utilised here for the determination of Fe(II) is specific to labile inorganic Fe(II). In addition, under these experimental conditions, the results demonstrate that DFB and protoporphyrin IX rapidly

remove Fe(II) in UV-FSW, whereas EDTA was required at 10 x the concentration of Fe(II) before CL signal quenching was observed. This reflects the fact that EDTA also binds other abundant divalent cations in seawater (e.g. Mg^{2+} and Ca^{2+}) albeit with lower affinity. Citrate, however, does not form stable complexes with Fe(II).

With regards to the use of the four model ligands during the assay experiments, these results would suggest that the use of DFB and protoporphyrin IX may result in an under estimatation of any Fe(II) generated due to re-complexation by these ligands prior to pre-concentration and determination. However, under the conditions used here, the use of EDTA and citrate would cause less removal of any Fe(II) generated.

5.3.4 Complexation of Fe(III) with Model Ligands

The previous section investigated the complexation of the model ligands with Fe(II). The purpose of this set of experiments was to investigate the complexation of EDTA, citrate, DFB and protoporphyrin IX with Fe(III) and what effect, if any, the complexed Fe(III)-ligand solutions would have on the Fe(II) chemiluminescence signal.

The stability constants for the four ligands (Table 5.1) are in the range Log $K_{Fe^{3+}L}$ 10.36 – 22.4 and would suggest that all the ligands form stable Fe(III)-complexes. In addition the ligands were pre-complexed with Fe(III) for > 24 h in UHP water to allow equilibration (without competition) prior to dilution in UV-FSW. The results from the analyses of the four complexed solutions are presented in Figure 5.8. These results, which are within two standard deviations of a control sample (UV-FSW), demonstrate that the four ligands bind to Fe(III). The complexes therefore present no interference on the CL signal.
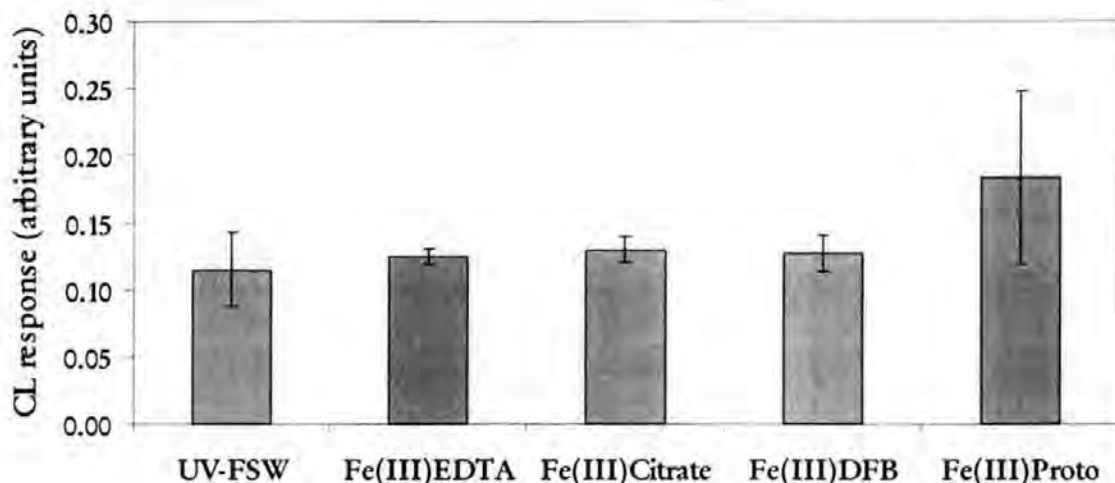
Figure 5.8 The CL response of the four complexed ligands. 20 nM Fe(III)-ligands with a 1:1 Fe:L ratio in UV-FSW. Analysis performed aerobically using the pre-concentration method. (Error bars represent ± 2 standard deviations).

However, the results for protoporphyin IX, while within 2 standard deviations of the UV-FSW control, would suggest that this ligand does not bind Fe(III) as efficiently as the other three under these experimental conditions. This is supported by a recent study using untreated Southern Ocean seawater (Rijkenberg et al., 2006), but is contrary to studies conducted by Rue and Bruland (1995) and Witter et al. (2000) who reported log K' values of 22.0 and 22.4 respectively for the Fe(III)-protoporphyrin IX complex using UV treated seawater. The data presented do not provide conclusive evidence that protoporphyrin IX binds with Fe(III), but for the purposes of this study, protoporphyrin IX was assumed to bind with Fe(III) and is supported by the results presented in the next section.

While these results indicate that the complexed solutions do not interfere with the CL signal, the results from protoporphyrin IX highlights the importance of including a control when performing the assay experiments, i.e. monitor the signal produced from the complexed solutions without the inclusion of cells within the assay experimental set-up. Another consideration for the assay experiments is the re-complexation of labile Fe(III) following oxidation of any generated Fe(II). This again highlights the importance of the immediate analysis of the filtrate flowing over the cells, prior to oxidation and re-complexation.

5.3.5 Phytoplankton Assays Investigating the Reduction of Fe(III)-ligands

Assay experiments, using the adapted FI-CL method, were carried out to investigate the reduction of Fe(III) bound to organic ligands by diatoms. As discussed in the Introduction above, the mechanisms through which diatom species acquire iron from the ocean environment are poorly understood. In this study, diatom cells supported in the in-line filter unit permitted solutions containing the Fe(III)-complexes of interest to be passed over the cells and the resultant Fe(II) signal to be continuously determined. In theory, reduction of Fe(III) may result from two possible mechanisms. The direct reduction at the cell surface of the Fe(III)-ligand by membrane bound reductases is one possible mechanism. The other is related to the presence of reactive oxygen species (O_2^-) in the cell micro-environment. In chapter four, it was demonstrated that *T. weissflogii* generated H_2O_2 (following disproportionation of its pre-cursor O_2^-) and that this generation increased when exposed to light. This generation may create both a reducing (from O_2^-) and/or oxidising (from H_2O_2) micro-environment around the cell which could affect the speciation of iron. Using the same species of diatom, *T. weissflogii*, similar light exposure assays, as presented in chapter four, were performed. In addition, diatoms cells grown under iron replete/starved conditions were used to assess the difference in response iron stress may present, also the use of ligands with different redox potentials could provide information on possible preferential reduction by the membrane bound reductases.

The results from the assays experiments are shown in the following graphs (Figures 5.9 – 5.13). Each figure consists of four individual graphs detailing the assay results. The data presented in each graph includes two sets of data, the response recorded with the diatom cells

in the filter unit and a control. The control was an assay procedure performed with each complexed ligand solution but without the diatom cells placed in the filter unit, it was performed in the same manner (with the same light/dark exposure timings) as the assays performed with the diatom cells. The four assays (represented by the four individual graphs) detailed in each Figure, were carried out on the same day and on the same batch of harvested diatom cells, for each of the four model ligands.

Different batches of cells may respond differently to stimulus / stress. Exposing the same batch of harvested cells, on the same day, to the same external stimulus reduces this biological variability. However, the time taken to complete all four assays for the four ligands, plus four controls, meant that some cells were kept suspended in the same media for long periods of time (> 4 h). Though kept cool (~ 5 – 6 °C) and in the dark, there will still therefore be some degree of variability in how the cells in each assay respond to stimuli. This is in addition to any external influence on the cell from the different ligands.

The first two set of graphs, Figures 5.9 and 5.10, are replicate assays performed using cells grown in iron replete media. The following two set of graphs, Figure 5.11 and 5.12, are replicate assays performed using iron starved diatom cells. An additional assay was also performed to complement the affect growth/nutrient status may have on the cells response. An organism can assimilate both nitrate (NO_3^-) and ammonium (NH_4^+) as part of its nitrogen requirements, however, NH_4^+ can be assimilated directly whereas NO_3^- must first be reduced to NH_4^+. This increases the energy requirement of the cells grown on NO_3^- and it is therefore considered that NH_4^+ is the preferred substrate (Maldonado and Price, 1996). An assay using cells grown on NH_4^+ was included in order to assess whether growth in this media influenced the response of the cells to complexed iron. The results from this assay are shown in Figure 5.13.

The concentrations of labile Fe(II) determined in all assays were low (< 3.5 nM). There was an observed increase in the Fe(II) CL signal, both for the control experiments and for the assays performed with the diatom cells. The difference in Fe(II) concentrations (Δ[Fe(II)]) determined in response to light exposure were very low (pM range) where

$$\Delta[\text{Fe(II)}] = \text{mean } [\text{Fe(II)}]_{\text{during light exposure}} - [\text{Fe(II)}]_{\text{preceding dark period}} \qquad (5.1)$$

The light responsive data from the control experiments indicates that the Fe(III)-ligands are reactive to the visible light from the light source resulting in a ligand to metal charge transfer reaction (LMCT). Subsequently the Fe(III) in the ligand is reduced to Fe(II) and dissociation occurs. Table 5.3 details ΔFe(II) in response to light for the four model ligands. Citrate produced the greater Fe(II) response when exposed to light resulting in a mean ΔFe(II) concentration of 100 ± 60 pM. The response from DFB, protoporphyrin IX and EDTA was marginally less resulting in mean ΔFe(II) concentrations of 70 ± 70 pM, 70 ± 40 pM and 50 ± 20 pM respectively.

Table 5.3 The difference in Fe(II) concentrations for the control experiments. Performed in the absence of diatom cells and reporting the difference in Fe(II) concentrations between dark periods and exposure to light for the four model ligands.*

Model ligand			
DFB	Protoporphyrin IX	Citrate	EDTA
70 ± 70§	70 ± 40	100 ± 60	50 ± 20
($n = 6$)	($n = 12$)	($n = 12$)	($n = 11$)

* All data given in pM. Error bounds indicate $\pm$ one standard deviation. The figures are calculated from the mean Fe(II) concentration in response to each light exposure performed during an assay (n) deducted from the Fe(II) concentration from the preceding dark period. This is compiled from the data presented in the graphs (Figure 5.9 – 5.13).
§ This data excludes 2 control experiments where the Fe(II) concentrations increased over the entire experimental period (Figures 5.10(a) and 5.11(a)).
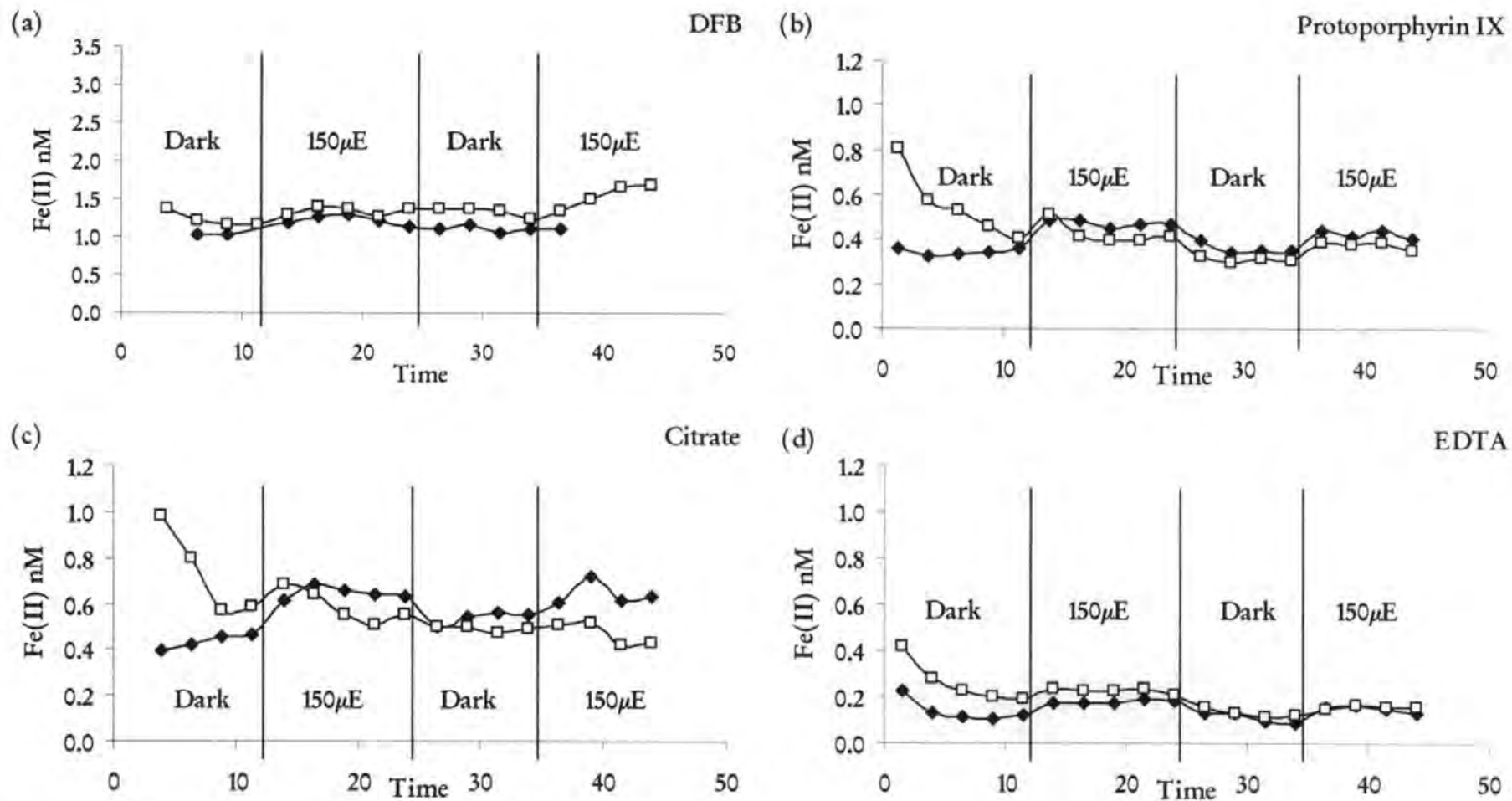
Figure 5.9. Initial assays performed without cells (♦ control) and in the presence of diatom cells (□) grown in iron replete media. Data shown reports the Fe(II) concentration determined during alternating periods of dark followed by exposure to light (150 mol photons m^{-2} s^{-1}) for the four model ligands (a) DFB, (b) protoporphyrin IX, (c) citrate and (d) EDTA. (Data from assays performed on 3rd Oct).
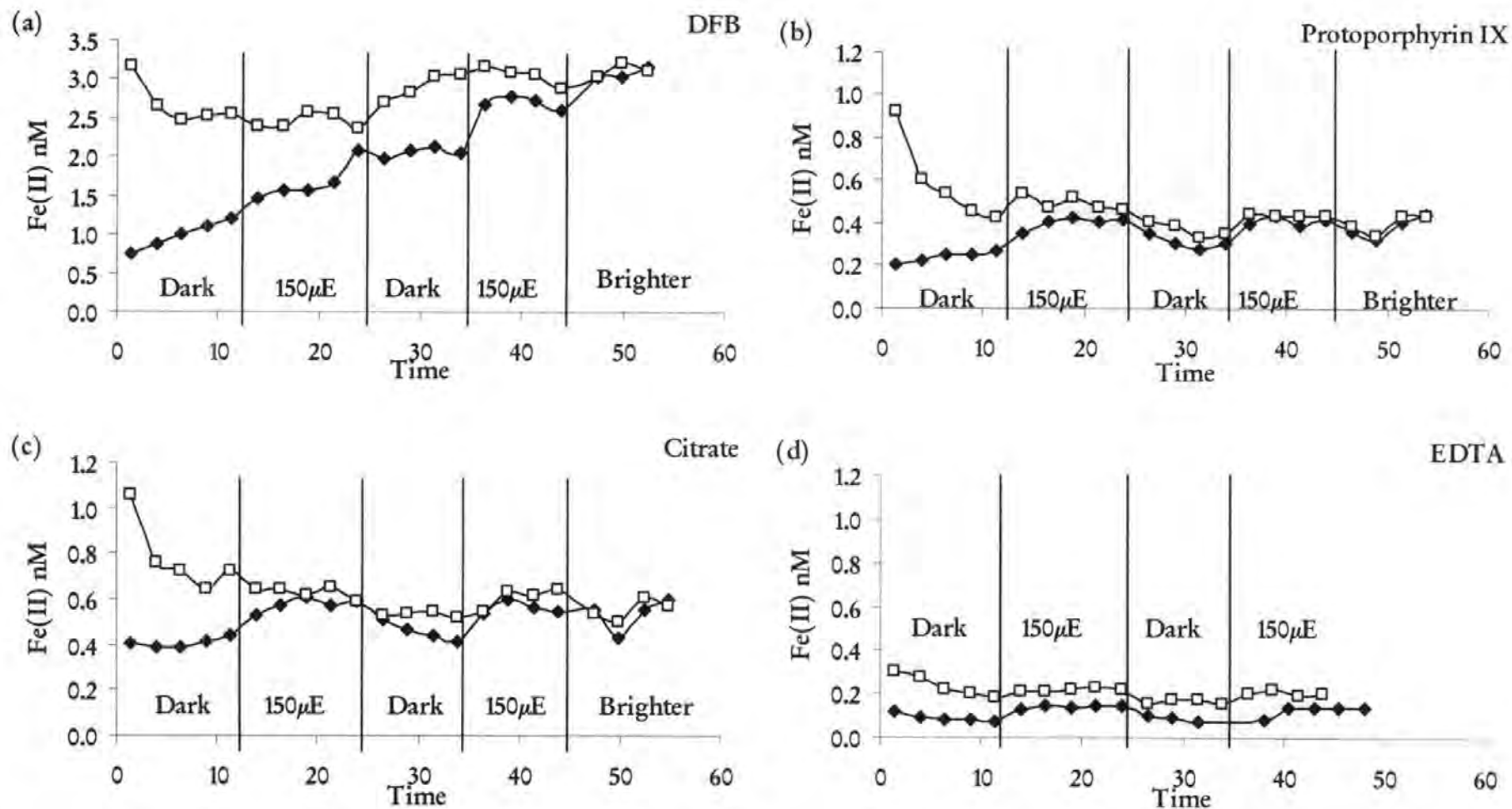
Figure 5.10. Duplicate assays performed without cells (♦ control) and in the presence of diatom cells (□) grown in iron replete media. Data shown reports the Fe(II) concentration determined during alternating periods of dark followed by exposure to light (150 mol photons m^{-2} s^{-1} and above) for the four model ligands (a) DFB, (b) protoporphyrin IX, (c) citrate and (d) EDTA.. (Data from assays performed on 17rd Oct).
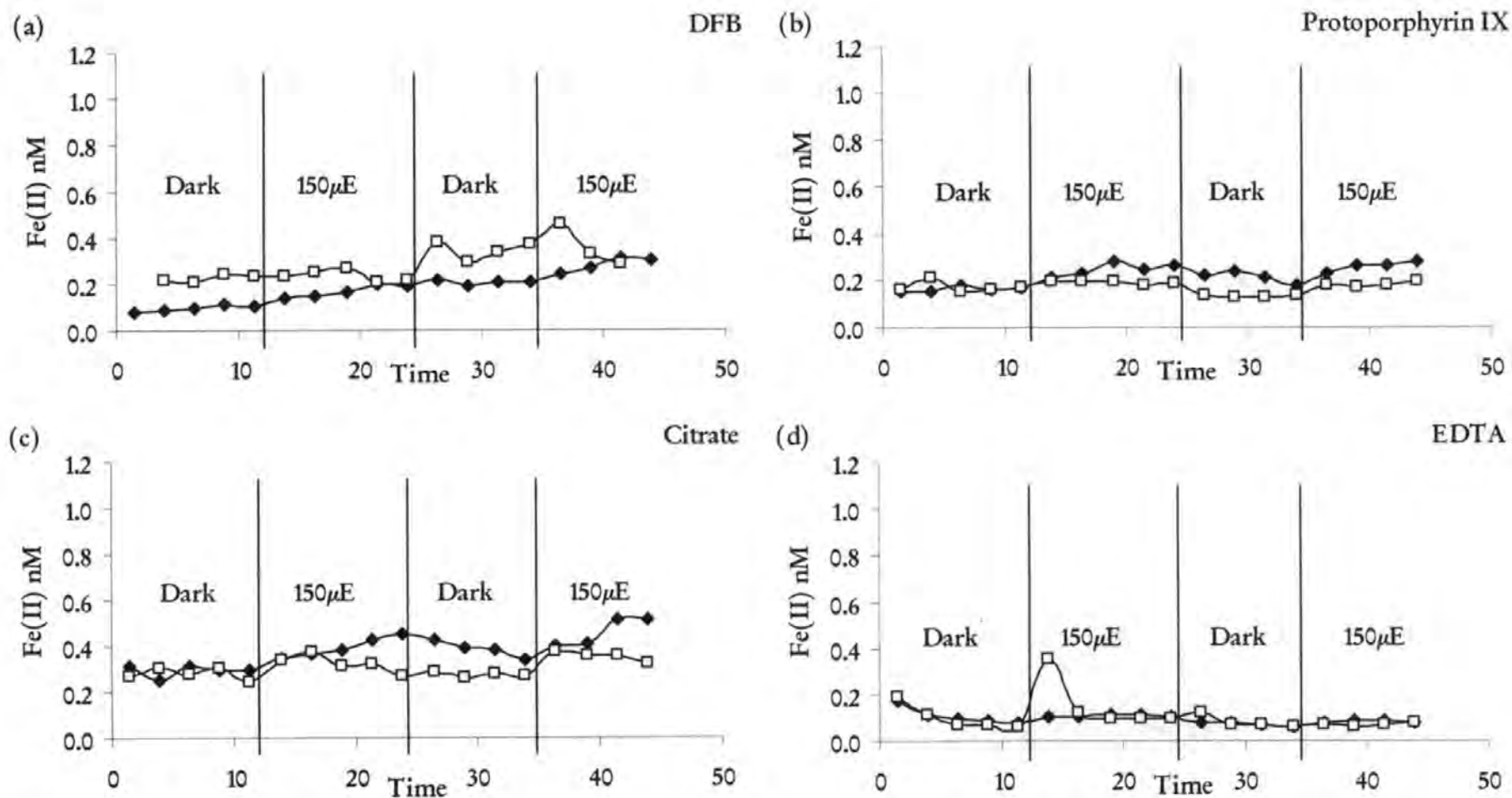
Figure 5.11. Initial assays performed without cells (♦ control) and in the presence of diatom cells (□) grown in iron limited media. Data shown reports the Fe(II) concentration determined during alternating periods of dark followed by exposure to light (150 mol photons m^{-2} s^{-1}) for the four model ligands (a) DFB, (b) protoporphyrin IX, (c) citrate and (d) EDTA. (Data from assays performed on 2nd Oct).
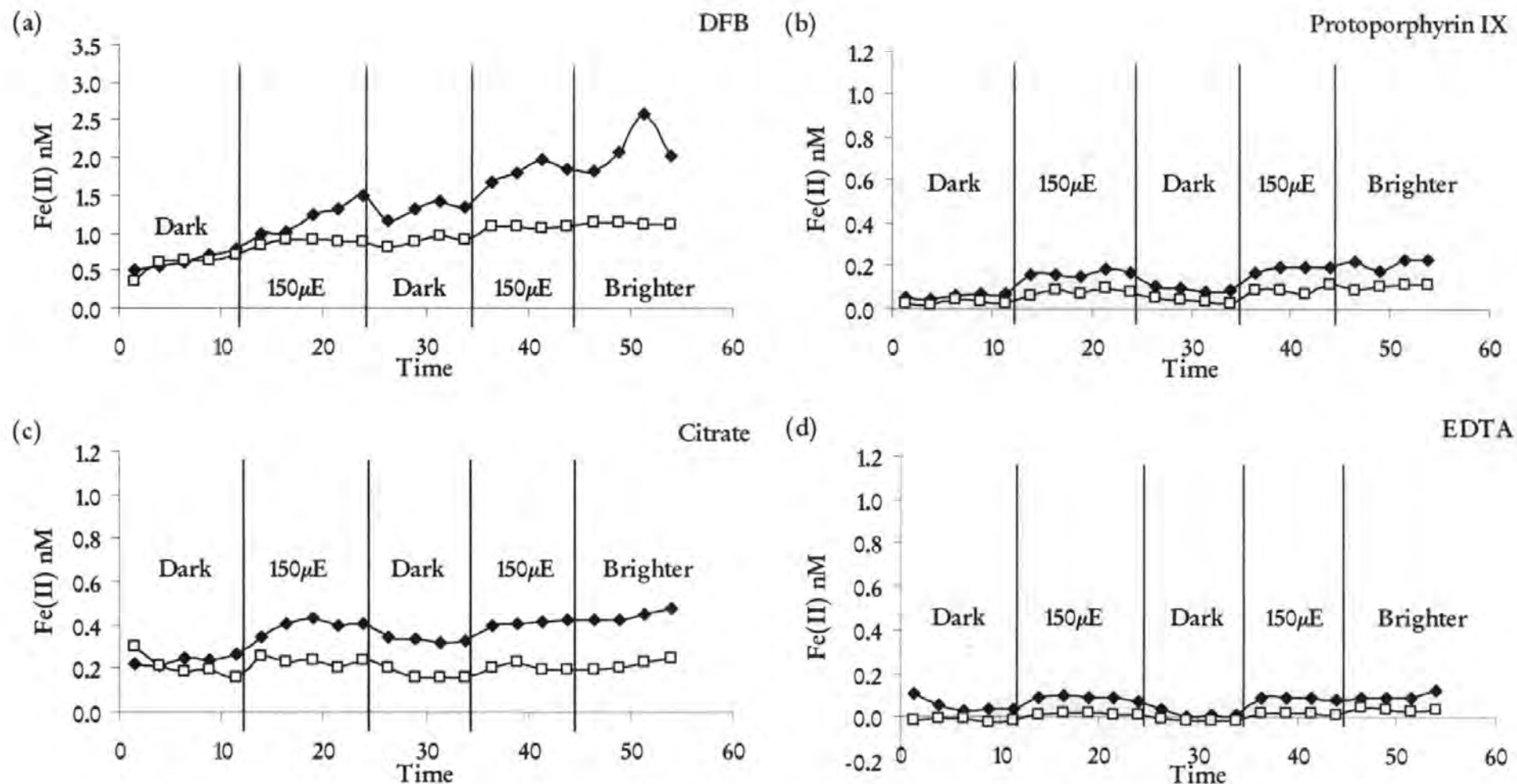
Figure 5.12. Duplicate assays performed without cells (♦ control) and in the presence of diatom cells (□) grown in iron limited media. Data shown reports the Fe(II) concentration determined during alternating periods of dark followed by exposure to light (150 mol photons m^{-2} s^{-1} and above) for the four model ligands (a) DFB, (b) protoporphyrin IX, (c) citrate and (d) EDTA. (Data from assays performed on 18th Oct).
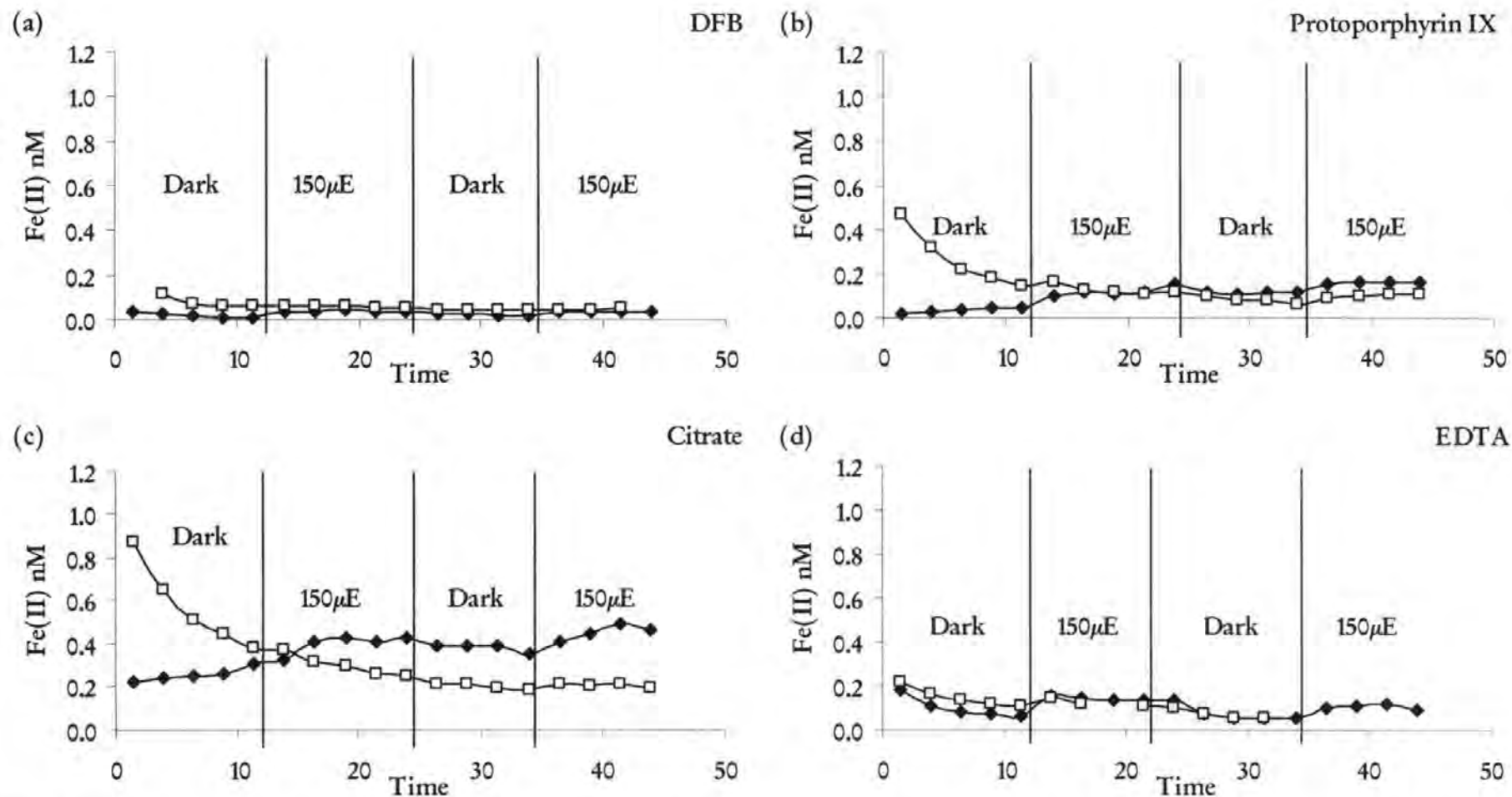
Figure 5.13. Assays performed without cells (♦ control) and in the presence of diatom cells (□) grown using ammonium as the nitrogen source. Data shown reports the Fe(II) concentration determined during alternating periods of dark followed by exposure to light (150 mol photons m^{-2} s^{-1}) for the four model ligands (a) DFB, (b) protoporphyrin IX, (c) citrate and (d) EDTA.. (Data from assays performed on 30th Sept).

A photoreactive effect has also been observed in other studies (Rijkenberg et al., 2006; Tang and Morel, 2006) for similar ligands, with the exception of DFB. Previous studies have reported DFB to be photostable (Barbeau et al., 2003; Borer et al., 2005), however these studies were performed at iron concentrations three orders of magnitude higher (μM) than this study (nM) and where the pM changes observed here, detailed in Table 5.3, would not be detected. It was noted, that while Rijkenberg et al. (2006) concluded that DFB was photo-stable, in the experiments performed at a concentration similar to those in this study (10 nM Fe(III): 20 nM DFB) an increase in the Fe(II) signal of ~ 50 pM is evident. However, this increase was not sustained and after ~ 15 min the signal started to decline. A similar response was also observed in three of the control assay performed in this study (Figure 5.9 (a), 5.11 (a) and 5.13 (a)). However, the DFB control data for the two other assay experiments (Figures 5.10 (a) and 5.12 (a)) show a continual increase in Fe(II) concentrations determined over the entire experimental period of ~ 50 min. There were no factors which could have contributed to the raised Fe(II) signal which were noted during the experiments and the reason for the increase is uncertain. For this reason the two sets of data from these assays is excluded from the data presented for DFB in Table 5.3. Based on the results observed in this study, it is not possible to confirm whether DFB is photo-stable or –reactive. The small pM changes observed here and by Rijkenberg et al. (2006), over 10 – 15 min timescales might be sufficient for cells to access Fe(II) and therefore is an area which requires further investigation.

Fe(II) generation in diatom assays

For the assays performed with the diatom cells included in the filter unit, a similar small (pM) but variable Fe(II) response was observed when the cells were exposed to light. Fe(II) concentrations were observed to increase in response to light (e.g. Figure 5.9 (b) and (d), Figure 5.12 (b) and (c)), however decreases in the Fe(II) signal were also observed (e.g. Figure 5.9 (c), 5.13 (b) and (c)). These changes do not appear to relate to the nutrient status of the diatoms cells or to a specific ligand. Table 5.4 details the range calculated (using equation

5.1) for the difference in Fe(II) concentrations determined between dark periods and exposure of the cells to light for all the assays. The data varies from negative values (- 84 pM, DFB iron replete) up to hundreds of pM (303 pM, DFB iron replete).

Table 5.4 The difference in Fe(II) concentrations for the diatom assays experiments. Reporting the difference in Fe(II) concentrations between dark periods and exposure to light for the four model ligands.[*]

Growth conditions of Diatoms	Model ligands			
	DFB	Protoporphyrin IX	Citrate	EDTA
Iron replete	- 84 to 303 ($n = 5$)	- 38 to 87 ($n = 5$)	- 53 to 90 ($n = 5$)	34 to 51 ($n = 4$)
Iron starved	- 19 to 171 ($n = 5$)	18 to 64 ($n = 5$)	12 to 85 ($n = 5$)	12 to 92 ($n = 5$)
Ammonium	- 4 to 3 ($n = 2$)	- 14 to 38 ($n = 2$)	- 83 to 17 ($n = 2$)	-18 ($n = 1$)

[*] All data given in pM. The figures are calculated from the mean Fe(II) concentration in response to each light exposure performed during an assay (n) deducted from the Fe(II) concentration from the preceding dark period. This is compiled from the data presented in the graphs (Figure 5.9 – 5.13).

While there is no overall observable pattern to the data, the Δ[Fe(II)] is wider for the diatoms grown in iron replete media. This is solely due to DFB (-84 to 303 pM) which also display this largest range for the iron starved cells (- 19 to 171 pM). It was noted that for two out of the five assays performed with the diatom cells using Fe(III)-DFB solution, the Fe(II) signal was overall higher than for the assay experiments performed with the other three model ligands (Figures 5.9 (a) and 5.10 (a)) (up to ~3.5 nM). As with the two sets of control data for Fe(III)-DFB, Figures 5.10 (a) and 5.12 (a), which were excluded from Table 5.3 due to a continual increase in Fe(II) concentrations over the assay period, there is no reason (or factors noted during the experiments) which could account for this higher Fe(II) signal The pre-complexed solutions for all the ligands were freshly prepared for each assay and, as previously demonstrated, Fe(III) fully complexes with DFB (Figure 5.8) therefore there should be no

positive interference from uncomplexed labile Fe(III) (Figure 2.12). The irregularity between the control runs when using DFB and the sometimes higher Fe(II) concentrations determined during assays cannot be readily explained from the data available here and requires further investigation.

The individual graphs from the five sets of assays performed, display a trend which can be observed by comparing the cell response to that of the control data. In general, for the assays performed with diatoms grown in iron replete media, the concentrations of Fe(II) determined are above that of the control. In contrast, the concentrations of Fe(II) determined in the assays performed with iron starved diatoms, and for those grown on ammonium, are below those of the control. These observed differences may have been due to a number of reasons:

1. The culture medium of the diatoms grown under iron replete conditions, is most likely supersaturated with ferric (oxyhydro-)oxide (FeO$_x$) which precipitates on the surface of the cell (Tang and Morel, 2006). This extracellular iron could be leaching into the solution flowing over the cells during assays and mechanisms occurring at the cell surface and/or in the near environment could result in Fe(III) reduction. The presence of organic ligands in the solution can increase or decrease Fe(III) photosensitivity e.g. Fe(III)-citrate can reduce iron oxide in the light (Waite and Morel, 1984) whereas studies have shown Fe(III)-DFB to be photostable (Borer et al., 2005; Rijkenberg et al., 2006).

2. The presence of photo-reactive ligands could add to increasing Fe(II) concentrations, through LMCT reaction resulting in the possible decomposition of the ligand (e.g. siderophore) and the production of Fe(II) (Barbeau et al. 2001).

3. The increase in Fe(II) signal may be from un-complexed labile Fe(III) produced as a result of reduction followed by re-oxidation.

4. In the assays performed using diatoms grown under iron starved conditions, the iron

158

in the flowing media may precipitate on the cell surface, however, this factor does not explain the similar response observed for the ammonium assays where the diatoms are not iron starved.

5. The lower Fe(II) concentrations observed in the iron limited and ammonium assays, may relate to the hypothesis of this study, that reduction of Fe(III)-ligands and the resultant labile Fe(II) is being taken up by metal transport proteins. In several graphs where the Fe(II) concentrations fall below the control (Figures 5.9 (c), 5.10 (c), 5.11 (b) and (c), 5.12 (a -c) and 5.13 (b – c)), and the point of divergence occurs after the initial exposure to light. The response to light was tested further by increasing the intensity to > 150 mol photons m^{-2} s^{-1} (Figures 5.10 and 5.12) however no additional/increased affects were observed. While the reduction of Fe(III)-ligands is a possibility, rapid re-complexation of Fe(II) with the ligand still present in solution is likely to occur before the filtrate passes over the 8-HQ pre-concentration column. Therefore, it may not be possible to determine all labile Fe(II) produced following reduction.

The hypothesis for this study was that diatom redox processes increase the concentrations of extra-cellular Fe(II) either through direct reduction or by indirect reactions due to the extra-cellular production of ROS generated at the cell surface. Our approach was to expose diatom cells to a range of Fe(III)-chelates and continuously monitor Fe(II) production at environmentally relevant concentrations. The results derived from this approach were inconclusive as there was no consistent relationship observed between labile Fe(II), the Fe(III)-ligand used and the light treatments. However, the procedures used have provided preliminary insight into the processes which may be occurring, under natural seawater pH conditions, in the micro-environment of the diatom cells under study. The cells were successfully incorporated into the adapted manifold of the FI-CL instrumentation and the concentrations of Fe(II) in the filtrate determined. Further experiments are now needed, both at the macro (community) and micro (individual cells) scale, to address the reduction

capacity (either the membrane bound reductases, electron transport enzymes or ROS production) of the diatoms used in this study and other species. Some suggestions to address the observations described above and for amendments to be included in future investigations using the methods described here are detailed below.

1. Included in the procedure should be a pre-wash of all cells (regardless of growth media) to remove cell surface iron, such as NaCl rinse followed by a oxalate-EDTA wash (Tang and Morel, 2006). This would remove the issue of any inorganic iron precipitates as a result of the growth media. Additionally, this amended protocol would also address the higher concentrations of Fe(II) observed in the first 5 min of a number of assays (e.g. Figure 5.9 (b) and (c)). This initial high concentration quickly reduces and could be a consequence of iron rich cell suspension solution still within the system. An alternative to the washing of cells would be to extend the washing time with the ligand solution prior to the assay (t = 0) commencing. However, a cell response to the ligand solution may be lost during washing.

2. To investigate possible interference from Fe(III) following any cellular influenced reduction and re-oxidation of Fe(II). Separate timed experiments could be performed where injections of Fe(II) standards are made and the time to pre-concentration varied. This should be followed by separate calibration to quantify the results.

3. Changes in the flow rate could allow for either a longer or shorter residence time of the complexed solution in the filter unit, allowing more contact with the cell surface membrane, though this would have to be balanced with potential losses through oxidation/re-complexation.

4. To minimise re-complexation with labile Fe(II), it is recommended that further experiments utilise citrate, as earlier experiments have demonstrated that this ligand does not form a stable complex with Fe(II) (Figures 5.5 and 5.6).

5. Finally, to provide further information into the mechanisms responsible for the reduction of Fe(III), both Fe(II) and H_2O_2 need to be determined simultaneously. Knowledge of

160

the concentration of ROS species would give an indication as to the oxidising/reducing environment surrounding the cell and therefore what influence the cell may have on iron speciation.

5.4 Conclusions

The overall aims and objectives of this study were to determine which iron-chelates diatoms may utilize to acquire iron via redox mechanisms at the cell surface. In order to accomplish this, an FI-CL system was successfully adapted and optimized for continuous in-line measurements of Fe(II) generated by diatom cells at pM concentrations. Initial interference studies revealed rapid complexation of Fe(II) by both DFB and protoporphyrin IX in UV-FSW. Interestingly, EDTA has been demonstrated to rapidly complex Fe(II) in UHP water, but does not preferentially complex Fe(II) in UV-FSW. The results for citrate, however, suggest that it does not form a stable complex with Fe(II) in either UHP water or UV-FSW. The rapid complexation of DFB and protoporphyrin IX with Fe(II) could result in a loss of any Fe(II) generated prior to determination. It is therefore difficult to assess whether generation of Fe(II) occurred in the diatom assays using these ligands unless the ligand decomposed and was unable to re-complex the labile Fe(II) (Barbeau et al., 2001). All four model ligands form a complex with Fe(III) and the model Fe(III)-ligand solutions did not interfere with the Fe(II) chemiluminescence signal.

In the study performed by Rose et al. (2005) it was also demonstrated that superoxide produced by the bacterium *L. majuscula* can serve as an electron shuttle and increase iron availability for the organism. It has also been demonstrated that superoxide will reduce a wide range of ferric-organic complexes to produce Fe(II) (Rose and Waite, 2005) and, in theory,

extracellular production of this reactive species should therefore increase iron availability for all organisms with high cellular redox processes (e.g. diatoms). High plasma membrane redox activity has been detected in diatoms (Davey et al., 2003), and the production of ROS by diatom cultures has been observed in recent studies (Kustka et al. 2005; Milne et al. submitted). However, the results from Kustka et al (2005) did not indicate an increase in available iron as a result of superoxide production. The investigations carried out here were to intended to bridge the gap between these two opposing reports and further assess the impact of cellular redox processes on iron availability. While, these initial studies have not been able to provide a conclusive outcome, small changes in the Fe(II) signal have been observed in response to light exposure. These pM Fe(II) changes need to be resolved from other factors which may be impacting on the Fe(II) signal (e.g. cell surface iron) to derive conclusions. A method and appropriate procedure are now in place to further investigate diatom cellular processes.

As with the technique adapted for the study of H_2O_2 production in diatoms, the technique described here can be applied to a wider range of further studies in different phytoplankton species. The versatility of the technique allows manipulation of the abiotic environment of the cells in order to study the affects of external parameters, such as temperature and nutrient limitation, and what consequences this may have on Fe(II) concentrations. All four ligands used in this study displayed photo-reactivity, each producing a small increase in Fe(II) concentrations when exposed to light ranging from 50 pM (EDTA) to 260 pM (DFB). While further studies could expand this range of ligands, it is recommended that ligands which do not readily bind Fe(II) be utilised (e.g. citrate) which would therefore remove the issue of re-complexation of labile Fe(II).

In summary, combining the methods for H_2O_2 and Fe(II) determination described in this thesis, has the potential to increase our understanding of the inter-relationship between iron, redox reactions and the role phytoplankton may have in this cycle.

Chapter 6

Conclusions and Future Work

6.1 Conclusions

Laboratory based studies were combined with field campaigns in order to study and understand the biogeochemical cycling of iron and hydrogen peroxide in the oceanic environment. Sensitive FI-CL techniques and suitable methods were adapted, optimised and evaluated in order to observe processes at the cellular level and combine these with studies of the ocean environment. Novel FI systems were subsequently used to determine Fe(II) and H_2O_2 in laboratory based assays with phytoplankton cells and the results presented in this thesis are the first to demonstrate real time production of H_2O_2 by the diatom species, *T. weissflogii*. In addition, a novel experimental approach was undertaken to determine Fe(II) generation following the reduction of organically bound Fe(III). The preliminary results presented here, indicate that the FI system developed can detect pM changes in Fe(II) concentrations in the assays performed using diatom cultures. Finally, the work undertaken has provided further insight into iron solubility (< 0.1 %) in seawater following a dust dissolution experiment.

Solubility of iron and aluminium in North Atlantic seawater

Iron solubility in North Atlantic seawater from the six dusts used in this study was very low, ranging from 0.001 – 0.04 %. In contrast, the release of aluminium from the dusts was two orders of magnitude higher, ranging from 0.06 - 9.0 %. Solubility varied depending on the particle concentration used (0.1 – 10 mg L^{-1}) resulting in lower solubilities at higher dust concentrations, a consequence of re-adsorption of the metal to particle surfaces confirming previously reported data (Bonnet and Guieu 2004; Zhuang et al. 1990; Spokes and Jickells 1996). Higher iron solubility was observed for a model rainwater solution (ammonium

acetate leach) which ranged from 0.15 - 1.48 % (mean 0.63 %), two orders of magnitude higher than that observed for seawater.

. The average iron/aluminium molar ratio (0.28) for the six dusts is comparable with reported data and would appear to be a good proxy for use in estimating iron release from dust deposition events. However, the range in the iron/aluminium ratio presented (0.38 – 0.70) shows the variability that can be encountered in dust/soil samples and it is therefore better to determine dissolved iron concentrations directly.

The solubility values reported. here for iron and aluminium are within the range previously observed (Bruland et al., 2001) and indicate low iron dissolution in North Atlantic surface waters from the six dusts under investigation. However Bonnet and Guieu (2004) showed that dust particles can release significant quantities of dissolved iron (0.07 – 1 nM) due to the long residence time in the mixed layer. The addition of dust carried out during this study stimulated phytoplankton growth in the natural phytoplankton community (Moore et al. 2006). All of these reports illustrate the importance of iron solubility from aerosols as a source of nutrients to the North Atlantic and hence controls primary productivity in this region.

Cellular H_2O_2 production and the effect on surface ocean water

While it is known that phytoplankton generate ROS (including H_2O_2), real time observations of such production have not been made before. In order to better understand the underlying biological processes behind H_2O_2 production, an analytical technique was required which would allow the manipulation of the abiotic environment of the cells whist performing real time analysis. A versatile and adaptable FI system was developed, with low

165

detection limits (<1 nM), excellent precision (1.1 – 1.8 %RSD) with the capability of sensitive real-time determination of H_2O_2 concentrations over a wide dynamic concentration range. Utilising this system in conjunction with a novel in-line filter approach, diatom H_2O_2 production has been demonstrated in laboratory based assay experiments. In addition, through field studies carried out in two different oceanic regions (English Channel and Ross Sea), a previously unreported correlation between phytoplankton biomass and surface H_2O_2 concentrations was observed. These results support recent studies which have suggested that biological production of H_2O_2 may be significant (Wolfe-Simon et al., 2005; Yuan and Shiller, 2005).

Reduction of Fe(III)-organic complexes by cellular processes

The production of H_2O_2 and ROS by diatom cultures has been observed in recent studies (Kustka et al. 2005; Milne et al. submitted) and high plasma membrane redox activity has been detected in diatoms (Davey et al., 2003). In order to assess whether membrane bound reductases and diatom produced ROS can reduce organically complexed iron to Fe(II) an appropriate analytical technique was required. The FI-CL instrumentation for the determination of Fe(II) was successfully adapted and optimised for the novel, continuous in-line measurements of Fe(II) generated by the diatom species, *T. weissflogii*. A highly sensitive (11 pM limit of detection) technique, with excellent precision (6.3 ± 3.2 % RSD) was used in the investigation. Using a similar in-line filter approach as utilised in the H_2O_2 assays, diatom cells were exposed to a range of Fe(III)-chelates and Fe(II) production at environmentally relevant concentrations continually determined. Preliminary results showed changes in Fe(II) concentrations, in relation to a control assay, in the range 84 to 303 pM following manipulation of the abiotic environment of the cells (light exposure). However, no consistent relationship was observed between labile Fe(II), the Fe(III)-ligand used and the light treatments.

166

6.2 Future Work

The work conducted in this thesis has shown the linkages between cellular processes and the acquisition of iron and has highlighted the key directions in which this research should be taken forward.

The results presented here (chapter four) in a laboratory based study, demonstrate that diatoms produce significant concentrations of H_2O_2 (and hence O_2^-). Field based studies indicated a correlation between fluorescence and H_2O_2 concentrations in coastal and open ocean surface waters. A continuation of the laboratory studies developed in this work using other key phytoplankton species e.g. coccolithophores, needs to be undertaken to investigate the contribution of these species to ROS. An in-situ study of natural progression of a phytoplankton bloom is required in order to relate the cellular processes observed in the laboratory to those in the natural environment.

A well defined knowledge of iron speciation is required in order to improve understanding of cell surface uptake. The results presented in chapter five indicate that both Fe(II) and Fe(III) species form complexes with organic ligands. Further investigation is needed into the complexation kinetics and equilibrium of Fe(II) and Fe(III) species between model phases and dissolved iron complexes under controlled laboratory conditions. Once this is completed, work needs to be directed into the natural environment. On-deck incubations are an ideal opportunity to study natural assemblages and should be used in conjunction with laboratory based studies to understand iron acquisition and cellular processes. Chemostats have the potential to mimic these natural processes by providing limiting nutrients (e.g. different sources of iron and nitrogen) continuously at low

concentrations, allowing growth rates to reach equilibrium with loss rates due to dilution. Adaptation of a continuous culture system for shipboard use to introduce limiting nutrients to natural plankton communities has been demonstrated by Hutchins and co-workers (2002). Chemotats are very versatile and offer the possibility of effectively simulating natural changes in nutrient supplies under controlled experimental conditions.

Integration of real-time satellite data and iron deposition may be possible in the future, but a better understanding of the dissolution of iron from aerosols is required. The work presented here (chapter three) and in previous studies (e.g. Bonnet and Guieu 2004) indicates that the dissolution of iron from particles occurs within the residence time of aerosols in surface waters (e.g. ~ 20 days) (Jickells, 1999). Further examination of the instantaneous release of dissolved iron from aerosols would enhance this knowledge and provide information into the kinetics of iron release over time. Variability due to structure, origin and atmospheric processing is more difficult to examine and requires access to a large and varied collection of samples. A broader understanding of the biogeochemical interactions and feedback mechanisms which occur in and across the air-sea interface can only be achieved through the integration of laboratory and field based studies and future work should therefore take a combined approach.

References

Achterberg, E.P. et al., 2001. Determination of iron in seawater. Analytica Chimica Acta, 442(1): 1-14.

Anderson, M.A. and Morel, F.M.M., 1982. The Influence of Aqueous Iron Chemistry on the Uptake of Iron by the Coastal Diatom Thalassiosira-Weissflogii. Limnology and Oceanography, 27(5): 789-813.

Arimoto, R. et al., 2004. Major ions and radionuclides in aerosol particles from the South Pole during ISCAT-2000. Atmospheric Environment, 38(32): 5473-5484.

Arrigo, K.R. et al., 2000. Phytoplankton taxonomic variability in nutrient utilization and primary production in the Ross Sea. Journal of Geophysical Research-Oceans, 105(C4): 8827-8845.

Arrigo, K.R. and van Dijken, G.L., 2003. Phytoplankton dynamics within 37 Antarctic coastal polynya systems. Journal of Geophysical Research-Oceans, 108(C8).

Asai, R., Matsukawa, R., Ikebukuro, K. and Karube, I., 1999. Highly sensitive chemiluminescence flow-injection detection of the red tide phytoplankton Heterosigma carterae. Analytica Chimica Acta, 390(1-3): 237-244.

Baker, A.R., French, M. and Linge, K.L., 2006a. Trends in aerosol nutrient solubility along a west-east transect of the Saharan dust plume. Geophysical Research Letters, 33(7).

Baker, A.R., Jickells, T.D., Witt, M. and Linge, K.L., 2006b. Trends in the solubility of iron, aluminium, manganese and phosphorus in aerosol collected over the Atlantic Ocean. Marine Chemistry, 98(1): 43-58.

Barbeau, K., Rue, E.L., Bruland, K.W. and Butler, A., 2001. Photochemical cycling of iron in the surface ocean mediated by microbial iron(III)-binding ligands. Nature, 413(6854): 409-413.

Barbeau, K., Rue, E.L., Trick, C.G., Bruland, K.T. and Butler, A., 2003. Photochemical reactivity of siderophores produced by marine heterotrophic bacteria and cyanobacteria based on characteristic Fe(III) binding groups. Limnology and Oceanography, 48(3): 1069-1078.

Benderliev, K.M. and Ivanova, N.I., 1994. High-Affinity Siderophore-Mediated Iron-Transport System in the Green-Alga Scenedesmus-Incrassatulus. Planta, 193(2): 163-

166.

Bergquist, B.A. and Boyle, E.A., 2006. Dissolved iron in the tropical and subtropical Atlantic Ocean. Global Biogeochemical Cycles, 20(1).

Bolwell, G.P., 1999. Role of active oxygen species and NO in plant defence responses. Current Opinion in Plant Biology, 2(4): 287-294.

Bonnet, S. and Guieu, C., 2004. Dissolution of atmospheric iron in seawater. Geophysical Research Letters, 31(3): art. no.L03303. doi:10.1029/2003GL018423.

Borer, P.M., Sulzberger, B., Reichard, P. and Kraemer, S.M., 2005. Effect of siderophores on the light-induced dissolution of colloidal iron(III) (hydr)oxides. Marine Chemistry, 93(2-4): 179-193.

Boukhalfa, H. and Crumbliss, A.L., 2002. Chemical aspects of siderophore mediated iron transport. Biometals, 15(4): 325-339.

Bowie, A.R. et al., 2006. A community-wide intercomparison exercise for the determination of dissolved iron in seawater. Marine Chemistry, 98(1): 81-99.

Bowie, A.R., Achterberg, E.P., Mantoura, R.F.C. and Worsfold, P.J., 1998. Determination of sub-nanomolar levels of iron in seawater using flow injection with chemiluminescence detection. Analytica Chimica Acta, 361(3): 189-200.

Bowie, A.R., Achterberg, E.P., Sedwick, P.N., Ussher, S. and Worsfold, P.J., 2002. Real-time monitoring of picomolar concentrations of iron(II) in marine waters using automated flow injection-chemiluminescence instrumentation. Environmental Science & Technology, 36(21): 4600-4607.

Bowie, A.R., Sedwick, P.N. and Worsfold, P., 2004. Analytical intercomparison between flow injection-chemiluminescence and flow injection-spectrophotometry for the determination of picomolar concentrations of iron in seawater. Limnology and Oceanography: Methods, 2: 42-54.

Bowie, A.R., Ussher, S.J., Landing, W.M. and Worsfold, P.J., 2007. Intercomparison between FI-CL and ICP-MS for the determination of dissolved iron in Atlantic seawater. Environmental Chemistry, 4(1): 1-4.

Boyd, P. and Harrison, P.J., 1999. Phytoplankton dynamics in the NE subarctic Pacific. Deep-Sea Research Part Ii-Topical Studies in Oceanography, 46(11-12): 2405-2432.

Boyd, P.W. et al., 2004. The decline and fate of an iron-induced subarctic phytoplankton

bloom. Nature, 428(6982): 549-553.

Boyd, P.W. et al., 2000. A mesoscale phytoplankton bloom in the polar Southern Ocean stimulated by iron fertilization. Nature, 407(6805): 695-702.

Boyle, E.A., Edmond, J.M. and Sholkovitz, E.R., 1977. The mechanism of iron removal in estuaries. Geochimica et Cosmochimica Acta, 41(9): 1313-1324.

Bruland, K.W. and Rue, E.L., 2001. Analytical methods for the determination of concentrations and speciation of iron. In: D.R. Turner and K.A. Hunter (Editors), The Biogeochemistry of Iron in Seawater. John Wiley & Sons Ltd, Chichester, pp. 255-289.

Bruland, K.W., Rue, E.L. and Smith, G.J., 2001. Iron and macronutrients in California coastal upwelling regimes: Implications for diatom blooms. Limnology and Oceanography, 46(7): 1661-1674.

Bruland, K.W., Rue, E.L., Smith, G.J. and DiTullio, G.R., 2005. Iron, macronutrients and diatom blooms in the Peru upwelling regime: brown and blue waters of Peru. Marine Chemistry, 93(2-4): 81-103.

Bruland, K.W. and Wells, S.G., 1995. The Chemistry of Iron in Seawater and Its Interaction with Phytoplankton - Introduction. Marine Chemistry, 50(1-4): 1-2.

Buck, C.S., Landing, W.M., Resing, J.A. and Lebon, G.T., 2006. Aerosol iron and aluminum solubility in the northwest Pacific Ocean: Results from the 2002 IOC cruise. Geochemistry Geophysics Geosystems, 7.

Canfield, D.E., 1989. Reactive Iron in Marine-Sediments. Geochimica Et Cosmochimica Acta, 53(3): 619-632.

Caron, D.A., Dennett, M.R., Lonsdale, D.J., Moran, D.M. and Shalapyonok, L., 2000. Microzooplankton herbivory in the Ross Sea, Antarctica. Deep-Sea Research Part Ii-Topical Studies in Oceanography, 47(15-16): 3249-3272.

Chester, R. et al., 1993. Factors Controlling the Solubilities of Trace-Metals from Nonremote Aerosols Deposited to the Sea-Surface by the Dry Deposition Mode. Marine Chemistry, 42(2): 107-126.

Cooper, W.J., Saltzman, E.S. and Zika, R.G., 1987. The Contribution of Rainwater to Variability in Surface Hydrogen-Peroxide. Journal of Geophysical Research-Oceans, 92(C3): 2970-2980.

Cooper, W.J., Shao, C.W., Lean, D.R.S., Gordon, A.S. and Scully, F.E., 1994. Factors

Affecting the Distribution of H2o2 in Surface Waters, Environmental Chemistry of Lakes and Reservoirs. Advances in Chemistry Series. Amer Chemical Soc, Washington, pp. 391-422.

Cooper, W.J. and Zepp, R.G., 1990. Hydrogen-Peroxide Decay in Waters with Suspended Soils - Evidence for Biologically Mediated Processes. Canadian Journal of Fisheries and Aquatic Sciences, 47(5): 888-893.

Cooper, W.J., Zika, R.G., Petasne, R.G. and Plane, J.M.C., 1988. Photochemical Formation of H2o2 in Natural-Waters Exposed to Sunlight. Environmental Science & Technology, 22(10): 1156-1160.

Croot, P.L. and Laan, P., 2002. Continuous shipboard determination of Fe(II) in polar waters using flow injection analysis with chemiluminescence detection. Analytica Chimica Acta, 466(2): 261-273.

Croot, P.L. et al., 2005. Spatial and temporal distribution of Fe(II) and H2O2 during EisenEx, an open ocean mescoscale iron enrichment. Marine Chemistry, 95(1-2): 65-88.

Croot, P.L., Streu, P. and Baker, A.R., 2004a. Short residence time for iron in surface seawater impacted by atmospheric dry deposition from Saharan dust events. Geophysical Research Letters, 31(23): L23S08. doi:10.1029/2004GL020153.

Croot, P.L., Streu, P., Peeken, I., Lochte, K. and Baker, A.R., 2004b. Influence of the ITCZ on H-2(2)O in near surface waters in the equatorial Atlantic Ocean. Geophysical Research Letters, 31(23): L23S04. doi:10.1029/2004GL020154.

Davey, M.S., Suggett, D.J., Geider, R.J. and Taylor, A.R., 2003. Phytoplankton plasma membrane redox activity: Effect of iron limitation and interaction with photosynthesis. Journal of Phycology, 39(6): 1132-1144.

de Baar, H.J.W. and de Jong, J.T.M., 2001. Distributions, sources and sinks of iron in seawater. In: D.R. Turner and K.A. Hunter (Editors), The Biogeochemistry of Iron in Seawater. John Wiley & Sons Ltd, Chichester, pp. 123-253.

de Jong, J.T.M. et al., 1998. Dissolved iron at subnanomolar levels in the Southern Ocean as determined by ship-board analysis. Analytica Chimica Acta, 377(2-3): 113-124.

DeSilva, D.M., Askwith, C.C. and Kaplan, J., 1996. Molecular mechanisms of iron uptake in eukaryotes. Physiological Reviews, 76(1): 31-47.

Dhungana, S. and Crumbliss, A.L., 2005. Coordination chemistry and redox processes in

siderophore-mediated iron transport. Geomicrobiology Journal, 22(3-4): 87-98.

Donat, J.R. and Bruland, K.W., 1988. Direct determination of dissolved cobalt and nickel in seawater by differential pulse cathodic stripping voltammetry preceded by adsorptive collection of cyclohexane-1,2-dione dioxime complexes. Analytical Chemistry, 60(3): 240-244.

Duce, R.A. and Tindale, N.W., 1991. Atmospheric Transport of Iron and Its Deposition in the Ocean. Limnology and Oceanography, 36(8): 1715-1726.

Evans, C., Malin, G., Mills, G.P. and Wilson, W.H., 2006. Viral infection of Emiliania huxleyi (Prymnesiophyceae) leads to elevated production of reactive oxygen species. Journal of Phycology, 42(5): 1040-1047.

Falkowski, P.G., 1994. The Role of Phytoplankton Photosynthesis in Global Biogeochemical Cycles. Photosynthesis Research, 39(3): 235-258.

Falkowski, P.G. and Raven, J.A., 1997. Aquatic Photosynthesis. Blackwell Scientific, Oxford.

Fridovich, I., 1998. The trail to superoxide dismutase. Protein Science, 7(12): 2688-2690.

German, C.R., Campbell, A.C. and Edmond, J.M., 1991. Hydrothermal Scavenging at the Mid-Atlantic Ridge - Modification of Trace-Element Dissolved Fluxes. Earth and Planetary Science Letters, 107(1): 101-114.

Gerringa, L.J.A., de Baar, H.J.W. and Timmermans, K.R., 2000. A comparison of iron limitation of phytoplankton in natural oceanic waters and laboratory media conditioned with EDTA. Marine Chemistry, 68(4): 335-346.

Gerringa, L.J.A., Rijkenberg, M.J.A., Timmermans, K.R. and Buma, A.G.J., 2004. The influence of solar ultraviolet radiation on the photochemical production of H2O2 in the equatorial Atlantic Ocean. Journal of Sea Research, 51(1): 3-10.

Gibbs, C.R., 1976. Characterization and Application of Ferrozine Iron Reagent as a Ferrous Iron Indicator. Analytical Chemistry, 48(8): 1197-1201.

Gledhill, M. and Vandenberg, C.M.G., 1994. Determination of Complexation of Iron(Iii) with Natural Organic Complexing Ligands in Seawater Using Cathodic Stripping Voltammetry. Marine Chemistry, 47(1): 41-54.

González-Davila, M., Santana-Casiano, J.M. and Millero, F.J., 2005. Oxidation of iron (II) nanomolar with H2O2 in seawater. Geochimica et Cosmochimica Acta, 69(1): 83-93.

Gordon, R.M., Martin, J.H. and Knauer, G.A., 1982. Iron in Northeast Pacific Waters. Nature,

299(5884): 611-612.

Granger, J. and Price, N.M., 1999. The importance of siderophores in iron nutrition of heterotrophic marine bacteria. Limnology and Oceanography, 44(3): 541-555.

Guieu, C. et al., 2002. Impact of high Saharan dust inputs on dissolved iron concentrations in the Mediterranean Sea. Geophysical Research Letters, 29(19).

Halliwell, B., 1982. Superoxide and Superoxide-Dependent Formation of Hydroxyl Radicals Are Important in Oxygen-Toxicity. Trends in Biochemical Sciences, 7(8): 270-272.

Hand, J.L. et al., 2004. Estimates of atmospheric-processed soluble iron from observations and a global mineral aerosol model: Biogeochemical implications. Journal of Geophysical Research-Atmospheres, 109(D17): D17205. doi:10.1029/2004JD004574.

Herring, J.G. and Morel, F.M.M., 1993. Principles and applications of Aquatic Chemistry. John Wiley & Sons, New York, 588 pp.

Hudson, R.J.M., Covault, D.T. and Morel, F.M.M., 1992. Investigations of Iron Coordination and Redox Reactions in Seawater Using Fe-59 Radiometry and Ion-Pair Solvent-Extraction of Amphiphilic Iron Complexes. Marine Chemistry, 38(3-4): 209-235.

Hudson, R.J.M. and Morel, F.M.M., 1990. Iron Transport in Marine-Phytoplankton - Kinetics of Cellular and Medium Coordination Reactions. Limnology and Oceanography, 35(5): 1002-1020.

Hutchins, D.A., Ditullio, G.R. and Bruland, K.W., 1993. Iron and Regenerated Production - Evidence for Biological Iron Recycling in 2 Marine Environments. Limnology and Oceanography, 38(6): 1242-1255.

Hutchins, D.A., Witter, A.E., Butler, A. and Luther, G.W., 1999. Competition among marine phytoplankton for different chelated iron species. Nature, 400(6747): 858-861.

Hydes, D.J., 1983. Distribution of Aluminum in Waters of the Northeast Atlantic 25-Degrees-N to 35-Degrees-N. Geochimica Et Cosmochimica Acta, 47(5): 967-973.

Hydes, D.J. and Liss, P.S., 1977. Behavior of Dissolved Aluminum in Estuarine and Coastal Waters. Estuarine and Coastal Marine Science, 5(6): 755-769.

Jickells, T., Church, T., Veron, A. and Arimoto, R., 1994. Atmospheric Inputs of Manganese and Aluminum to the Sargasso Sea and Their Relation to Surface-Water Concentrations. Marine Chemistry, 46(3): 283-292.

Jickells, T.D., 1999. The inputs of dust derived elements to the Sargasso Sea; a synthesis.

Marine Chemistry, 68(1-2): 5-14.

Jickells, T.D. et al., 2005. Global iron connections between desert dust, ocean

biogeochemistry, and climate. Science, 308(5718): 67-71.

Jickells, T.D. and Spokes, L.J., 2001. Atmospheric iron inputs to the oceans. In: D.R. Turner

and K.A. Hunter (Editors), The Biogoechemistry of Ion in Seawater. John Wiley &

Sons Ltd, Chichester, pp. 85-121.

Johnson, K.S. et al., 2001. The annual cycle of iron and the biological response in central

California coastal waters. Geophysical Research Letters, 28(7): 1247-1250.

Johnson, K.S. et al., 2003. Surface ocean-lower atmosphere interactions in the Northeast

Pacific Ocean Gyre: Aerosols, iron, and the ecosystem response. Global

Biogeochemical Cycles, 17(2): art. no.-1063.

Johnson, K.S., Gordon, R.M. and Coale, K.H., 1997. What controls dissolved iron

concentrations in the world ocean? Marine Chemistry, 57(3-4): 137-161.

Kieber, R.J., Peake, B., Willey, J.D. and Jacobs, B., 2001a. Iron speciation and hydrogen

peroxide concentrations in New Zealand rainwater. Atmospheric Environment,

35(34): 6041-6048.

Kieber, R.J., Williams, K., Willey, J.D., Skrabal, S. and Avery, G.B., 2001b. Iron speciation in

coastal rainwater: concentration and deposition to seawater. Marine Chemistry, 73(2):

83-95.

Kim, Y.C., Miller, C.D. and Anderson, A.J., 1999. Transcriptional regulation by iron and role

during plant pathogenesis of genes encoding iron- and manganese-superoxide

dismutases of Pseudomonas syringae pv. syringae B728a. Physiological and Molecular

Plant Pathology, 55(6): 327-339.

King, D.W., Lounsbury, H.A. and Millero, F.J., 1995. Rates and Mechanism of Fe(II)

Oxidation at Nanomolar Total Iron Concentrations. Environmental Science &

Technology, 29(3): 818-824.

Konigsberger, L.C., Konigsberger, E., May, P.M. and Hefter, G.T., 2000. Complexation of

iron(III) and iron(II) by citrate. Implications for iron speciation in blood plasma.

Journal of Inorganic Biochemistry, 78(3): 175-184.

Kraemer, S., Borer, P. and Sulzberger, B., 2004. Light induced dissolution of iron(III)(HYDR)

oxides in the presence of siderophores. Abstracts of Papers of the American Chemical

Society, 227: U1106-U1106.

Kustka, A.B., Shaked, Y., Milligan, A.J., King, D.W. and Morel, F.M.M., 2005. Extracellular
production of superoxide by marine diatoms: Contrasting effects on iron redox
chemistry and bioavailability. Limnology and Oceanography, 50(4): 1172-1180.

Landing, W.M. and Bruland, K.W., 1987. The Contrasting Biogeochemistry of Iron and
Manganese in the Pacific-Ocean. Geochimica Et Cosmochimica Acta, 51(1): 29-43.

Landing, W.M., Haraldsson, C. and Paxeus, N., 1986. Vinyl Polymer Agglomerate Based
Transition-Metal Cation Chelating Ion-Exchange Resin Containing the 8-
Hydroxyquinoline Functional-Group. Analytical Chemistry, 58(14): 3031-3035.

Lee, T.Y. et al., 1995. Chemiluminescence Detection of Red Tide Phytoplankton Chattonella-
Marina. Analytical Chemistry, 67(1): 225-228.

Lewis, B.L. et al., 1995. Voltammetric Estimation of Iron(III) Thermodynamic Stability-
Constants for Catecholate Siderophores Isolated from Marine- Bacteria and
Cyanobacteria. Marine Chemistry, 50(1-4): 179-188.

Lin, J. and Kester, D.R., 1992. The Kinetics of Fe(II) Complexation by Ferrozine in Seawater.
Marine Chemistry, 38(3-4): 283-301.

Liu, X.W. and Millero, F.J., 1999. The solubility of iron hydroxide in sodium chloride
solutions. Geochimica Et Cosmochimica Acta, 63(19-20): 3487-3497.

Lohan, M.C., Aguilar-Islas, A.M., Franks, R.P. and Bruland, K.W., 2005. Determination of
iron and copper in seawater at pH 1.7 with a new commercially available chelating
resin, NTA Superflow. Analytica Chimica Acta, 530(1): 121-129.

Lohan, M.C. and Bruland, K.W., 2006. Importance of vertical mixing for additional sources of
nitrate and iron to surface waters of the Columbia River plume: Implications for
biology. Marine Chemistry, 98(2-4): 260-273.

Luo, C. et al., 2005. Estimation of iron solubility from observations and a global aerosol
model. Journal of Geophysical Research-Atmospheres, 110(D23): D23307.
doi:10.1029/2005JD006059.

Macrellis, H.M., Trick, C.G., Rue, E.L., Smith, G. and Bruland, K.W., 2001. Collection and
detection of natural iron-binding ligands from seawater. Marine Chemistry, 76(3): 175-
187.

Maldonado, M.T. and Price, N.M., 1996. Influence of N substrate on Fe requirements of

marine centric diatoms. Marine Ecology-Progress Series, 141(1-3): 161-172.

Maldonado, M.T. and Price, N.M., 1999. Utilization of iron bound to strong organic ligands by plankton communities in the subarctic Pacific Ocean. Deep-Sea Research Part Ii-Topical Studies in Oceanography, 46(11-12): 2447-2473.

Maldonado, M.T. and Price, N.M., 2000. Nitrate regulation of Fe reduction and transport by Fe-limited Thalassiosira oceanica. Limnology and Oceanography, 45(4): 814-826.

Maldonado, M.T. and Price, N.M., 2001. Reduction and transport of organically bound iron by Thalassiosira oceanica (Bacillariophyceae). Journal of Phycology, 37(2): 298-309.

Maldonado, M.T., Strzepek, R.F., Sander, S. and Boyd, P.W., 2005. Acquisition of iron bound to strong organic complexes, with different Fe binding groups and photochemical reactivities, by plankton communities in Fe-limited subantarctic waters. Global Biogeochemical Cycles, 19(4).

Marchetti, A., Sherry, N.D., Kiyosawa, H., Tsuda, A. and Harrison, P.J., 2006. Phytoplankton processes during a mesoscale iron enrichment in the NE subarctic Pacific: Part I - Biomass and assemblage. Deep-Sea Research Part Ii-Topical Studies in Oceanography, 53(20-22): 2095-2113.

Maring, H.B. and Duce, R.A., 1987. The Impact of Atmospheric Aerosols on Trace-Metal Chemistry in Open Ocean Surface Seawater .1. Aluminum. Earth and Planetary Science Letters, 84(4): 381-392.

Martell, A.E. and Smith, R.M., 1997. Critical Stability Constants, 3. Plenum, New York.

Martin, J.H. et al., 1994. Testing the Iron Hypothesis in Ecosystems of the Equatorial Pacific-Ocean. Nature, 371(6493): 123-129.

Martin, J.H., Fitzwater, S.E., Gordon, R.M., Hunter, C.N. and Tanner, S.J., 1993. Iron, Primary Production and Carbon Nitrogen Flux Studies During the Jgofs North-Atlantic Bloom Experiment. Deep-Sea Research Part II-Topical Studies in Oceanography, 40(1-2): 115-134.

Martin, J.H. and Gordon, R.M., 1988. Northeast Pacific Iron Distributions in Relation to Phytoplankton Productivity. Deep-Sea Research Part a-Oceanographic Research Papers, 35(2): 177-196.

Martin, J.H., Gordon, R.M., Fitzwater, S. and Broenkow, W.W., 1989. Vertex - Phytoplankton / Iron Studies in the Gulf of Alaska. Deep-Sea Research Part I - Oceanographic

Research Papers, 36(5): 649-680.

Martin, J.H., Gordon, R.M. and Fitzwater, S.E., 1990. Iron in Antarctic Waters. Nature, 345(6271): 156-158.

Measures, C.I., 1995. The Distribution of Al in the Ioc Stations of the Eastern Atlantic between 30-Degrees-S and 34-Degrees-N. Marine Chemistry, 49(4): 267-281.

Measures, C.I. and Brown, E.T., 1996. Estimating dust input to the Atlantic Ocean using surface water Al concentrations. In: S.a.C. Guerzoni, R. (Editor), The Impact of Desert Dust across the Mediterranean. Kluwer, Dordrecht, pp. 301-311.

Measures, C.I. and Vink, S., 1999. Seasonal variations in the distribution of Fe and Al in the surface waters of the Arabian Sea. Deep-Sea Research Part II-Topical Studies in Oceanography, 46(8-9): 1597-1622.

Measures, C.I. and Vink, S., 2000. On the use of dissolved aluminum in surface waters to estimate dust deposition to the ocean. Global Biogeochemical Cycles, 14(1): 317-327.

Measures, C.I., Yuan, J. and Resing, J.A., 1995. Determination of Iron in Seawater by Flow Injection-Analysis Using in-Line Preconcentration and Spectrophotometric Detection. Marine Chemistry, 50(1-4): 3-12.

Merenyi, G., Lind, J. and Eriksen, T.E., 1990. Luminol Chemi-Luminescence - Chemistry, Excitation, Emitter. Journal of Bioluminescence and Chemiluminescence, 5(1): 53-56.

Miller, W.L. and Kester, D.R., 1994. Peroxide Variations in the Sargasso Sea. Marine Chemistry, 48(1): 17-29.

Millero, F.J., 2006. Chemical Oceanography. Taylor and Francis.

Millero, F.J. and Sotolongo, S., 1989. The Oxidation of Fe(II) with H2O2 in Seawater. Geochimica Et Cosmochimica Acta, 53(8): 1867-1873.

Millero, F.J., Sotolongo, S. and Izaguirre, M., 1987. The Oxidation-Kinetics of Fe(II) in Seawater. Geochimica Et Cosmochimica Acta, 51(4): 793-801.

Millero, F.J., Sotolongo, S., Stade, D.J. and Vega, C.A., 1991. Effect of Ionic Interactions on the Oxidation of Fe(Ii) with H2o2 in Aqueous-Solutions. Journal of Solution Chemistry, 20(11): 1079-1092.

Mills, M.M., Ridame, C., Davey, M., La Roche, J. and Geider, R.J., 2004. Iron and phosphorus co-limit nitrogen fixation in the eastern tropical North Atlantic. Nature, 429(6989): 292-294.

Moffett, J.W. and Zafiriou, O.C., 1993. The Photochemical Decomposition of Hydrogen-Peroxide in Surface Waters of the Eastern Caribbean and Orinoco River. Journal of Geophysical Research-Oceans, 98(C2): 2307-2313.

Moffett, J.W. and Zika, R.G., 1987. Reaction-Kinetics of Hydrogen-Peroxide with Copper and Iron in Seawater. Environmental Science & Technology, 21(8): 804-810.

Moore, C.M. et al., 2006. Iron limits primary productivity during spring bloom development in the central North Atlantic. Global Change Biology, 12(4): 626-634.

Moore, R.M., Burton, J.D., Williams, P.J.L. and Young, M.L., 1979. Behavior of Dissolved Organic Material, Iron and Manganese in Estuarine Mixing. Geochimica Et Cosmochimica Acta, 43(6): 919-926.

Neilands, J.B., 1995. Siderophores - Structure and Function of Microbial Iron Transport Compounds. Journal of Biological Chemistry, 270(45): 26723-26726.

O' Sullivan, D.W., Hanson, A.K. and Kester, D.R., 1995. Stopped-Flow Luminol Chemiluminescence Determination of Fe(II) and Reducible Iron in Seawater at Subnanomolar Levels. Marine Chemistry, 49(1): 65-77.

Obata, H., Karatani, H., Matsui, M. and Nakayama, E., 1997. Fundamental studies for chemical speciation of iron in seawater with an improved analytical method. Marine Chemistry, 56(1-2): 97-106.

Obata, H., Karatani, H. and Nakayama, E., 1993. Automated-Determination of Iron in Seawater by Chelating Resin Concentration and Chemiluminescence Detection. Analytical Chemistry, 65(11): 1524-1528.

Oda, T. et al., 1997. Generation of reactive oxygen species by raphidophycean phytoplankton. Bioscience Biotechnology and Biochemistry, 61(10): 1658-1662.

Orians, K.J. and Bruland, K.W., 1986. The Biogeochemistry of Aluminum in the Pacific-Ocean. Earth and Planetary Science Letters, 78(4): 397-410.

Ozsoy, T. and Saydam, A.C., 2001. Iron speciation in precipitation in the North-Eastern Mediterranean and its relationship with Sahara dust. Journal of Atmospheric Chemistry, 40(1): 41-76.

Petasne, R.G. and Zika, R.G., 1997. Hydrogen peroxide lifetimes in South Florida coastal and offshore waters. Marine Chemistry, 56(3-4): 215-225.

Powell, R.T. and Donat, J.R., 2001. Organic complexation and speciation of iron in the South

and Equatorial Atlantic. Deep-Sea Research Part Ii-Topical Studies in Oceanography, 48(13): 2877-2893.

Powell, R.T., King, D.W. and Landing, W.M., 1995. Iron Distributions in Surface Waters of the South-Atlantic. Marine Chemistry, 50(1-4): 13-20.

Price, D., Fauzi, R., Mantoura, C. and Worsfold, P.J., 1998. Shipboard determination of hydrogen peroxide in the western Mediterranean sea using flow injection with chemiluminescence detection. Analytica Chimica Acta, 371(2-3): 205-215.

Price, D., Worsfold, P.J. and Mantoura, R.F.C., 1994. Determination of Hydrogen-Peroxide in Sea-Water by Flow- Injection Analysis with Chemiluminescence Detection. Analytica Chimica Acta, 298(1): 121-128.

Price, N.M. and Morel, F.M.M., 1998. Biological cycling of iron in the ocean. In: A. Sigel and S. H. (Editors), Metal Ions on Biological Systems: Iron Transport and Storage in Micro-organisms, Plants and Animals. Marcel Dekker, New York, pp. 1-36.

Prospero, J.M., Nees, R.T. and Uematsu, M., 1987. Deposition Rate of Particulate and Dissolved Aluminum Derived from Saharan Dust in Precipitation at Miami, Florida. Journal of Geophysical Research-Atmospheres, 92(D12): 14723-14731.

Reid, R.T., Live, D.H., Faulkner, D.J. and Butler, A., 1993. A Siderophore from a Marine Bacterium with an Exceptional Ferric Ion Affinity Constant. Nature, 366(6454): 455-458.

Ren, J.L., Zhang, J., Luo, J.Q., Pei, X.K. and Jiang, Z.X., 2001. Improved fluorimetric determination of dissolved aluminium by micelle-enhanced lumogallion complex in natural waters. Analyst, 126(5): 698-702.

Ridame, C. and Guieu, C., 2002. Saharan input of phosphate to the oligotrophic water of the open western Mediterranean Sea. Limnology and Oceanography, 47(3): 856-869.

Rijkenberg, M.J.A., Gerringa, L.J.A., Carolus, V.E., Velzeboer, I. and de Baar, H.J.W., 2006. Enhancement and inhibition of iron photoreduction by individual ligands in open ocean seawater. Geochimica Et Cosmochimica Acta, 70(11): 2790-2805.

Rose, A.L., Salmon, T.P., Lukondeh, T., Neilan, B.A. and Waite, T.D., 2005. Use of superoxide as an electron shuttle for iron acquisition by the marine cyanobacterium Lyngbya majuscula. Environmental Science & Technology, 39(10): 3708-3715.

Rose, A.L. and Waite, D., 2006. Role of superoxide in the photochemical reduction of iron in

seawater. Geochimica Et Cosmochimica Acta, 70(15): 3869-3882.

Rose, A.L. and Waite, T.D., 2001. Chemiluminescence of luminol in the presence of iron(II) and oxygen: Oxidation mechanism and implications for its analytical use. Analytical Chemistry, 73(24): 5909-5920.

Rose, A.L. and Waite, T.D., 2005. Reduction of organically complexed ferric iron by superoxide in a simulated natural water. Environmental Science & Technology, 39(8): 2645-2650.

Rue, E.L. and Bruland, K.W., 1995. Complexation of Iron(Iii) by Natural Organic-Ligands in the Central North Pacific as Determined by a New Competitive Ligand Equilibration Adsorptive Cathodic Stripping Voltammetric Method. Marine Chemistry, 50(1-4): 117-138.

Rue, E.L. and Bruland, K.W., 1997. The role of organic complexation on ambient iron chemistry in the equatorial Pacific Ocean and the response of a mesoscale iron addition experiment. Limnology and Oceanography, 42(5): 901-910.

Saito, M.A. and Moffett, J.W., 2002. Temporal and spatial variability of cobalt in the Atlantic Ocean. Geochimica Et Cosmochimica Acta, 66(11): 1943-1953.

Saito, M.A., Moffett, J.W. and DiTullio, G.R., 2004. Cobalt and nickel in the Peru upwelling region: A major flux of labile cobalt utilized as a micronutrient. Global Biogeochemical Cycles, 18(4).

Saito, M.A. and Schneider, D.L., 2006. Examination of precipitation chemistry and improvements in precision using the Mg(OH)(2) preconcentration inductively coupled plasma mass spectrometry (ICP-MS) method for high-throughput analysis of open-ocean Fe and Mn in seawater. Analytica Chimica Acta, 565(2): 222-233.

Salmon, T.P., Rose, A.L., Neilan, B.A. and Waite, T.D., 2006. The FeL model of iron acquisition: Nondissociative reduction of ferric complexes in the marine environment. Limnology and Oceanography, 51(4): 1744-1754.

Sanudo-Wilhelmy, S.A., Rivera-Duarte, I. and Flegal, A.R., 1996. Distribution of colloidal trace metals in the San Francisco Bay estuary. Geochimica Et Cosmochimica Acta, 60(24): 4933-4944.

Sarthou, G. and Jeandel, C., 2001. Seasonal variations of iron concentrations in the Ligurian Sea and iron budget in the Western Mediterranean Sea. Marine Chemistry, 74(2-3):

115-129.

Sarthou, G. et al., 1997. Fe and H2O2 distributions in the upper water column in the Indian sector of the Southern Ocean. Earth and Planetary Science Letters, 147(1-4): 83-92.

Schmidt, W., 1999. Mechanisms and regulation of reduction-based iron uptake in plants. New Phytologist, 141(1): 1-26.

Shaked, Y., Kustka, A.B., Morel, F.M.M. and Erel, Y., 2004. Simultaneous determination of iron reduction and uptake by phytoplankton. Limnology and Oceanography-Methods, 2: 137-145.

Smith, W.O., Marra, J., Hiscock, M.R. and Barber, R.T., 2000. The seasonal cycle of phytoplankton biomass and primary productivity in the Ross Sea, Antarctica. Deep-Sea Research Part Ii-Topical Studies in Oceanography, 47(15-16): 3119-3140.

Soriadengg, S. and Horstmann, U., 1995. Ferrioxamine-B and Ferrioxamine-E as Iron Sources for the Marine Diatom Phaeodactylum-Tricornutum. Marine Ecology-Progress Series, 127(1-3): 269-277.

Statham, P.J., Yeats, P.A. and Landing, W.M., 1998. Manganese in the eastern Atlantic Ocean: processes influencing deep and surface water distributions. Marine Chemistry, 61(1-2): 55-68.

Sunda, W., 2001. Bioavailability and bioaccumulation of iron in the sea. In: D.R. Turner and K.A. Hunter (Editors), The Biogeochemistry of Iron in Seawater. John Wiley & Sons Ltd, Chichester, pp. 41-84.

Sunda, W.G. and Huntsman, S.A., 1995. Iron Uptake and Growth Limitation in Oceanic and Coastal Phytoplankton. Marine Chemistry, 50(1-4): 189-206.

Sunda, W.G., Litaker, R.W., Hardison, D.R. and Tester, P.A., 2005. Dimethylsulfoniopropionate (DMSP) and its relation to algal pigments in diverse waters of the Belize coastal lagoon and barrier reef system. Marine Ecology-Progress Series, 287: 11-22.

Tang, D.G. and Morel, F.M.M., 2006. Distinguishing between cellular and Fe-oxide-associated trace elements in phytoplankton. Marine Chemistry, 98(1): 18-30.

Taylor, A.R. and Chow, R.H., 2001. A microelectrochemical technique to measure trans-plasma membrane electron transport in plant tissue and cells in vivo. Plant Cell and Environment, 24(7): 749-754.

Taylor, S.R., 1964. Abundance of chemical elements in the continental crust: a new table. Geochimica et Cosmochimica Acta, 28(8): 1273-1285.

Thomson, M. and Banerjee, E.K., 1991. Atomic Absorption Methods in Applied Geochemistry. In: S.J. Haswell (Editor), Atomic Absorption Spectrometry: Theory, Design and Applications. Elsevier, Amsterdam, pp. 289-320.

Trick, C.G., 1983. Examination of hydroxamate-siderophore production by neritic eukaryotic marine phytoplankton. Marine Biology, 75: 9-17.

Trick, C.G. and Wilhelm, S.W., 1995. Physiological-Changes in the Coastal Marine Cyanobacterium Synechococcus Sp Pcc-7002 Exposed to Low Ferric Ion Levels. Marine Chemistry, 50(1-4): 207-217.

Turner, A. and Millward, G.E., 1994. Partitioning of Trace-Metals in a Macrotidal Estuary - Implications for Contaminant Transport Models. Estuarine Coastal and Shelf Science, 39(1): 45-58.

Twiner, M.J. and Trick, C.G., 2000. Possible physiological mechanisms for production of hydrogen peroxide by the ichthyotoxic flagellate Heterosigma akashiwo. Journal of Plankton Research, 22(10): 1961-1975.

Ussher, S., Achterberg, E.P. and Worsfold, P., 2004. Marine Biogeochemistry of Iron. Environmental Chemistry, 1: 67-80.

Ussher, S.J., Yaqoob, M., Achterberg, E.P., Nabi, A. and Worsfold, P.J., 2005. Effect of model ligands on iron redox speciation in natural waters using flow injection with luminol chemiluminescence detection. Analytical Chemistry, 77(7): 1971-1978.

van den Berg, C.M.G., 1995. Evidence for Organic Complexation of Iron in Seawater. Marine Chemistry, 50(1-4): 139-157.

Vasconcelos, M., Leal, M.F.C. and van den Berg, C.M.G., 2002. Influence of the nature of the exudates released by different marine algae on the growth, trace metal uptake, and exudation of Emiliania huxleyi in natural seawater. Marine Chemistry, 77(2-3): 187-210.

Von Damm, K.L. and Bischoff, J.L., 1987. Chemistry of Hydrothermal Solutions from the Southern Juan-De-Fuca Ridge. Journal of Geophysical Research-Solid Earth and Planets, 92(B11): 11334-11346.

Waite, T.D. and Morel, F.M.M., 1984. Photoreductive Dissolution of Colloidal Iron-Oxide -

Effect of Citrate. Journal of Colloid and Interface Science, 102(1): 121-137.

Watson, A.J., 2001. Iron limitation in the oceans. In: D.R. Turner and K.A. Hunter (Editors), The Biogeochemistry of Iron in Seawater. John Wiley & Sons Ltd, Chichester, pp. 9-39.

Wedepohl, K.H., 1995. The Composition of the Continental-Crust. Geochimica Et Cosmochimica Acta, 59(7): 1217-1232.

Weger, H.G., Middlemiss, J.K. and Petterson, C.D., 2002. Ferric chelate reductase activity as affected by the iron-limited growth rate in four species of unicellular green algae (Chlorophyta). Journal of Phycology, 38(3): 513-519.

Wells, M.L., 2003. The level of iron enrichment required to initiate diatom blooms in HNLC waters. Marine Chemistry, 82(1-2): 101-114.

Whitfield, M., 2001. Interactions between phytoplankton and trace metals in the ocean Advances in Marine Biology. Academic Press, pp. 1-128.

Wilhelm, S.W., MacAuley, K. and Trick, C.G., 1998. Evidence for the importance of catechol-type siderophores in the iron-limited growth of a cyanobacterium. Limnology and Oceanography, 43(5): 992-997.

Witter, A.E., Hutchins, D.A., Butler, A. and Luther, G.W., 2000. Determination of conditional stability constants and kinetic constants for strong model Fe-binding ligands in seawater. Marine Chemistry, 69(1-2): 1-17.

Wolfe-Simon, F., Grzebyk, D., Schofield, O. and Falkowski, P.G., 2005. The role and evolution of superoxide dismutases in algae. Journal of Phycology, 41(3): 453-465.

Wu, J.F., Boyle, E., Sunda, W. and Wen, L.S., 2001. Soluble and colloidal iron in the olgotrophic North Atlantic and North Pacific. Science, 293(5531): 847-849.

Wu, J.F. and Boyle, E.A., 1998. Determination of iron in seawater by high-resolution isotope dilution inductively coupled plasma mass spectrometry after Mg(OH)(2) coprecipitation. Analytica Chimica Acta, 367(1-3): 183-191.

Wu, J.F. and Luther, G.W., 1995. Complexation of Fe(Iii) by Natural Organic-Ligands in the Northwest Atlantic-Ocean by a Competitive Ligand Equilibration Method and a Kinetic Approach. Marine Chemistry, 50(1-4): 159-177.

Yocis, B.H., Kieber, D.J. and Mopper, K., 2000. Photochemical production of hydrogen peroxide in Antarctic waters. Deep-Sea Research Part I: Oceanographic Research

Papers, 47(6): 1077-1099.

Yoshida, T., Tanaka, M. and Okamoto, K., 2002. Immunoglobulin G induces microglial
superoxide production. Neurological Research, 24(4): 361-364.

Yuan, J. and Shiller, A.M., 2001. The distribution of hydrogen peroxide in the southern and
central Atlantic ocean. Deep-Sea Research Part II: Topical Studies in Oceanography,
48(13): 2947-2970.

Yuan, J.C. and Shiller, A.M., 1999. Determination of subnanomolar levels of hydrogen
peroxide in seawater by reagent-injection chemiluminescence detection. Analytical
Chemistry, 71(10): 1975-1980.

Yuan, J.C. and Shiller, A.M., 2000. The variation of hydrogen peroxide in rainwater over the
South and Central Atlantic Ocean. Atmospheric Environment, 34(23): 3973-3980.

Yuan, J.C. and Shiller, A.M., 2005. Distribution of hydrogen peroxide in the northwest Pacific
Ocean. Geochemistry Geophysics Geosystems, 6(9): Q09M02.
doi:10.1029/2004GC000908.

Zhu, X.R., Prospero, J.M., Millero, F.J., Savoie, D.L. and Brass, G.W., 1992. The Solubility of
Ferric Ion in Marine Mineral Aerosol Solutions at Ambient Relative Humidities.
Marine Chemistry, 38(1-2): 91-107.

Zhuang, G., Duce, R.A. and Kester, D.R., 1990. The Dissolution of Atmospheric Iron in
Surface Seawater of the Open Ocean. Journal of Geophysical Research-Oceans,
95(C9): 16207-16216.

Zhuang, G.S. and Duce, R.A., 1993. The Adsorption of Dissolved Iron on Marine Aerosol-
Particles in Surface Waters of the Open-Ocean. Deep-Sea Research Part I-
Oceanographic Research Papers, 40(7): 1413-1429.

Zika, R.G., Moffett, J.W., Petasne, R.G., Cooper, W.J. and Saltzman, E.S., 1985. Spatial and
Temporal Variations of Hydrogen-Peroxide in Gulf of Mexico Waters. Geochimica Et
Cosmochimica Acta, 49(5): 1173-1184.